

15

1169-40313-322
NASA CR-106301

REPORT
of
1967 SUMMER "TYCHO" MEETING
Contract No: NSR-24-005-047



**CASE FILE
COPY**

"TYCHO" STUDY GROUP
ELECTRICAL ENGINEERING DEPARTMENT
UNIVERSITY OF MINNESOTA

TG #31

REPORT
of
1967 SUMMER "TYCHO" MEETING
Contract No: NSR-24-005-047

Prepared by

UNIVERSITY OF MINNESOTA
Minneapolis, Minnesota

For

HEADQUARTERS, NATIONAL AERONAUTICS & SPACE ADMINISTRATION
Washington, D. C. 20546

PREFACE

This report is the result of the "TYCHO" Study Group Summer Study Session held at Dartmouth College, Hanover, New Hampshire, during the period June 20 to July 21, 1967.

The report is organized into a basic section and appendices containing a series of scientific papers written by individual "TYCHO" Study Group Members as research contributions. The basic section contains recommendations, partially supported by the appendices, concerning NASA's proposed planetary explorations program.

The 1967 "TYCHO" Summer Study Session investigations were confined to matters relating to atmospheric and surface conditions of the planets Venus and Mars of importance to proposed manned or unmanned landings. The investigations consisted of a comprehensive analysis of published data and presentations by the best available experts in the field.

TABLE OF CONTENTS

Edge Index

<u>Title</u>	<u>Page</u>
Summary and Recommendations	1
Discussion.	5
Mars.	5
Venus	7

RESEARCH CONTRIBUTIONS

<u>Appendix</u>	<u>Title</u>	<u>Page</u>
A	On the Radio Occultation Method for Studying Planetary Atmospheres; Anderson, D. L. and Phinney, R. A.. . . .	A1-12
B	The Case for a Mars Orbiter, Collins, R. J.. (To be distributed later)	B1-15
C	Variations in the Radar Cross Section of Venus; Evans, J. V.	C1-30
D	Radar Observations of Venus and Mars; Evans, J. V.	D1-39
E	Reflection and Diffraction in a Bistatic Radar Occultation Experiment; Hagfors, T..	E1-12
F	Water Vapor & Ice in the Martian Atmosphere; Heffner, H.	F1-12
G	The Venus Atmosphere: Further Experiments and Present Knowledge; Hopfield, J. J. and Phinney, R. A..	G1-15
H	Microwave Spectroscopy; Lax, B..	H1-11
I	Some Comments on the Scattering of Thermal Microwave Radiation Beneath a Planetary Surface; Smith, B. G..	I1-16
J	Water on Mars; Smoluchowski, R..	J1-11

REPORT

OF

1967 "TYCHO" SUMMER STUDY SESSION

June/July 1967

SUMMARY AND RECOMMENDATIONS

During July, 1967, the "TYCHO" Study Group met at Dartmouth College to examine various aspects of the NASA program for planetary exploration. Considerations of the group indicated that in the near future greatest scientific interest would be associated with unravelling the nature of the atmosphere of Venus and the details of the surface of Mars. The major impetus for planetary exploration stems in large measure from the opportunities to shed light on the origin of the solar system and the origin of life. These two questions were considered by the National Academy of Science and discussed in the Woods Hole Report. In response to this report, NASA proposed the planetary exploration program shown in Fig. 1. This program amply responds to all of the issues raised. Recognizing the completeness of both the report and the outlined program, the present study group raised the question, "What should result if delays arise as a result of either fiscal or technical problems?" In response to

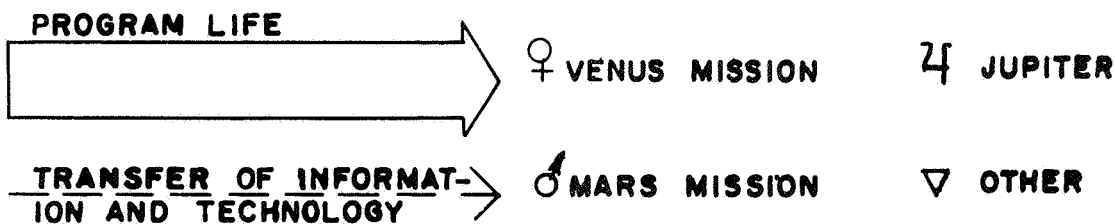
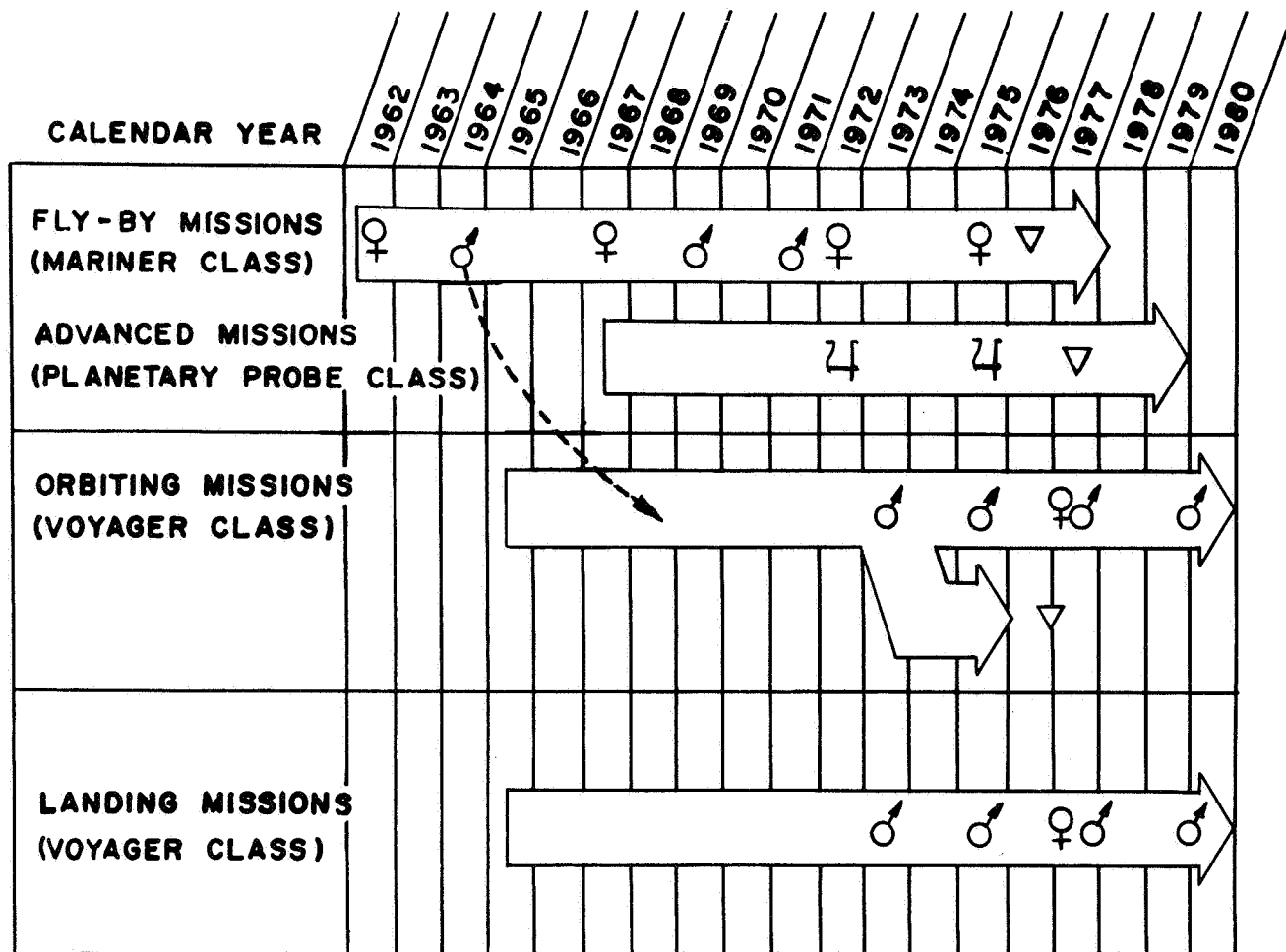


Figure 1 Evolution and Development of Planetary Missions. Following the Voyager missions to Mars, starting in 1973, will be the Voyager missions to Venus, starting in 1977. In the 1980's, Voyagers will be used to explore the outer planets. It is important to note that, during the period in which the large Voyager system is first used for Mars, there is a continuing need for Mariner-class spacecraft for precursor missions to Venus and to the outer planets. Within the restrictions of launch opportunities and the lead times needed to develop and test spacecraft, the sequence of missions shown remains highly flexible. Scientific and technical information gained from previous flights feed into subsequent missions. (From "Summary of the Voyager Program," NASA unnumbered publication, January 1967.)

this question, the following recommendations are made:

Recommendation 1.-Following the successful Mariner fly-by mission (1969) and the Mariner atmospheric probe mission (1971) the 1973 opposition of Mars should be used (as planned) for an orbiting-landing vehicle (Voyager). In the event that the Voyager 1973 spacecraft will not be available, an additional Mariner spacecraft of the 1969 type should be used in an orbiting mode. This mission should be designed to supply multiple occultation experiments, high resolution optical surface mapping with a TV camera system, and an infrared mapping of the surface. The data obtained could provide information on the seasonal and diurnal fluctuations and give a better understanding of the atmospheric effects than would be possible with a second atmospheric probe. Furthermore, the multiple passes would allow the radio occultation experiment to provide some information on the contour of the terrain.

Recommendation 2.-Recognizing the great uncertainty associated with the density and composition of the atmosphere of Venus, the next mission (1972) to Venus should be (as is planned) an atmospheric probe. In the event of delays or shortages in the Mariner program, the Mariner spacecraft/atmospheric probe scheduled for Mars in 1971 should be rescheduled for the 1972 Venus opposition.

Recommendation 3.-Recognizing that the contributions from ground-based astronomy and in particular radar astronomy have been of significant importance to the space program (e.g., the definition of the astronomical unit, orbit elements of the planets, rotation rates of Venus and Mercury, terrain elevation of Mars, and mean surface slopes of the planets), NASA should take positive steps to ensure the continuation of those radar activities now being carried on as peripheral activities at installations supported by the Department of Defense and other agencies.

The recommendation concerning an orbiting spacecraft about the planet Mars reflects the view that the 1964, 1969, and 1971 Mariners will give enough information required for successful landing on the surface. However, in order to put a lander to best use, detailed information concerning the character of the surface will be needed. The 1973 orbiting spacecraft with a TV camera system would yield this information and allow examination of many possible landing sites. Additional studies of seasonal fluctuations of the dark and light areas would also be possible. (For detailed recommendations concerning the Mars' probe, see Appendix B.)

The principal question related to Venus is the constitution and pressure of the lower atmosphere and its interaction with the surface. The current (1967) Venus fly-by can be expected to yield some information concerning the atmospheric density. However, until the composition of the clouds and the surface pressure is determined our knowledge of conditions there will remain extremely incomplete, and it will be impossible to make models for the physics and chemistry of this planet. For this reason the 1972 mission to Venus should include an atmospheric probe. In light of the success of the 1964 Mariner IV occultation results and the fortunate coincidence that nearly the entire atmosphere can be attributed to one component (CO_2), the need for an atmospheric probe of Mars is not pressing. Thus, it may even be desirable to reschedule the 1971 Mars/Mariner spacecraft probe to 1972 Venus. (For details concerning the Venus atmospheric probe, see Appendix G.)

Various particular questions are considered in Appendices A through J.

DISCUSSION

The impetus for planetary exploration stems in large measure from the opportunities this program offers to shed light on the origin of the solar system and the origin of life. In the process of answering these questions a necessary first step is determination of the physical environment. At the present time, two most important scientific questions are the possible presence of surface or subsurface water on Mars and the gross features of the composition and the pressure of the atmosphere of Venus.

Mars

In recent years the study of Mars by optical and infrared spectroscopy, radar reflectivity, and the Mariner IV space probe has added much to the knowledge of observational astronomy, but little to a detailed understanding of the geology of the surface or interior. Factors now considered well determined are the atmospheric pressure, gross composition of the atmosphere, and the surface temperature. (See Appendix F). Of those Martian features apparent even to the early optical observers--dark and light areas, polar caps and dust storms to say nothing of the fabled canals--virtually no information has been added within the last decade. The Mariner IV mission radio occultation experiments successfully determined the number density of the atmospheric particles as a function of altitude. The same Mariner IV pictures, however, added an additional unresolved question. This result is the occurrence of large craters with an absence of sharp features. The implied erosion seems too effective to have been caused by winds alone.

The question of the presence of water on Mars is of great interest because it has an important bearing upon the problem of extra-terrestrial biology and because it is closely related to our understanding of the degree and mechanism of erosion on that planet.

The range of pressures and of surface temperatures on Mars straddles the triple point of water: 6.11 mb and 273°K, and thus, in principle, one could expect to encounter ice, liquid water and water vapor in amounts varying with altitude, latitude, time of day and year. While there is evidence for water vapor in the atmosphere there is no comparable information about ice or liquid water. Polar caps are probably solid CO₂ but permafrost or ice may exist at preferred locations under a rather shallow coverage of soil. Intergranular moisture and a thin liquid top layer of permafrost could provide a suitable milieu for bacterial life. The dark areas on Mars are known to be warmer than the bright areas and if the recent radar studies are correct in indicating that these areas are topographic depressions rather than high plateaus, then it is natural to assume that they have more subsurface liquid water or ice than the rest of the planet. This difference may account not only for their higher radar reflectivity, but also for the darker color either following the biological hypothesis or according to some of the inorganic models. It is recommended that radar reflectivity and surface temperature of the dark areas be measured as a function of diurnal and seasonal variations of insolation. Such observations could be best made from a Martian orbiter but ground-based studies could also be important.

The present knowledge concerning Mars allows a reasonable coherent picture to be constructed of the pressure temperature composition of the atmosphere. This model has been used to predict global wind patterns. The next series of questions concerning the Mars planet are related to the properties and character of the surface:

- 1) What mechanism is responsible for the erosion?
- 2) What is the origin of the season of color changes?

- 3) What is the nature of the polar cap?
- 4) What is the relative terrain of the dark and light areas?

The above questions will not be answered until samples of the surface are available along with detailed studies of the topology. The implication of this statement is that a landing on the surface of Mars with a modest automated laboratory will ultimately be necessary. This laboratory should be self contained, able to maintain observations during seasonal changes and have the possibility for executing a simple chemical analysis as well as monitoring the local weather. The present ignorance of the surface terrain features suggests that prior to landing it will be necessary to obtain relatively high definition optical photographs of a certain fraction of the surface. The fraction of the surface subjected to such examination should include areas subject to seasonal changes. It is because of the selection of a suitable landing site for the automated laboratory that the lander probe of an orbiting mission was recommended in the previous section.

Venus

The planet Venus presents a more interesting challenge to the scientific community of 1967 than does Mars. This difference arises not from the amount of knowledge concerning Venus but rather the lack of it. Optical observations of Venus reveal only a generally mottled disk usually interpreted as clouds. The origin and composition of the clouds--a topic of much debate--has not yet been resolved. Present spectrographic information has indeed revealed the presence of CO_2 and H_2O . These observations and the infrared and radar temperatures have been used to imply the presence of ice crystals or water vapor as the dominant mechanism producing clouds. However, alternate approaches involving high surface pressure and perpetual dust storms can be offered to present a consistent picture of the observed data. The conclusion from

these observations is that evidence obtained through spectroscopy, radar reflection, radio emission, or infrared temperatures will not yield a satisfactory model for the planetary atmosphere or its surface until the composition of the atmosphere is available. For this reason it is essential to program an early Venus fly-by equipped with an atmospheric probe which will determine the composition of the clouds and identify a composition profile of the atmosphere.

The near equality of the radii, masses and uncompressed density of the Earth and Venus suggests that the composition and internal evolution of these two planets should be similar. The atmosphere of Venus is apparently quite different than that of the Earth even when the effects of geological activity of Earth are taken into account. Although still an unsettled problem the amount of H_2O in the atmosphere of Venus is apparently a great deal less than exists on the Earth. If the atmospheres of the Earth and Venus are secondary, i.e. due to outgassing of the interior, we would expect the amount of water outgassed from Venus to be similar to the amount of water outgassed from the Earth if the primitive compositions of the planets were the same.

The lack of water on Venus, if verified, could be due to:

- 1) Less water available in the primordial accreting material from which Venus accreted as H_2O or as water of hydration in silicates. This is a possibility since Venus presumably accreted nearer the Sun than the Earth and the primitive particles were, therefore, slightly hotter.
- 2) Less hydrogen available in Venus (relative to carbon) for reduction purposes.
- 3) More effective removal of H_2O from the atmosphere of Venus by photodissociation and loss of hydrogen.

If the latter possibility is important, then the lack of water in the atmosphere of Venus becomes less cosmologically

important. One can ask, what would happen to the Earth's atmosphere if the Earth:

- 1) Were moved to the orbit of Venus
- 2) Had its axis of rotation less tilted to its plane or revolution, thereby decreasing seasonal effects
- 3) Had its period of rotation increased to 243 days
- 4) Had its magnetic field removed

Would the cloud cover increase, the surface temperature rise to 600°K , and would coldtrapping effects be less effective in retaining water? These are essentially the observed differences between the Earth and Venus, and it is important to decide whether these differences are meteorological rather than cosmological.

Some of these questions can be tackled by methods of theoretical meteorology, but a Venus atmosphere probe would tell us immediately the composition of the Venusian atmosphere and would allow us to compute the rate of escape of these components or their dissociation products.

This is just one aspect of the problem of the origin and evolution of the solar system. The differences in composition of the Earth, Venus, Mars, Moon, Mercury, and the meteorites must be explained in any theory of the solar system, and it is important that differences which arise during evolution of the planets, such as the possibility of increased H_2O loss from Venus, be separated from primordial differences in the composition of the protoplanetary clouds.

TG # 32

APPENDIX A
(Report of 1967 Summer "TYCHO" Meeting, TG # 31)

ON THE RADIO OCCULTATION METHOD
FOR STUDYING PLANETARY ATMOSPHERES

D. L. Anderson and R. A. Phinney
July, 1967

Contract No. NSR-24-005-047

Prepared by

UNIVERSITY OF MINNESOTA
Minneapolis, Minnesota

For

HEADQUARTERS, NATIONAL AERONAUTICS & SPACE ADMINISTRATION
Washington, D. C. 20546

ON THE RADIO OCCULTATION METHOD
FOR STUDYING PLANETARY ATMOSPHERES

ABSTRACT

The problem of determining the refractivity profile of a planetary atmosphere from optical or radio occultation data is identical in principle to the problem of determining the variation of seismic velocities in the earth from the travel times of seismic body waves observed at the surface of the earth. In either case a complete set of data can be inverted uniquely, the only constraints being those fundamental to geometric optics.

Expressions are given for converting radar doppler data to the index of refraction as a function of depth in the atmosphere, and for the effects of geometric spreading and absorption on the amplitude of the signal.

TABLE OF CONTENTS

<u>Title</u>	<u>Page</u>
Introduction	A-1
Reduction of the Data.	A-3
Transformation to a Refractive Index Profile	A-5
Discussion	A-7
Bibliography	A-11

LIST OF ILLUSTRATIONS

<u>Figure</u>	<u>Title</u>	<u>Page</u>
1	Geometry of the Occultation Experiment	A-2
2	Schematic $\theta(p)$ Curve for Different Atmospheres.	A-8

ON THE RADIO OCCULTATION METHOD FOR
STUDYING PLANETARY ATMOSPHERES

D. L. Anderson and R. A. Phinney

July, 1967

INTRODUCTION

The purpose of this note is to point out a direct method of transforming radar doppler data from an occultation experiment directly into a profile of refractive index versus radius. Fjeldbo and Eshleman (1965) discuss in some detail the types of information contained in the phase and amplitude of a radio signal occulted by a planet. Their method of determining the refractive index profile is approximate but it should give good results without iteration for a planet with a thin atmosphere. They applied their technique to the interpretation of the Mariner IV occultation experiment on Mars. Kliore, et al. (1966), Kliore, et al. (1965a), Cain, et al. (1965), Kliore, et al. (1965b), Fjeldbo, et al. (1965), Fjeldbo, et al. (1966a, 1966b). For a thick atmosphere where strong bending of the rays is expected, a more general method of interpretation is desirable. Such a method, due to Herglotz, Wiechert, and others, has been well developed in the seismological literature.

The Herglotz-Wiechert method is used to determine velocity-depth profiles in the earth from the observed variation of travel time with arc distance between source and seismometer. We give here a brief derivation in a form appropriate to the radio occultation experiment and a discussion of its applicability. For further discussion of such effects as focusing and defocusing, shadow formation, etc., we recommend Bullen's (1963) text.

The geometry of the occultation experiment is summarized in Fig. 1. The coordinates are referred to the center of mass of

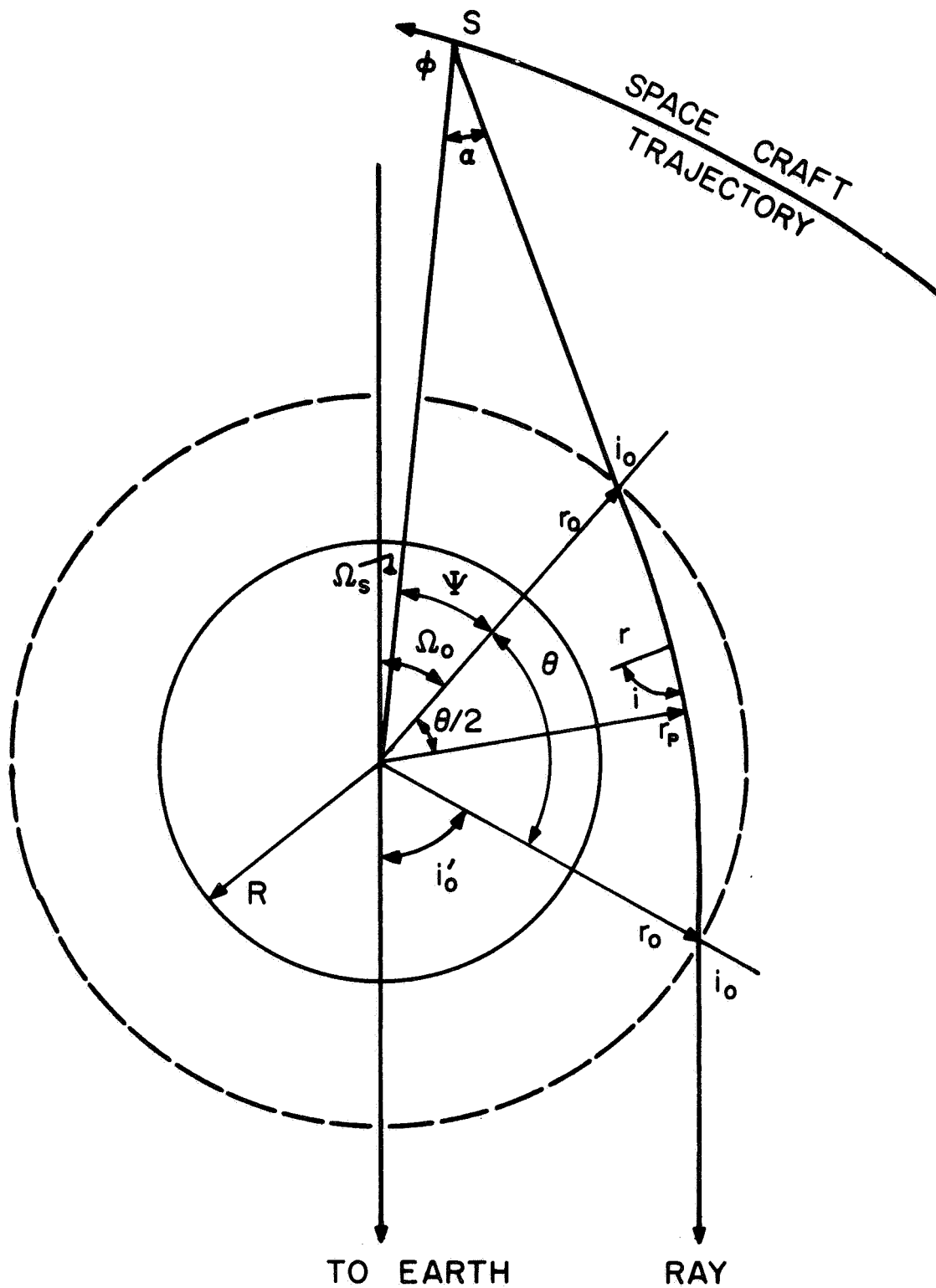


Figure 1 Geometry of the Occultation Experiment.

the planet. The refractive index, n , is a function of r in a shell $R < r < r_0$ where r_0 is an arbitrary level lying effectively above all the mass of the atmosphere, and R is the radius of the solid planet. The ray path is straight-line outside the atmosphere. It is assumed that the trajectories of the spacecraft and the earth are known with respect to the center of mass of the planet. The indicated spacecraft trajectory is the projection of the actual trajectory in the plane defined by the centers of mass of the spacecraft, earth, and planet. If the properties of the atmosphere depend only on r , then only components of velocity in the plane of the figure contribute to the observed Doppler shift.

This research was performed as part of the 1967 "TYCHO" Summer Study at Dartmouth College under NASA Contract No. NSR-24-005-047 with the University of Minnesota. The authors are indebted to G. Fjeldbo for his discussion of the problem with the "TYCHO" group.

REDUCTION OF THE DATA

The observed Doppler shift is corrected for the relative motion of the earth-based receiver and the planetary center of mass. The residual Doppler shift is then converted into a total phase by

$$\phi(t) = 2\pi t \Delta f(t) \quad (1)$$

where the zero of time is taken shortly prior to occultation. In the ray-optical description of the experiment, one can set up a family of constant phase surfaces and orthogonal rays. The selection of a time zero provides a unique value to the phase function as a function of the spatial coordinates. The spacecraft trajectory provides a sampling of the phase along an arc. This information determines the angle of emission of the ray from the spacecraft and, eventually, the refractive index profile.

The eiconal equation for the phase is

$$(\nabla\Phi)^2 = \frac{n^2 w^2}{c^2} \quad (2)$$

Assuming the spacecraft is above the atmosphere

$$|\nabla\Phi| = w/c \quad (3)$$

From the Doppler data, the directional derivative $\frac{\partial\Phi}{\partial s}$ is determined along the spacecraft trajectory. The angle between the ray and the trajectory then follows:

$$\cos(\alpha + \Phi) = \frac{\partial\Phi}{\partial s} / |\nabla\Phi| = \frac{c}{2\pi f} \frac{\partial\Phi}{\partial s} \quad (4)$$

where f may without error be taken as constant during the occultation. Since Φ is known, α follows immediately.

The ray is now projected to a reference sphere r_o . The angle of incidence on this surface is:

$$\sin i_o = r_s \sin \alpha / r_o \quad (5)$$

(the subscript s refers to spacecraft coordinates). Solution of the triangles in Fig. 1 gives the entry point angle

$$\sin(\Omega_o - \Omega_s) = \frac{\sin \alpha}{r_o} [r_s \cos \alpha - r_o \cos i_o] \quad (6)$$

and the angle subtended by the portion of the ray in the atmosphere:

$$\theta = \pi - i'_o - \Omega_o \quad (7)$$

The rays to earth are sufficiently parallel that we can take $i'_o = i_o$.

Instead of Doppler as a function of spacecraft position, we now have the angle of incidence at the top of the atmosphere as a function of θ . We now transform to a relation between refractive index and radius, using the method described by Herglotz (1907), Bateman (1910), and Wiechert and Geiger (1910).

TRANSFORMATION TO A REFRACTIVE INDEX PROFILE

A ray parameter, p , is defined

$$p = nr \sin i \quad (8)$$

which is constant along a ray, by Snell's law, and serves as a label of the ray. In the absence of an atmosphere p would be the radius of closest approach, and may be called the impact parameter of the ray. We have immediately:

$$p = r_0 \sin i_0 = r_p n_p \quad (9)$$

where the subscript p refers to the turning point of the ray. As an auxiliary variable, define η , which varies along a ray, taking the value r_0 at $r = r_0$ and the value p at $r = r_p$:

$$\eta = nr = p/\sin i \quad (10)$$

Integrating along the ray gives the total arc subtended:

$$\theta(p) = 2 \int_{r_p}^{r_0} (p/r)(\eta^2 - p^2)^{-1/2} dr = 2 \int_p^{r_0} (p/r)(\eta^2 - p^2)^{-1/2} \frac{dr}{d\eta} d\eta \quad (11)$$

The path length in the atmosphere is

$$s = 2 \int_p^{r_0} r n (\eta^2 - p^2)^{-1/2} dr \quad (12)$$

Now set

$$y = \eta^2 - r_0^2 \quad (13)$$

$$w = p^2 - r_0^2$$

Then

$$\theta(p) = 2p \int_w^0 (y-w)^{-1/2} \frac{d \ln r}{dy} dy \quad (14)$$

This integral equation for $\ln r(y)$ is in the form of the Abel integral equation and may be solved by reference to the Abel transform pair

$$f(w) = K \int_0^w g'(y)(y-w)^{-1/2} dy \quad (15)$$

$$g(y) = (K\pi)^{-1} \int_0^y f(w)(w-y)^{-1/2} dw$$

By inspection:

$$\ln [r(y)/r_0] = \frac{1}{\pi} \int_0^y \theta(w) 2p(w)^{-1}(w-y)^{-1/2} dw \quad (16)$$

or

$$\ln [r(\eta)/r_0] = \frac{1}{\pi} \int_{r_0}^{\eta} \frac{\theta(p) dp}{(p^2 - \eta^2)^{1/2}}$$

The right hand side is solved by the substitution $p = \eta \cosh q$ and integration by parts:

$$\ln[r/r_0] = \frac{1}{\pi} \left[\theta \cosh^{-1}(p/\eta) \right] \int_{r_0}^{\eta} - \frac{1}{\pi} \int_{r_0}^{\eta} \cosh^{-1}(p/\eta) \frac{d\theta}{dp} dp \quad (17)$$

The first term on the right hand side vanishes and exponentials can be taken:

$$r(\eta) = r_0 \exp \left\{ - \frac{1}{\pi} \int_{r_0}^{\eta} \cosh^{-1} (p/\eta) \frac{d\theta}{dp} dp \right\} \quad (18)$$

The integral is always positive; $r_0 > \eta$ and $\frac{d\theta}{dp}$ is normally negative. It is possible to make $\frac{d\theta}{dp}$ positive over certain ranges of p due to sharp gradients in n ($n < 1$), but the integral must always be positive.

The refractive index profile $r(\eta)$ follows from Eq. (18) and from the definition of η , Eq. (10).

DISCUSSION

Some of the hazards in applying Eq. (18) are discussed in Jeffreys (1959) and Bullen (1963). Being due to the nature of the optical problem rather than the method of analysis, these considerations are equally applicable whatever method is used to derive the refractive index profile. In summary:

1) $d\theta/dp$ may be positive for a limited range of p (Fig. 2). The function $p(\theta)$ is then multivalued for certain ranges, due to multipath propagation. The spacecraft must be able to distinguish all multiple rays in order for an interpretation to be correct.

2) In a neutral atmosphere, the increase of refractive index with depth causes the rays to be curved downward. In order that a ray emerge from the atmosphere by a direct refraction path the radius of curvature of the ray must exceed that of the tangent sphere. Since the downward curvature of a ray is given by

$$\rho = - \frac{d \ln n}{dr} \quad (19)$$

this condition is

$$- \frac{dn}{dr} < \frac{n}{r} \approx \frac{1}{r} \quad (20)$$

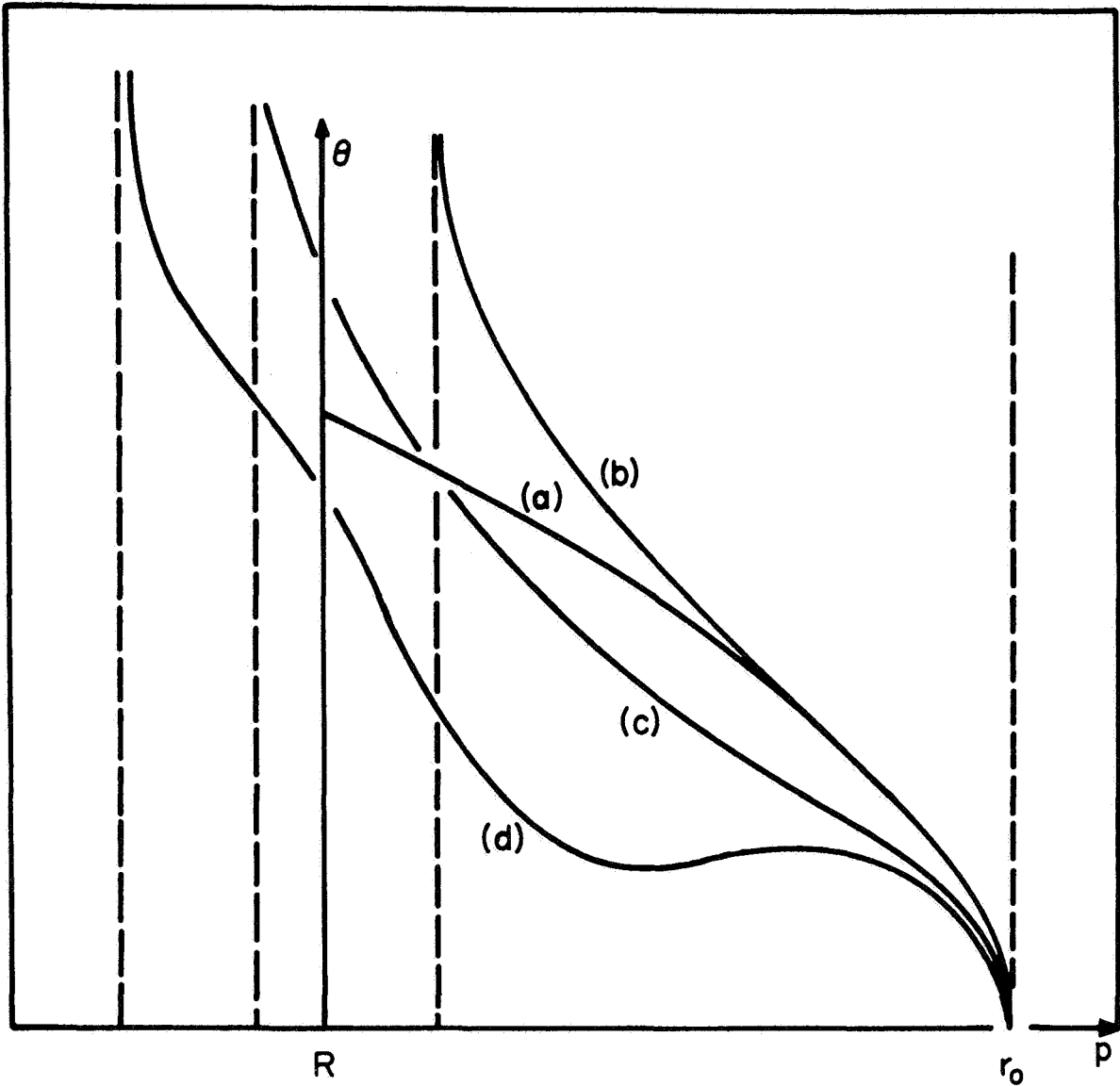


Figure 2 Schematic $\theta(p)$ Curves for Different Atmospheres.

- (a) No atmosphere: $\theta = 2\cos^{-1} \left(\frac{p}{r_0} \right)$; $p > R$.
- (b) Strongly refracting neutral atmosphere
- (c) Weakly refracting ionosphere and weakly refracting atmosphere
- (d) Strongly refracting ionosphere and strongly refracting atmosphere

(a) and (c) end occultation; (b) and (d) end asymptotically at an optical shadow.

In the lower atmosphere of a planet like Venus Eq. (20) may not be satisfied, and rays with p below a critical value can emerge from the atmosphere only by reflection from the solid surface. The essence of this, or any equivalent inversion method is that the turning points (r_p) of the rays considered must range continuously through the atmosphere. Since this is true only from r_0 down to the critical level, Eq. (18) cannot be applied to the atmosphere below the critical level. In seismology, refractive index decreases at great depth result in the eventual emergence of the downward refracted rays, but this is extremely unlikely in atmospheric studies.

A slightly different condition defines when a ray having the accessible range of p , $0 < p < r_0$, can have a turning point at depth r :

$$n r < r_0 \quad (21)$$

If a screening region of low index (ionosphere) lies above the neutral atmosphere, Eq. 21 is replaced by the more stringent condition.

$$n r < n^* r^* \quad (22)$$

where $*$ refers to the ionospheric level of maximum nr . For an ionosphere with the scale determined for Mars by Mariner IV, about 6×10^8 electrons/cm³ would be required. Consequently, Eq. 22 is unlikely to apply in a real case.

The intensity variation of the refracted signal due to focusing and defocusing can be stated in the notation of this paper. Neglecting diffraction effects at caustics,

$$\frac{I(\text{exit})}{I(\text{entry})} = \frac{\sin \psi}{\sin(\theta+\psi)} \left[\frac{d\theta/dp}{\left(\frac{(\tan i_0 - \tan \alpha) \sin \alpha}{r_0 \cos \psi} + \frac{\tan \psi^{-1}}{r_0 \sin i_0} \right)} \right]^{-1} \quad (23)$$

where $\psi = \Omega_0 - \Omega_s$. If r_s is nearly equal to r_0 , the expression in braces is small and positive; $I(\text{exit})$ will be very large (focusing) if $\frac{d\theta}{dp} = 0 + \{\} \approx 0$. If $r_s \rightarrow \infty$, $\alpha \rightarrow 0$, $\psi \rightarrow i_0$, and focusing will occur if $\frac{d\theta}{dp} = \tan i_0$. In the study of atmospheres, i_0 is always near $\pi/2$ and that condition will not be satisfied (Fig. 2).

Rays which are refracted downward at nearly the curvature of the planet have large $\frac{d\theta}{dp}$ and are severely defocused.

BIBLIOGRAPHY

- Bateman, H., (1910), The Solution of the Integral Equation which connects the Velocity of Propagation of an Earthquake Wave in the Interior of the Earth with the Times which the Disturbance takes to Travel to the Different Stations on the Earth's Surface, Phil. Mag. (6), 19, pp. 576-587.
- Bullen, K. E., An Introduction to the Theory of Seismology, Cambridge University Press, (1963).
- Cain, D. L., F. D. Drake, V. R. Eshleman, G. Fjeldbo, A. Kliore, and G. S. Levy, Proc. Ionospheric Research Committee of the Avionics Panel, AGARD, NATO, Rome, Italy, September 21-25, 1965.
- Fjeldbo, G., V. R. Eshleman, A. J. Kliore, D. L. Cain, G. S. Levy, and F. D. Drake, Preliminary Results of the Mariner IV Radio Occultation Measurement of the Upper Atmosphere of Mars, ibid, (1965).
- Fjeldbo, G., W. C. Fjeldbo, and V. R. Eshleman, Atmosphere of Mars: Mariner IV Models Compared, Science, 153, pp. 1518-1523, 1966b.
- Fjeldbo, G., W. C. Fjeldbo, and V. R. Eshleman, Models for the Atmosphere of Mars based on the Mariner IV Occultation Experiment, J. Geophys. Res. 71, No. 9, pp. 2307-2316, (1966a).
- Herglotz, G., (1907) Uber das Benndorfsche Problem der Fortpflanzungsgeschwindigkeit der Erdbebenstrahlen, Phys. Z. 8, pp. 145-147.
- Jeffreys, H., The Earth, Cambridge University Press, (1959).
- Kliore, A., D. L. Cain, and G. S. Levy, Radio Occultation Measurement of the Martian Atmosphere over two Regions by the Mariner IV Space Probe, Proceedings Seventh International Space Science Symposium, (COSPAR), Vienna, Austria, May 11-17, 1966.

BIBLIOGRAPHY (continued)

- Kliore, A., D. L. Cain, G. S. Levy, V. R. Eshleman, G. Fjeldbo, and F. D. Drake, Preliminary Results of the Mariner IV Occultation Measurement of the Atmosphere of Mars, Proceedings of the CalTech-JPL Lunar and Planetary Conference, September 13-18, 1965.
- Kliore, A., D. L. Cain, G. S. Levy, V. R. Eshleman, G. Fjeldbo and F. D. Drake, Occultation Experiment: Results of the First Direct Measurement of Mars' Atmosphere and Ionosphere, Science, 149, p. 1243, September 10, 1965.
- Wiechert, E., and L. Geiger, Bestimmung des Weges der Erdbebenwellen im Erdinnern, Phys. Z., 11, pp. 294-312, 1910.

TG #33

APPENDIX B

(Report of 1967 Summer "TYCHO" Meeting, TG #31)

THE CASE FOR A MARS ORBITER

R.J. Collins

Note: This paper has been delayed and will be distributed separately at a later date.

APPENDIX C
(Report of 1967 Summer "TYCHO" Meeting, TG # 31)

VARIATIONS IN THE RADAR CROSS
SECTION OF VENUS

J. V. Evans
June/July, 1967

Contract No: NSR-24-005-047

Prepared by

UNIVERSITY OF MINNESOTA
Minneapolis, Minnesota

For

HEADQUARTERS, NATIONAL AERONAUTICS & SPACE ADMINISTRATION
Washington, D. C. 20546

VARIATIONS IN THE RADAR CROSS SECTION OF VENUS

ABSTRACT

Variations in the radar cross section of Venus have been reported by a number of observers. At decimeter wavelengths these are of the order of $\pm 50\%$ of the mean and have been attributed to variations in the nature of the terrain occupying the subradar point. At 3.8 cm the cross section is most frequently observed to be $\sim .012\%$ of the projected area of the disk, but values three times larger have been reported. The suggestion has been made that these increases result from changes in the amount of attenuation caused by the atmosphere of Venus. This would imply large scale variations in the distribution of the microwave absorbing agent and would have serious consequences for many of the atmospheric models that have been proposed.

This paper reviews the evidence for variations in the cross section and provides revised values of the cross section at 3.8 cm. The mean value for the cross section observed in 1966 is now placed at .017. A closer examination of one instance in which the cross section at 3.8 cm was seen to increase reveals that this event was associated with the passage of a large feature through the region of the subradar point. This suggests that the variations observed at this wavelength, like those at longer wavelengths are associated with the nature of the terrain at the subradar point and are not the result of weather-like phenomena on Venus.

TABLE OF CONTENTS

<u>Title</u>	<u>Page</u>
Introduction	C-1
Meterwave and Decimeter Observations	C-1
Centimeter Wave Observations	C-8
Radar Calibration Errors	C-10
Signal-to-Noise Ratio Errors	C-11
Corrections for Terrestrial Absorption and Pointing Error.	C-13
Longitude Variation	C-21
A Major Surface Feature on Venus	C-21
Summary.	C-28
Bibliography	C-30

ILLUSTRATIONS

<u>Figure</u>	<u>Title</u>	<u>Page</u>
1	Millstone Hill ($\lambda = 23$ cm) and Arecibo Ionospheric Observatory ($\lambda = 70$ cm) cross section measurements as a function of date in 1964.	C-4
2	The measurement shown in Fig. 1 replotted as a function of the longitude of the subradar point.	C-6
3	Cross section measurements reported by Evans, et al. (1966) at 3.8 cm.	C-9
4	Variation of the equivalent echo temperature of Venus at 3.8 cm with zenith angle χ on February 9, 1966.	C-16
5	Variation of the equivalent echo temperature of Venus at 3.8 cm with zenith angle on March 30, 1966.	C-17

ILLUSTRATIONS - Continued

<u>Figure</u>	<u>Title</u>	<u>Page</u>
6	The variation of the gain of the Haystack antenna with elevation angle according to radio star observations (Allen, 1967).	C-19
7	Comparison of the decimeter cross section measurements (Fig. 2) scaled by a factor 1/10 with revised values obtained at 3.8 cm (Table 5).	C-22
8	Spectrum of Venus signals March 21, 1966.	C-23
9	Spectrum of Venus signals March 21, 1966, with runs in which doppler tracking was believed poor removed.	C-24
10	Spectrum of Venus signals March 30, 1966	C-26
11	Spectrum of Venus signals April 15, 1966.	C-27

LIST OF TABLES

<u>Table</u>	<u>Title</u>	<u>Page</u>
1	Cross Section Observations of Venus.	C-2
2	CW Cross Section Measurements of Venus at 3.8 cm	C-10
3	Signal-to-Noise Uncertainty in the 3.8 cm Cross Section Measurements	C-12

LIST OF TABLES - Continued

<u>Table</u>	<u>Title</u>	<u>Page</u>
4	Corrections Applied to the 3.8 cm Cross Section Measurements for Atmospheric Attenuation and Pointing Error	C-14
5	Revised Values for the Cross Section at 3.8 cm	C-20

VARIATIONS IN THE RADAR CROSS SECTION OF VENUS

J. V. Evans

Lincoln Laboratory+

Massachusetts Institute of Technology

INTRODUCTION

In a companion paper we have reviewed the results of radar studies of the planets Venus and Mars. In that paper we discussed the variability in the radar cross section of Mars, but did not report on similar variations observed for Venus. In this report we review the evidence for variations in the cross section of Venus, and present hitherto unpublished data which throws light on the behavior at 3.8 cm wavelength.

We are indebted to the staff of the Haystack Microwave Facility who were responsible for making the 3.8 cm measurements, to Dr. G. H. Pettengill for helpful advise and discussions, and to Dr. I. I. Shapiro and his colleagues for furnishing a tabulation of the longitude and latitude of the subradar point on Venus as a function of date. This work was performed during the course of the "TYCHO" Study Group meeting at Dartmouth College, Hanover, New Hampshire, June-July, 1967.

METERWAVE AND DECIMETER OBSERVATIONS

Measurements at the radar cross section of Venus have been made at meter wavelengths by James and Ingalls (1964) and Klemperer et al. (1964) at the wavelengths listed in Table 1. Both groups found that the mean cross section was a little under 0.2 of the projected area of the disk, but that values as large as 0.6 were occasionally observed.

+Supported by the U. S. Air Force

TABLE 1

CROSS SECTION OBSERVATIONS OF VENUS

Observer	Wavelength	Period
James and Ingalls (1964)	7.84 m.	11/6/62 - 12/7/62
Klemperer et al. (1964)	6.00 m.	11/28/62 - 12/7/62
Pettengill et al. (1967)	70.00 cm.	2/22/64 - 9/20/64
Evans et al. (1965)	23.00 cm.	3/5/64 - 8/26/64
Goldstein (1964)	12.60 cm.	9/7/62 - 12/15/62
Carpenter (1966)	12.60	5/10/64 - 7/18/64
Evans et al. (1966)	3.80	1/18/66 - 6/27/66

In the case of the $\lambda = 7.84$ m measurements plane polarized signals were transmitted and received, and hence some of the observed variability must have been caused by Faraday rotation in the earth's ionosphere. An additional fading mechanism can be anticipated; namely, the constructive and destructive interference of signals reflected from different portions of the surface of Venus. Klemperer et al. (1964) show that the echo amplitudes have a Rayleigh distribution as would be expected due to this effect. Similar fading is encountered for the moon as its aspect changes with respect to a terrestrial observer, and has been studied extensively (Evans 1965). In the case of Venus near inferior conjunction the fading period would be of the order of ≥ 20 sec at $\lambda = 6$ m so that in a five-minute observing period there would be 15 or less independent echo samples. Hence, much of the variability observed by James and Ingalls (1964) can be attributed simply to the small number of independent signal samples obtained per run. Long period variability in the cross section may also have been present in their result, but is probably masked by these short period fluctuations.

Measurements of the cross section at decimeter wavelengths have been reported by Pettengill et al. (1967), Evans et al. (1965), Goldstein (1964), and Carpenter (1966) for the time periods and wavelengths listed in Table 1. At these wavelengths the fading period is reduced to the order of one second so that the statistical sample obtained during a single 5-minute observation period is considerably improved. In addition, all these observers employed antennas which could follow Venus, and thus were able to make repeated observations during the course of the day. In these measurements, therefore, the principal sources of uncertainty in the cross section were those introduced by poor signal-to-noise ratio and the calibration of the radar equipment.

Goldstein (1964) obtained a mean value for the radar cross section of $.095 \pi r^2$ (where r is the radius of Venus) with departures from the mean as large as $\pm 50\%$, which he attributed to variability in the scattering behavior of the planet. Carpenter (1966) reported a mean value of $.114 \pi r^2$ at the same wavelength, and found variations in this of the order of $\pm 20\%$. No explanation for the difference between this result and Goldstein's has been offered.

Evans et al. (1965) and Pettengill et al. (1967) found somewhat larger variations at $\lambda = 23$ and 70 cm respectively. Since the mean of the values published by Evans et al. is about $0.13 \pi r^2$, and the mean of the values obtained by Pettengill et al. (1967) is $.14 \pi r^2$, we have compared the two sets of data in a single plot (Fig. 1) showing cross section vs date. Much of the variation shown in Fig. 1 must be introduced by the errors of measurement. These would be least in June and July (i.e. around inferior conjunction) and become progressively larger away from this time. Despite this the occasional values that are either half or twice the mean probably represent real changes in the cross section.

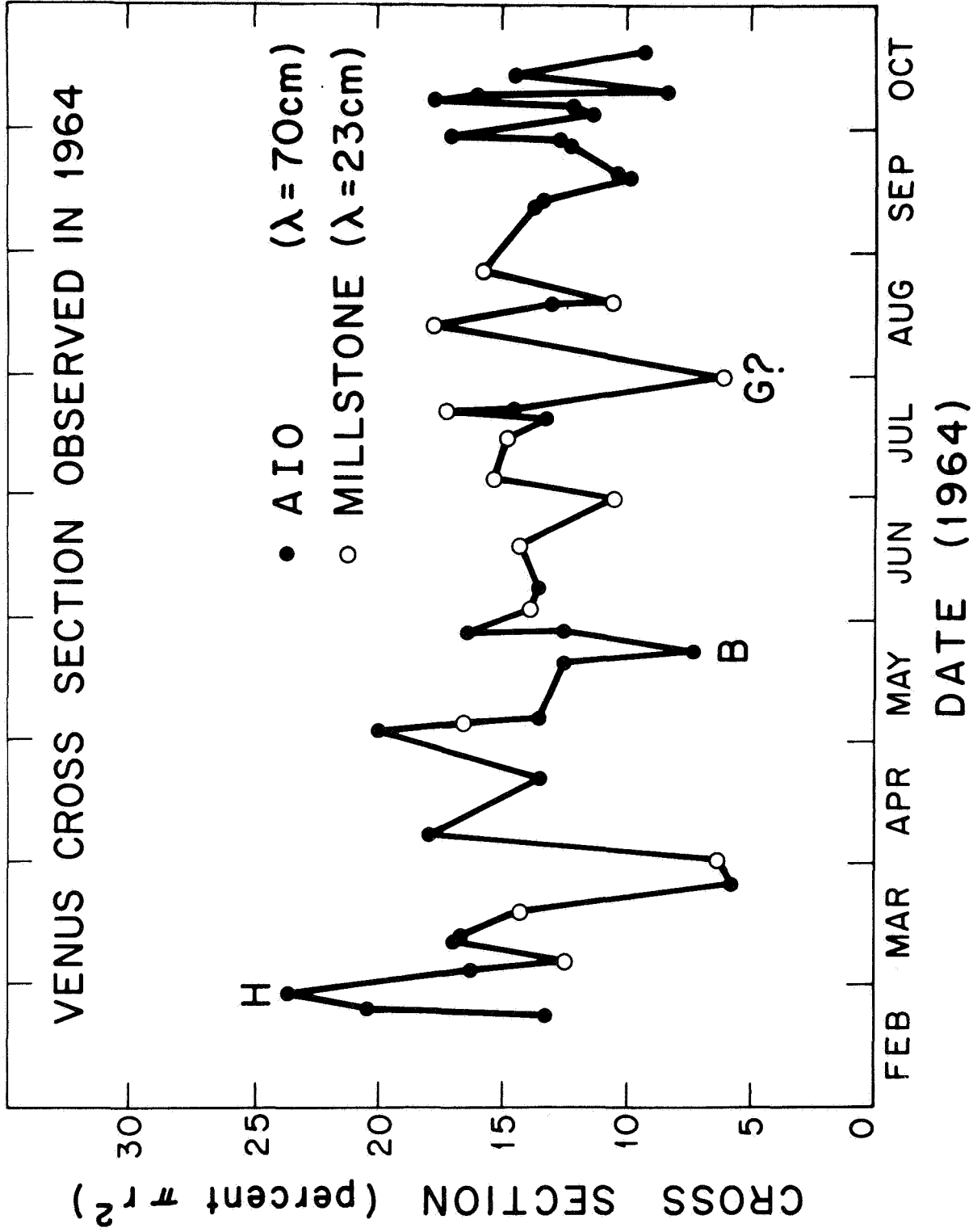


Figure 1 Millstone Hill ($\lambda = 23\text{ cm}$) and Arecibo Ionospheric Observatory ($\lambda = 70\text{ cm}$) cross section measurements as a function of date in 1964.

The data shown in Fig. 1 span a time interval longer than the axial rotation period of Venus with respect to the earth (~ 5 months). Thus some longitudes were viewed more than once. The variation in the latitude of the subradar point during the entire period shown in Fig. 1 was within the range -3.6 to $+5.8^\circ$ (assuming a pole position $\delta = 66^\circ$, $\alpha = 270^\circ$). Since, however, 50% of the echo power is returned in the first 300 μ sec from the leading edge (Evans et al. 1965) corresponding to a region of $\pm 7^\circ$ about the subradar point, to a first approximation we may ignore the variation of latitude with time and simply plot the cross section versus longitude. This is done in Fig. 2 employing a coordinate system proposed by I. I. Shapiro and colleagues. In this system, the prime meridian is defined as being the central meridian at 0.0h U. T. January 1, 1961. The pole position adopted is that given above, and a rotation period of -243.2 days has been assumed. Since the region from which the radar return chiefly arises is of the order of 15° in longitude, it is evident that much of the fine structure in this figure is spurious.

Anomalous scattering regions on the surface of Venus have been detected by a number of workers, and their location studied extensively by Carpenter (1966). We have attempted to see if there is any correlation between the major changes in cross section shown in Fig. 2 with the passage of such features through the subradar region. This is somewhat complicated by the difference in the coordinate systems employed by Shapiro and Carpenter. Very crudely Carpenter's longitudes will be obtained by subtracting 240° from those shown in Fig. 2. However, this transformation is not exact since Carpenter (1966) employed a pole position of ($\delta = 68^\circ$, $\alpha = 255^\circ$) and a rotation period of 250 days.

One suggested identification is that the dip in cross section at 162° longitude is associated with the passage of the feature

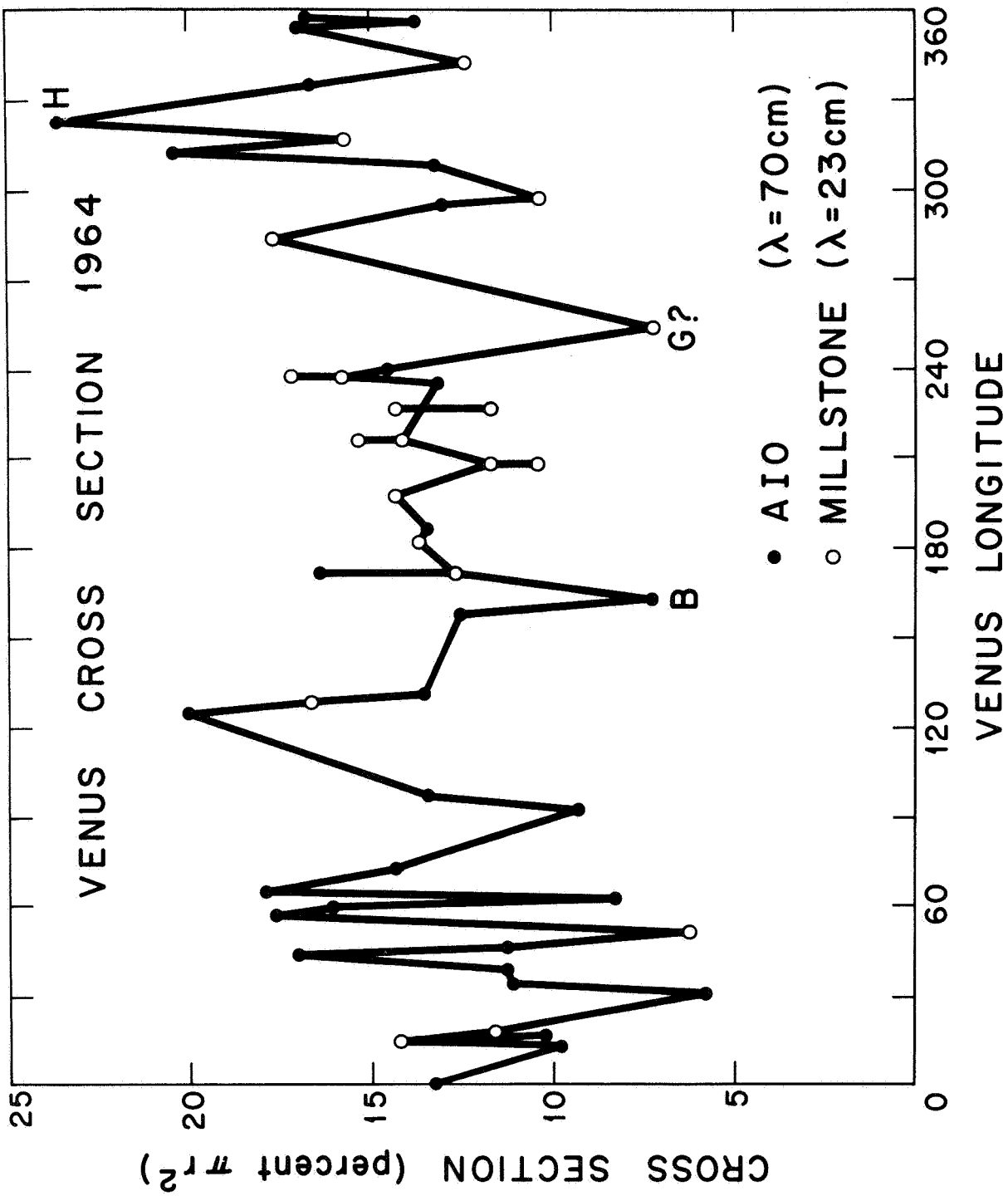


Figure 2 The measurements shown in Fig. 1 replotted as a function of the longitude of the subradar point. The coordinate system is defined in the text.

B of Carpenter's list through the subradar region. A second dip occurs when the feature G would lie on the central meridian, but if Carpenter's value for the latitude of G is correct, then it seems that this feature would lie outside the central region that chiefly governs the echo strength. The peak at 320° (labeled H) in Fig. 2 occurs at the same longitude as an increase at 3.8 cm wavelength was observed (next section).

In sum, Venus rotates with respect to the Earth such that the longitude of the subradar point changes at a rate of between 3° per day (at superior conjunction) and $\sim 1^\circ$ per day (near inferior conjunction). Some 50% of the echo power is returned from a region at the subradar point extending some 15° in longitude. Thus, we might expect significant changes in the cross section to occur on a time scale of the order of 5 days or longer. The accuracy and the sampling afforded by the published data is too poor to permit the construction of a reliable cross section versus longitude map. However, there is nothing in the data to suggest that what real variation does exist is not simply a consequence of changes in the roughness and/or reflectivity of the subradar region.

Week to week changes of the roughness have been reported by Evans et al. (1965) and increases in roughness would be expected to lower the observed cross section. Thus major dips are consistent with the view that a large rough area has moved to occupy the subradar region. The converse probably does not hold. The average scattering properties of Venus are sufficiently near specular that it would not be possible to make a major increase in the cross section by placing a completely smooth region at the subradar point. This follows because the back-scattering gain g of a sphere with a gently undulating surface is $1 + a^2$ where a is the rms surface slope. For most regions on Venus $a \sim 0.1$ and thus the gain is indistinguishable from that

of a perfect sphere. It follows that increases in cross section must result from increases in the reflection coefficient at the subradar point (or of the roughness of a large area surrounding this region).

CENTIMETER WAVE OBSERVATIONS

Whereas the cross section reported for meter and decimeter observations lies in the range $0.1-0.2 \pi r^2$, Karp et al. (1964) reported a cross section at 3.6 cm of $0.01 \pi r^2$. This was subsequently confirmed by Evans et al. (1966) who were able to show that, at least in part, this low value is caused by attenuation in the atmosphere of Venus. Observations at this wavelength thus hold special interest in that they may provide information concerning the nature of the atmosphere and possible day-to-day changes.

Figure 3 shows the cross section measurements reported by Evans et al. (1966). These values are also listed in Table 2. Near close approach (i.e., up to day 50) the accuracy of measurement was limited by uncertainty in the performance of the radar (e.g., the antenna gain, transmitter power, etc), together with the amount of atmospheric attenuation introduced by the earth's atmosphere. Subsequently, the signal-to-noise ratio deteriorated, and the uncertainty in the determination of the echo power increased as reflected by the error bars in Fig. 3. In what follows we discuss these three principle sources of error in order to determine whether the two large cross section increases observed (Fig. 3) may be attributed to errors of measurement.

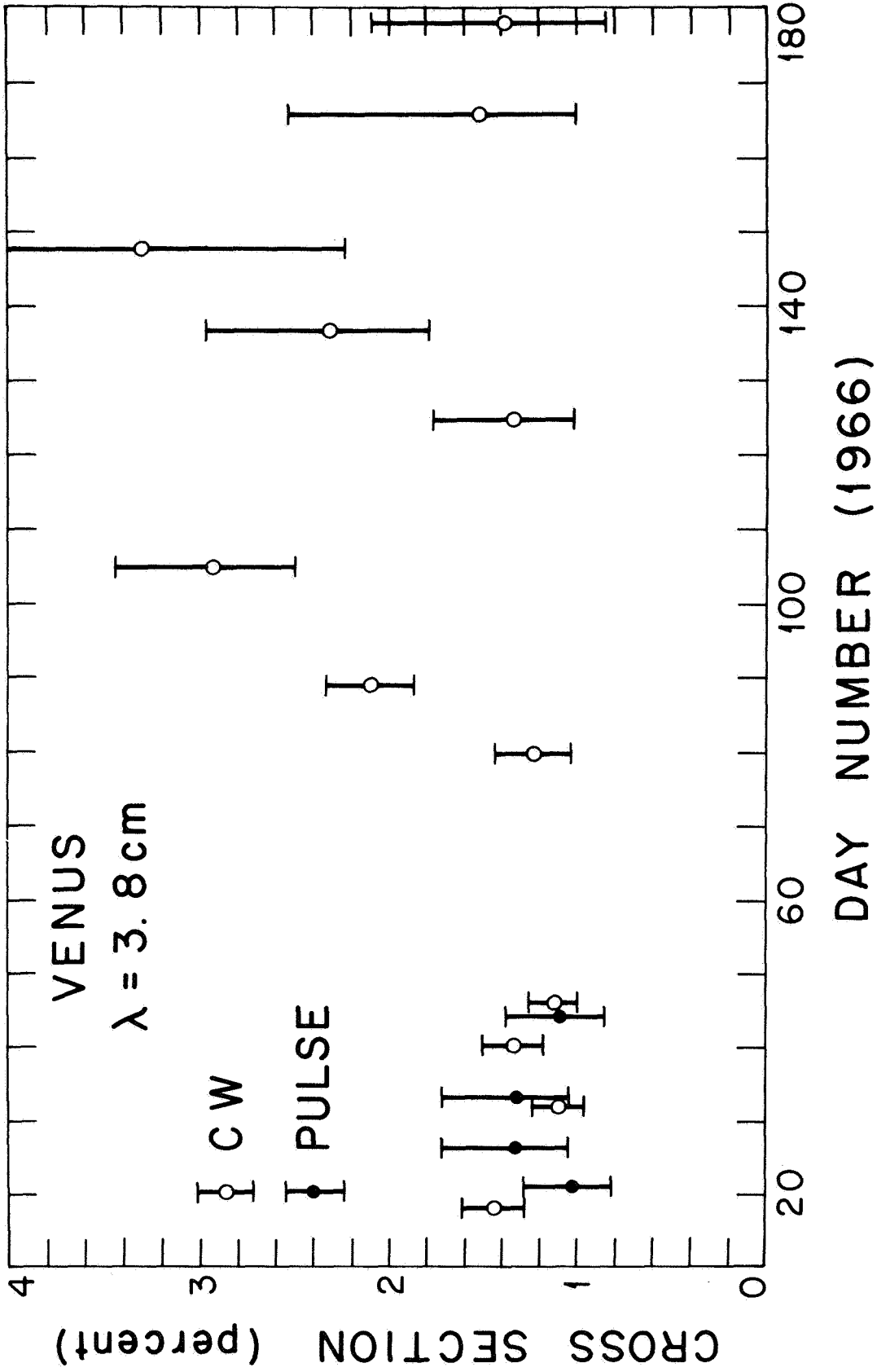


Figure 3. Cross section measurements reported by Evans, et al. (1966) at 3.8 cm.

TABLE 2

C. W. CROSS SECTION MEASUREMENTS OF VENUS AT 3.8 cm
(Evans et al. 1966)

Date	No.	Echo Power (dbw)	Flight Time (sec)	Cross Section db below πr^2	Cross Section (% πr^2)
Jan. 18	18	-181.41	274.85	-18.41	1.44
Feb. 1	32	-182.65	275.89	-19.59	1.10
Feb. 9	40	-183.48	300.54	-18.73	1.34
Feb. 15	46	-185.78	308.77	-19.56	1.11
Mar. 21	80	-194.50	557.45	-19.12	1.22
Mar. 30	89	-194.32	626.59	-16.81	2.08
Apr. 15	105	-197.22	752.89	-15.34	2.92
May 5	125	-202.70	909.02	-18.75	1.33
May 17	137	-202.33	1000.36	-16.40	2.29
May 28	148	-203.66	1082.40	-14.84	3.28
June 15	166	-207.09	1208.53	-18.07	1.56
June 27	178	-208.72	1285.56	-18.88	1.29

Radar Calibration Errors

Evans et al. (1966) estimated that the overall accuracy of the calibration of the radar is probably not better than ± 2 db. Thus, the absolute values reported may be in error by as much as $\pm 50\%$. However, the operation of the equipment was monitored sufficiently well that variations in performance larger than ± 0.5 db would not have escaped notice. Thus the relative accuracy of the measurements should not be worse than $\pm 10\%$. It follows that instrumental effects can be excluded as the prime cause of the variability shown in Fig. 3.

Signal-to-Noise Ratio Errors

The spectrum of the signals (in the presence of noise) was determined by digital spectrum analysis of the output of a 500 c/s wide channel (i.e., wider than the signal bandwidth). The output of the same channel was also analyzed when the signal was absent, and this "noise only" spectrum subtracted from the "signal-plus-noise." To remove gain differences between the two runs, the two spectra were normalized before subtraction to have the same mean value in two frequency intervals located on either side of the band occupied by the echo. This operation introduces the largest uncertainty in the determination of the echo intensity. If the combined bandwidth of the two windows is b c/s, and the duration of a run is t seconds, there will be a baseline uncertainty after subtraction of ΔT where

$$\Delta T = T_n \sqrt{2/bt} \text{ } ^\circ\text{K} \quad (1)$$

where T_n is the system noise temperature ($^\circ\text{K}$). If n runs are averaged, this becomes

$$\Delta T = T_n \sqrt{2/nbt} \text{ } ^\circ\text{K} \quad (2)$$

If the mean echo temperature over the frequency band occupied by the signal is \bar{T} $^\circ\text{K}$, then the uncertainty in the echo power is simply $\Delta T/\bar{T}$ *. Table 3 lists values of \bar{T} , T_n , b , nt , ΔT , and $\Delta T/\bar{T}$. It can be seen that the accuracy declined with time, although improvements in T_n and b were made which served to reduce ΔT . On June 15 and 27 the comparison bands were widened to the point where they occupied portions of the echo spectrum. Thus, the echo contributions from the limb region were not included in the computation of \bar{T} , and the cross section values for these two days reported in Table 2 should be increased by about 10% to allow for this effect.

*The uncertainty introduced by the stochastic nature of the signal itself has here been neglected.

TABLE 3

SIGNAL-TO-NOISE UNCERTAINTY
 IN THE 3.8 cm CROSS SECTION MEASUREMENTS
 (Evans et al. 1966)

Date	\bar{T} (°K)	\bar{T}_n (°K)	b (c/s)	nt (sec)	ΔT (°K)	$\Delta \bar{T}/\bar{T}$ (%)
Jan. 18	400.0	156	107.4	3510	0.36	0.09
Feb. 1	325.6	173	107.4	2700	0.47	0.14
Feb. 9	213.5	185	179.7	4200	0.30	0.14
Feb. 15	105.2	237	179.7	2400	0.51	0.48
Mar. 21	8.89	209.7	93.7	3240	0.54	6.0
Mar. 30	9.28	119.2	93.7	5670	0.16	2.1
Apr. 15	4.51	123.1	93.7	5250	0.25	5.5
May 5	1.28	121.6	93.7	5400	0.24	18.9
May 17	1.39	127.4	93.7	8000	0.21	14.9
May 28	1.02	197.5	93.7	7560	0.33	32.4
June 15	1.23	126.5	250	7248	0.14	10.8
June 27	0.83	114.0	250	6425	0.09	11.0

Table 3 shows that the uncertainty in the signal-to-noise ratio cannot have contributed to the day-to-day variability to a greater extent than variations in system performance. These two sources combined would be expected to introduce an rms fluctuation of the order of 45% at most. This is far less than the fluctuation observed (Fig. 3).

CORRECTIONS FOR TERRESTRIAL ABSORPTION AND POINTING ERROR

Two corrections were applied to the values of echo power (Table 2) in order to obtain the values for the cross section given. The first of these took account of the fact that the true and apparent positions of Venus differed. That is, the direction to which the antenna should be pointed to place the greatest amount of transmitter power on the surface is not precisely the same as that for receiving the largest echo signal owing to the motion of Venus. In the early measurements the antenna was maintained pointing in the apparent position, and although the apparent motion of Venus was greatest at this time, the flight time was sufficiently short that the pointing error so introduced was negligible. Later, by pointing at the apparent position the effective gain in the "transmit" interval was reduced. An estimate of this reduction was made from the antenna beam pattern and the angular separation between the true and apparent positions. The largest correction that was necessary to apply due to this effect was 0.5 db (Table 4) and the accuracy of this correction is judged to be better than ± 0.2 db.

Atmospheric attenuation occurs in the earth's atmosphere even in fine weather. The one-way attenuation with the beam in the zenith is at most 0.1 db and at the zenith distance for which most of these measurements were made would be ≤ 0.2 db (Evans et al. 1966). Thus, the two-way loss would be ≤ 0.4 db. This correction was not applied to the results listed in Table 2. On some days observations were carried out during rain or heavy snow and the increased terrestrial atmospheric absorption present was reflected in higher system noise temperatures T_n . Corrections for the additional loss on these days were obtained as follows. The mean of the system temperature values encountered on fine days \bar{T}_n was obtained and the system temperature observed during bad

weather then used to compute the loss L from

$$T_{\text{sky}} (1-L) + T_{\text{R}}L + \bar{T}_{\text{n}} = T_{\text{n}} \quad (3)$$

where T_{sky} is the radio temperature of the sky background at this wavelength (taken to be 5°K) and T_{R} is room temperature (taken to be 270°K). This is not a very satisfactory procedure and can be criticized on a number of counts. The proper way to proceed would be to determine the atmospheric extinction directly by observing the apparent cross section as a function of zenith distance.

TABLE 4

CORRECTIONS APPLIED TO THE 3.8 cm CROSS SECTION MEASUREMENTS
FOR ATMOSPHERIC ATTENUATION AND POINTING ERROR

(Evans et al. 1966)

Date	Pointing Correction		Atmospheric Correction		Total Correction	
Jan. 18	0	db	0	db	0	db
Feb. 1	0	db	0	db	0	db
Feb. 9	0	db	0.2	db	0.2	db
Feb. 15	0	db	1.2	db	1.2	db
Mar. 21	0.1	db	0	db	0.1	db
Mar. 30	0.2	db	0	db	0.2	db
Apr. 15	0.2	db	0	db	0.2	db
May 5	0	db	0	db	0	db
May 17	0.45	db	0	db	0.45	db
May 28	0.5	db	1.3	db	1.8	db
June 15	0	db	0	db	0	db
June 27	0	db	0	db	0	db

An examination of the data has been undertaken in order to attempt this. Unfortunately, the signal-to-noise ratio of the runs taken beyond March 30 is too poor to permit one to detect small changes in cross section from run to run. Prior to this date the elevation of Venus was low ($\sim 30^\circ$) and data taking generally stopped when the elevation fell to 20° . Thus, the range of zenith distances over which observations were made is small. A further difficulty is that the system temperature T_n varied with zenith distance, but was not usually measured at frequent enough intervals to permit the cross section to be determined accurately for individual runs. (This follows because the value of T_n assumed for the baseline determines the overall calibration of the signal spectrum.) Figure 4 shows an attempt to obtain a relation between the echo temperature and the zenith distance for February 9. Two sets of points are shown. The open circles represent values obtained by assuming a constant value of T_n (taken to be the mean of all the measured values). The closed circles (thought to be more accurate) represent values obtained by taking estimates of T_n for each run (obtained by reasonable extrapolation through the measured values). A similar attempt with the data of March 30 is presented in Fig. 5. The straight lines shown in Figs. 4 and 5 have been fitted by eye. That shown in Fig. 4 implies a two-way zenithal absorption of 0.44 db and Fig. 5 some 0.56 db. The uncertainty in the value derived for March 30 is considered far larger than that for February 9 in view of the wider scatter of the points (Fig. 5).

R. Allen (1967) has examined the variation of the intensity of a number of radio sources observed with the Haystack antenna as a function of zenith distance χ . Each measurement was corrected for the atmospheric extinction according to a theoretically obtained dependence.

$$F = F_0 \exp (-.025 \sec \chi) \quad (4)$$

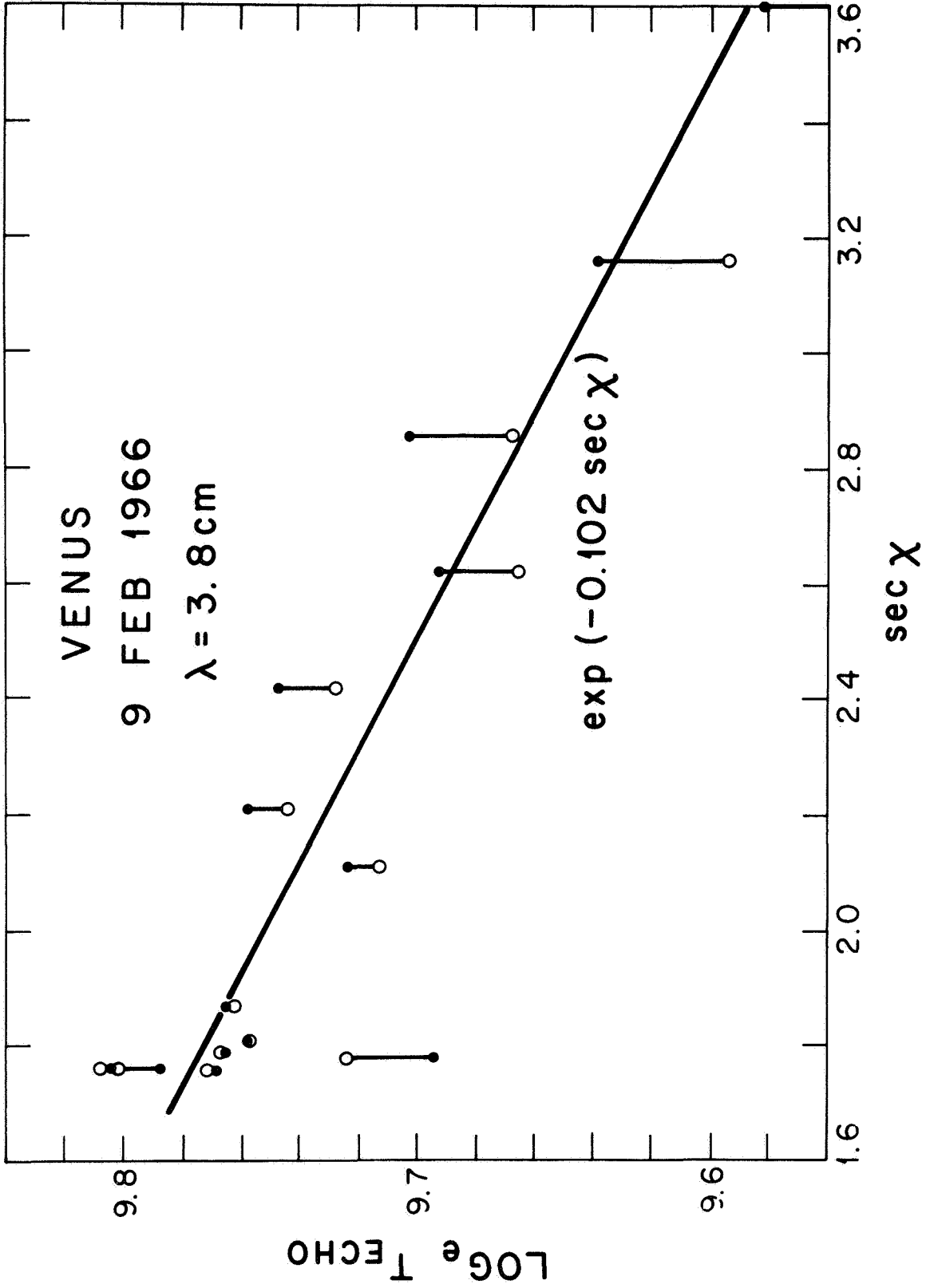


Figure 4 Variation of the equivalent echo temperature of Venus at 3.8 cm with zenith angle χ on Feb. 9, 1966. Open circles represent values obtained assuming a constant receiver temperature. Closed circles are values based upon estimates of how the receiver temperature varied with zenith distance and should be more accurate.

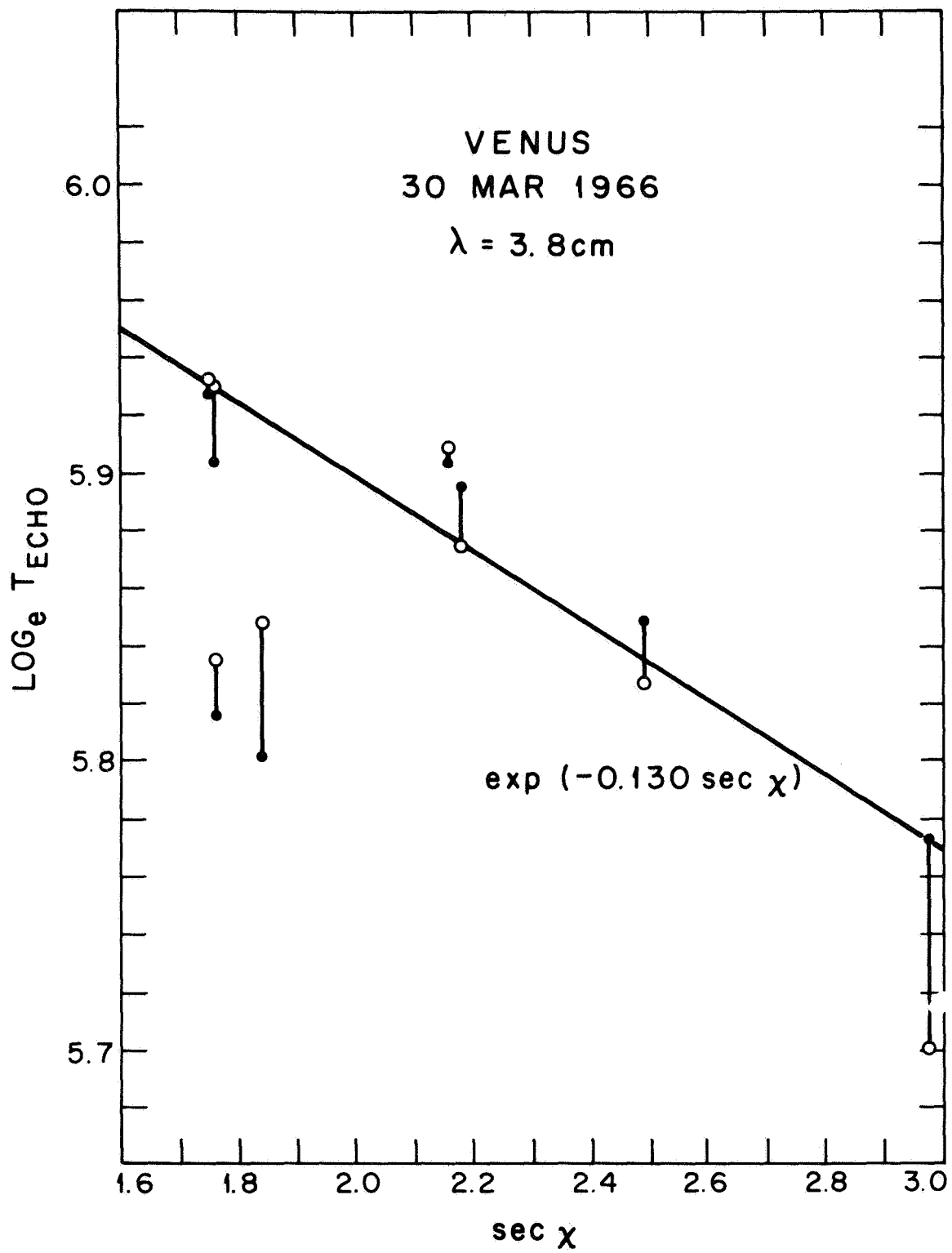


Figure 5 Variation of the equivalent echo temperature of Venus at 3.8 cm with zenith angle on March 30, 1966.

where F is the observed flux and F_0 would be the flux in the absence of atmospheric attenuation. According to this law the one-way zenithal absorption is 0.055 db. When the corrected values of flux were plotted against χ a residual variation was found which was attributed to variation in the antenna gain. Figure 6 shows the dependence in the observed gain G as a function of the elevation angle between 20° and 40° . Allen's results imply that over this elevation range

$$G = G_0 \exp (-.0256 \sec \chi) \quad (5)$$

The similar dependence of this expression to that for atmospheric extinction (Eq. 4) suggests that the latter effect may have been underestimated.

The antenna gain employed in the radar equation in order to reduce the observed echo power to a radar cross section was established from observations at high elevations. Thus these two expressions should be combined, and allowing for the two-way nature of both effects we would expect the radar cross section to vary as

$$\sigma = \sigma_0 \left[\exp (-0.101 \sec \chi + 0.051) \right] \quad (6)$$

This is close to the law determined empirically (Figs. 4 and 5). Since most of the radar observations of Venus were conducted at a zenith distance of $\sim 60^\circ$ ($\sec \chi = 2$) we believe that the values reported in Table 2 are systematically low by approximately 0.8 db.

Adopting an average value of 0.11 db for the one-way attenuation we can estimate that the atmosphere contributes some 6.7° to the system temperature T_n even under fine conditions. This is sufficiently small that the expression employed to derive the correction for atmospheric extinction (Eq. 3) in wet weather is probably not seriously in error. In retrospect, however, it seems unwise to apply large corrections to the result in view of the

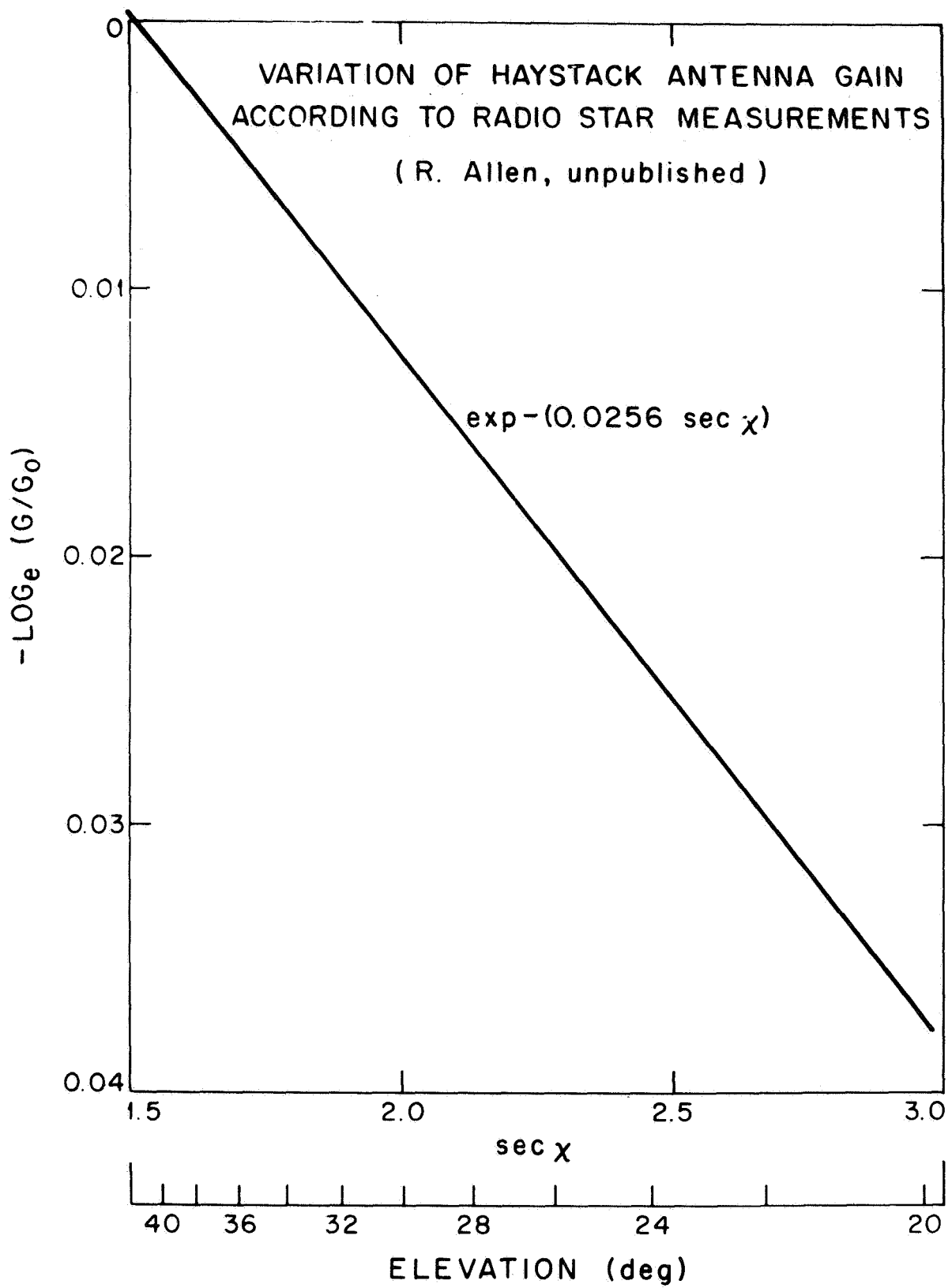


Figure 6 The variation of the gain of the Haystack antenna with elevation angle according to radio star observations (Allen, 1967).

cumulative effect of errors in T_n . If by chance an erroneously high value of T_n is measured, then a cross section will be derived which is correspondingly high. This will then be scaled by a factor to allow for atmospheric attenuation which is also an overestimate. Accordingly, it seems best to discard the values reported for February 15 and May 28, and Table 5 presents a revised list of cross sections in which this has been done. In this table a correction of 0.8 db has uniformly been applied to the results to allow for the combined effects of atmospheric extinction and gain degradation.

TABLE 5

REVISED VALUES FOR THE CROSS SECTION AT 3.8 cm

Date	Uncorrected Value (db below πr^2)	Atmospheric Correction (db)	Corrected Value (db below πr^2)	(% πr^2)
Jan. 18	-18.41	-0.8	-17.61	1.74
Feb. 1	-19.59	-0.8	-18.79	1.32
Feb. 9	-18.73	-0.8	-17.93	1.61
Mar. 21	-18.32 ⁽¹⁾	-0.8	-17.52	1.77
Mar. 30	-16.81	-0.8	-16.01	2.51
Apr. 15	-15.34	-0.8	-14.54	3.50
May 5	-18.75	-0.8	-17.95	1.60
May 17	-16.40	-0.8	-15.60	2.75
June 15	-17.57 ⁽²⁾	-0.8	-16.77	2.10
June 27	-18.38 ⁽²⁾	-0.8	-17.58	1.75

(1) Revised value; allows for 0.8 db estimated additional waveguide loss on this day.

(2) Revised value; allows for 0.5 db reduction in cross section due to narrow bandwidth.

Longitude Variation

Table 5 contains three large values (March 30, April 15, and May 17). The mean of the remainder is $0.017 \pi r^2$. Thus the largest increase is of the order of 100%. Similar increases have been observed at decimeter wavelengths (Figs. 1 and 2). Fig. 7 compares some of the values listed in Table 5 with the cross section observed at 23 and 70 cm (Fig. 2). The data are too sparse to draw any firm conclusions, but we do notice that the first increase in the 3.8 cm cross section occurred roughly at the longitude for which the decimeter cross section appears to be highest. In conclusion, we believe that cross section variations of a factor of two do occur at 3.8 cm wavelength, but it is impossible to decide from the foregoing whether these result from changes in the absorption by the atmosphere of Venus or from variations in the surface reflectivity.

A MAJOR SURFACE FEATURE ON VENUS

The spectra obtained for Venus near inferior conjunction by Evans et al. (1966) at 3.8 cm were carefully examined in order to obtain the mean scattering function. Subsequently the spectra were not examined in any great detail though Evans et al. (1966) observed a tendency for them to become asymmetrical prior to an increase in the cross section.

Fig. 8 shows the average echo spectrum observed on March 21 together with the mean curve expected based upon earlier observations. Difficulties were encountered with the doppler tuning on this day, and the echo power to the right of the expected curve was thought to result from instrumental smearing. Figure 9 shows a spectrum obtained for the same day by combining only runs during which the doppler compensation was known to have been applied correctly. A large feature can be seen on the approaching

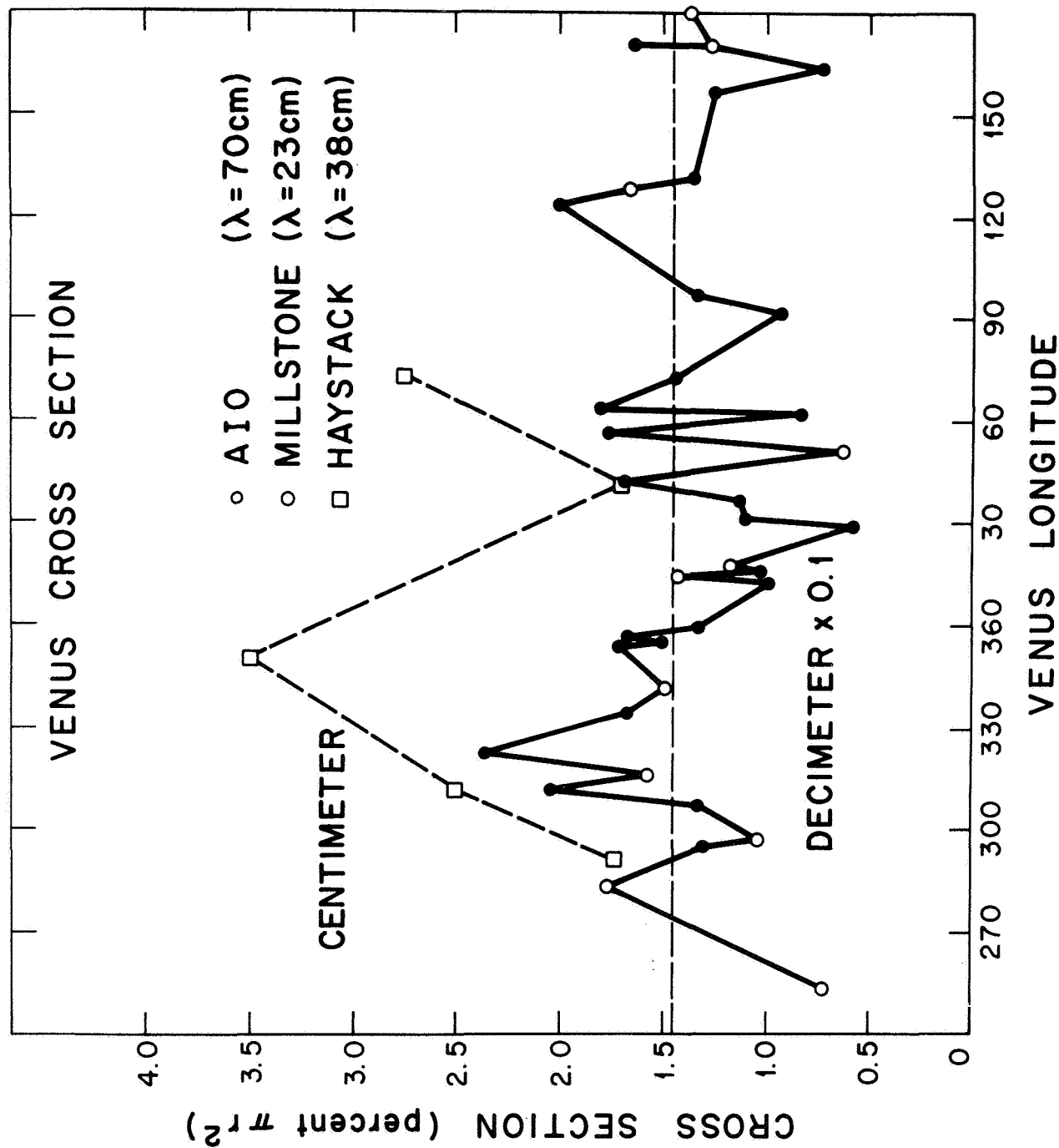


Figure 7 Comparison of the decimeter cross section measurements (Fig. 2) scaled by a factor 1/10 with revised values obtained at 3.8 cm (Table 5).

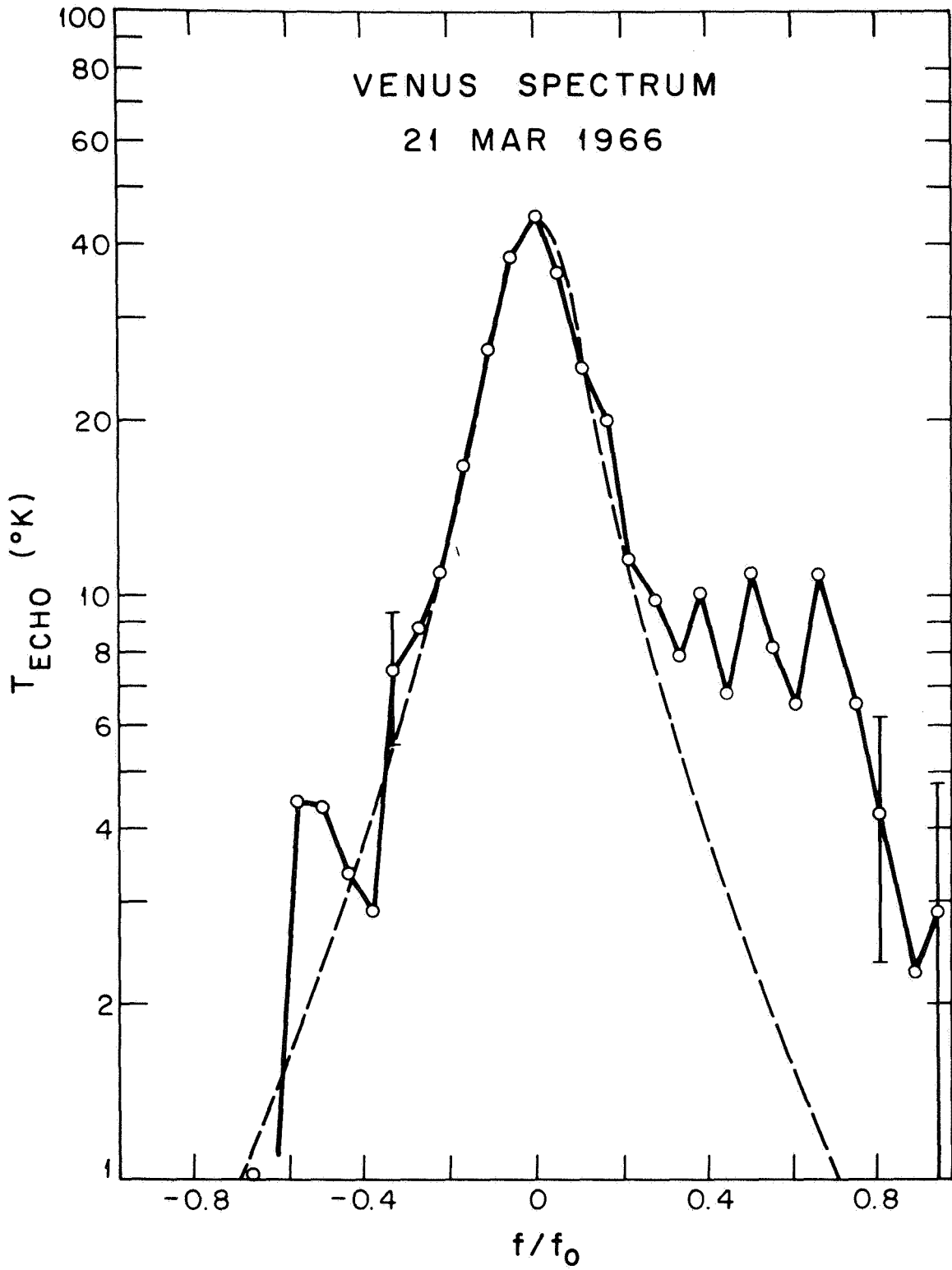


Figure 8 Spectrum of Venus signals March 21, 1966.

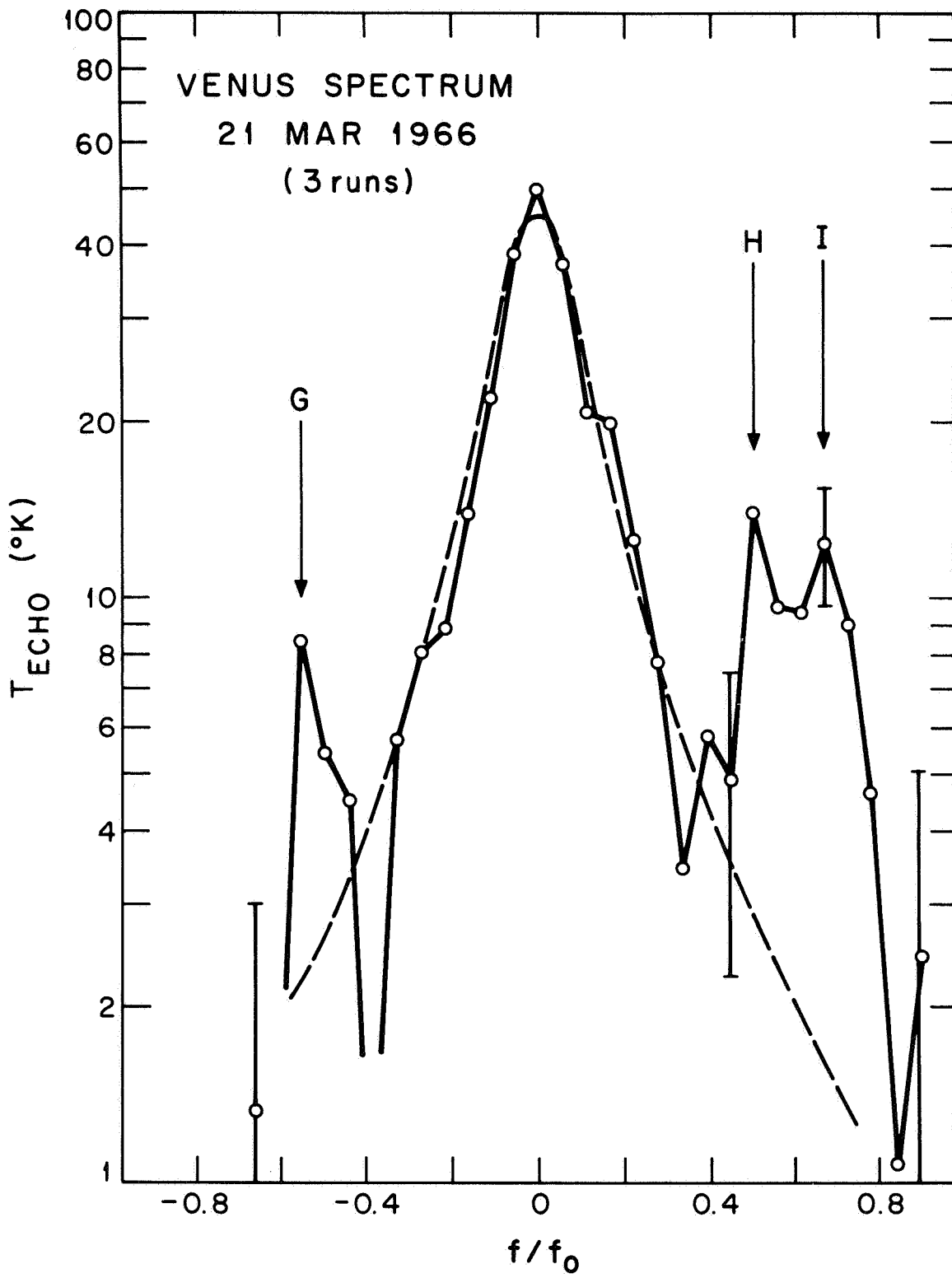


Figure 9 Spectrum of Venus signals March 21, 1966, with runs in which doppler tracking was believed poor removed.

limb and one on the receding limb. The latter can be identified with G of Carpenter's list, while the former has here been labeled H and I at the points of greatest intensity. On March 30 (Fig. 10) the approaching feature had moved to within 10° of the subradar point and extended westwards to at least 20° in longitude and possibly further. By April 15 (Fig. 11) the identifiable peaks H and I lay on the receding limb. Based upon the assumption that the regions responsible for these reflections lie close to the equator, we find that they move in the expected manner. The longitudes obtained for the two peaks are $H = 332 \pm 1^\circ$; $I = 322 \pm 1^\circ$.

It is possible to compute what contribution these features make to the total cross section assuming that the area beneath the broken curve corresponds to the mean value of $.017\pi r^2$. The increases are, respectively, 12, 36 and 35% for March 21, 30 and April 15. The cross sections measured (Table 5) correspond to increases of 5, 60, and 100% above the mean. In the case of April 15 the proper position of the expected curve is by no means obvious, and it is possible that it should be lower than shown, thereby reducing the above discrepancy. Such might be the case, if (as seems likely) the feature extends a further 20° westward beyond I. In this event the feature would occupy a 40° region in longitude and be considerably longer even than the complex region β discovered by Goldstein (1965).

In the case of March 30 the difference in the cross section derived directly and by comparison with the mean curve is 0.7 db which is certainly within the experimental accuracy expected.

In sum, it seems that the increase in cross section observed early in April is associated with the appearance of a large feature on the disc of Venus. When sufficiently removed from the region of the subradar point the increase in cross section is probably attributable to the increased power contributed by this feature. It follows that we cannot hope for perfect

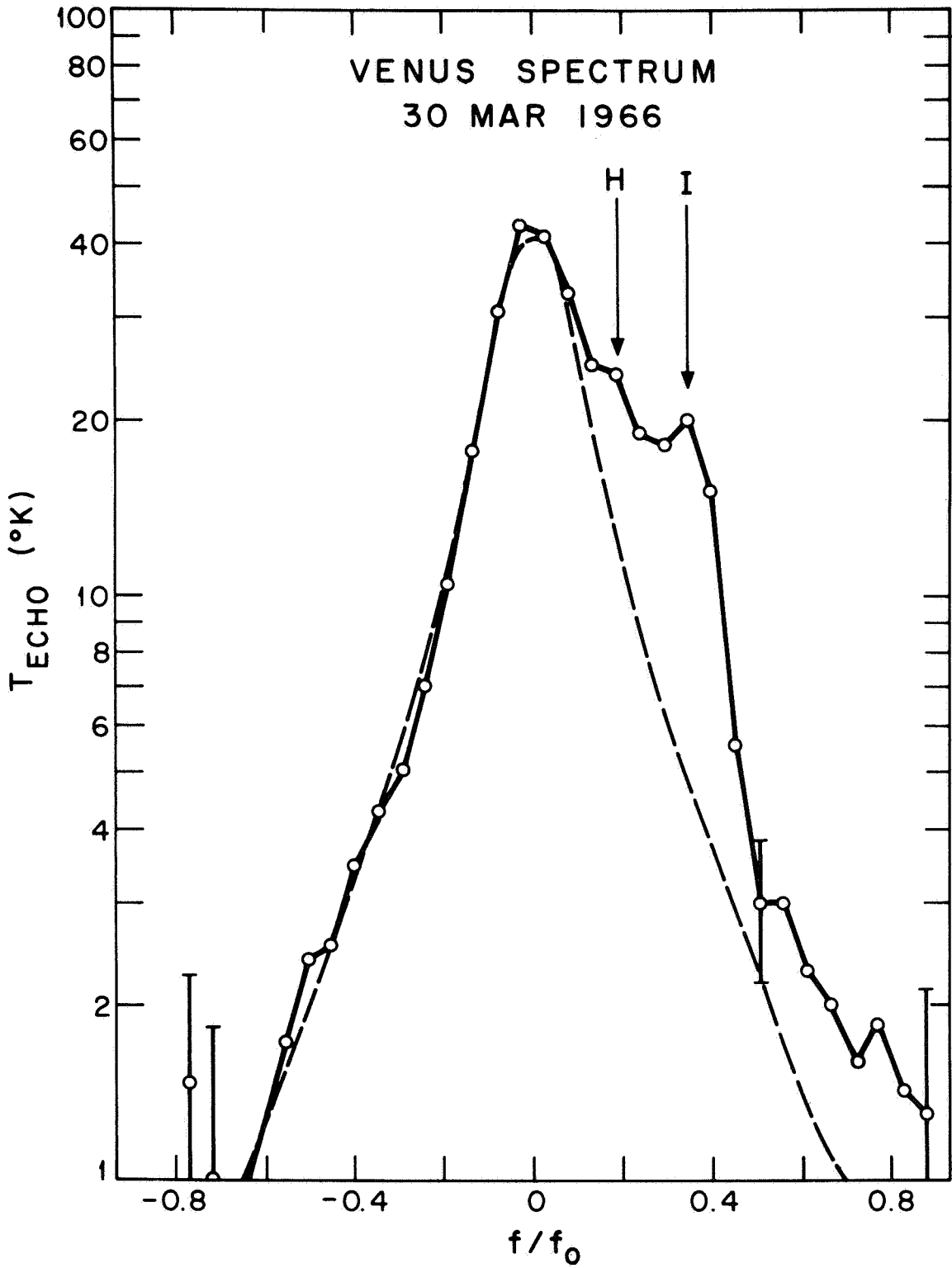


Figure 10 Spectrum of Venus signals March 30, 1966.
C-26

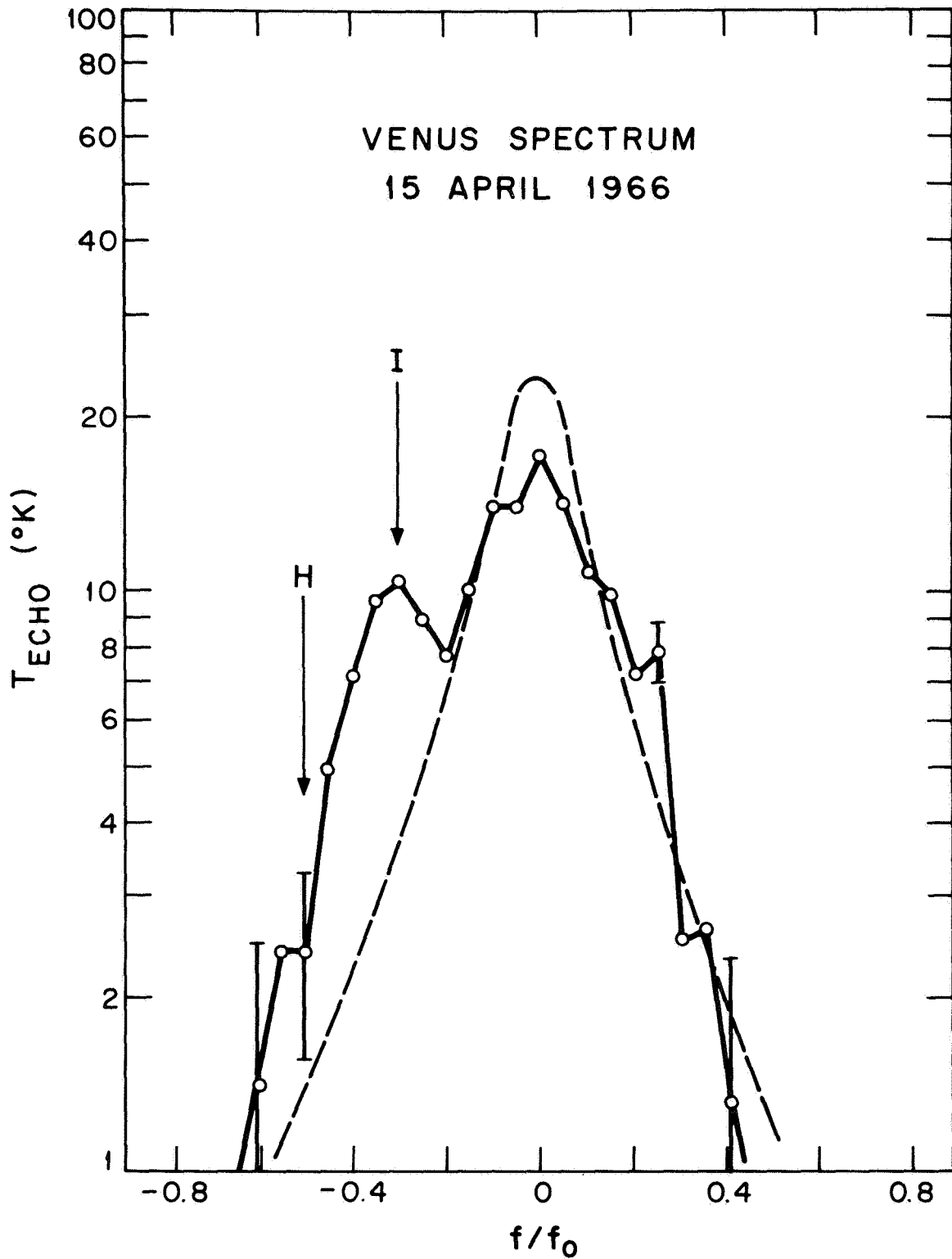


Figure 11 Spectrum of Venus signals April 15, 1966.

correlation between the results of the decimeter and centimeter measurements compared in Fig. 7. In the pulse-type decimeter measurements, the amplitude of the echo attributable to the near surface was taken as a measure of the overall cross section, it being assumed that the scattering law does not change with time.

It is interesting that the highest cross section thus far reported at decimeter wavelengths occurred when the peak H lay on the meridian (Fig. 7). Thus it must be supposed that the region H has a higher reflectivity than average. Yet we are also required to make region H rougher than average in order to account for why--relative to its environs--it gets brighter the further it lies from the center of the disc (Figs. 9-11). The increase in cross section observable at 3.8 cm wavelength may result from reflectivity and roughness variations and/or height variations of the surface resulting from changes in the atmospheric absorption. Precise cross section measurements at two wavelengths together with accurate range measurements should help to resolve this question.

SUMMARY

Variations of the cross section of Venus have been reported by a number of observers (Table 1). Because of its long rotation period with respect to the earth (~ 5 months) it has been difficult to construct a reflectivity vs longitude plot for Venus corresponding to those now available for Mars. Difficulties arise in maintaining the performance of the radar constant (or at least known) and from the large variation in the absolute signal strength due to range changes. Figure 2 represents a first crude attempt at such a plot and includes data obtained at 23 and 70 cm. Much of the fine structure in Fig. 2 must be spurious since the region from which 50% of the echo power is returned occupies some 15° in longitude, and thus there should be good correlation over longitude intervals of half this amount.

Variations in the cross section are to be expected depending upon the roughness of the terrain occupying the subradar region. Direct observations of roughness changes are available from scattering law measurements (Evans et al. 1965) and from the detection of anomalous scattering regions on the surface (Carpenter, 1966), some of which appear to move through the subradar point. Increasing the roughness at the subradar point can readily account for a reduction in the cross section by a factor of 2. An increase in the cross section must largely be caused by increased reflectivity.

Measurements at 3.8 cm by Evans et al. (1966) have been re-examined in this paper. The possible sources of error in these measurements were discussed and it was concluded that attenuation in the earth's atmosphere and degradation of the antenna gain with zenith distance were the most serious of these. As a result, two of the measurements were discarded and the remainder were revised upward (Table 5). The revised values exhibit increases above the mean ($0.017 \pi r^2$) of the order of 100%. By examining the spectra of the signals obtained during one such instance, it was found that the increase appeared to be associated with the passage across the disk of a large anomalously scattering region, occupying approximately the longitude interval $320^\circ - 350^\circ \pm 10^\circ$. We are led to conclude, therefore, that fluctuations in the cross section at this wavelength are probably related to variations in the nature of the terrain visible to the radar (e.g., reflectivity, roughness, and perhaps height), and are not the result of weather-like phenomena in the atmosphere.

BIBLIOGRAPHY

- Allen, R. J., "Observations of Several Discrete Radio Sources at 3.64 and 1.94 Centimeters," Ph.D. Thesis, MIT, January, 1967.
- Carpenter, R. L., "Study of Venus by CW-Radar 1964 Results," *Astron. J.* 71, pp. 142-152 (1966).
- Evans, J. V., "Radar Studies of the Moon," *J. Res. Nat. Bur. Stds.*, 69D, pp. 1637-1659 (1965).
- Evans, J. V., R. A. Brockelman, J. C. Henry, G. M. Hyde, L. G. Kraft, W. A. Reid, and W. W. Smith, "Radio Echo Observations of Venus and Mercury at 23 cm Wavelength," *Astron. J.* 70, pp. 486-501, (1965).
- Evans, J. V., R. P. Ingalls, L. P. Rainville, and R. R. Silva, "Radar Observations of Venus at 3.8 cm Wavelength," *Astron. J.* 71, pp. 902-915 (1966).
- Goldstein, R. M., "Venus Characteristics by Earth-Based Radar," *Astron. J.* 69, pp. 12-18 (1964).
- Goldstein, R. M., "Preliminary Venus Radar Results," *J. Res. Nat. Bur. Stds.* 69D, pp. 1623-1625 (1965).
- James, J. C. and R. P. Ingalls, "Radar Observations of Venus at 38 Mc/sec," *Astron. J.* 69, pp. 19-22 (1964).
- Karp, D., W. E. Morrow and W. B. Smith, "Radar Observations of Venus at 3.6 cm," *Icarus* 3, pp. 473-475 (1964).
- Klemperer, W. K., G. R. Ochs and K. L. Bowles, "Radar Echoes from Venus at 40 Mc/sec" *Astron. J.* 69, pp. 22-28 (1964).
- Pettengill, G. H., R. B. Dyce and D. B. Campbell, "Radar Measurement at 70 cm at Venus and Mercury," *Astron. J.* 72, pp. 330-337 (1967).

APPENDIX D
(Report of 1967 Summer "TYCHO" Meeting, TG # 31)

RADAR OBSERVATIONS OF
VENUS AND MARS

J. V. Evans

July, 1967

Contract No. NSR-24-005-047

Prepared by

UNIVERSITY OF MINNESOTA
Minneapolis, Minnesota

For

HEADQUARTERS, NATIONAL AERONAUTICS & SPACE ADMINISTRATION
Washington, D C. 20546

RADAR OBSERVATIONS OF VENUS AND MARS

ABSTRACT

Planetary radar observations commenced in 1960 with the successful detection of echoes from Venus by groups in the U. S., U. K., and the U. S. S. R. Since then Venus has been extensively studied by radar, and similar though less extensive measurements have been made on Mercury and Mars.

Possibly of greatest utility to the space program are the revisions obtained by radar to the values for the astronomical unit, the earth-moon mass ratio, the radii of the planets and the elements of their orbits. These revisions make it possible to direct a deep-space probe to within the immediate vicinity of the planet where earlier optical data would have been grossly in error.

In addition to the improvements to planetary positions radar has provided new values for the rotation periods of Mercury and Venus, and estimates of their surface roughness and composition. In the case of Venus some information concerning the absorption of radio waves by the atmosphere has also been obtained. For Mars the reflectivity and surface elevation vs Martian longitude have been determined for a region in the Martian tropics. These quantities show interesting correlation with visual (i.e. dark) features.

TABLE OF CONTENTS

<u>Title</u>	<u>Page</u>
Introduction.	D-1
Radar Contributions to Planetary Sizes and Motions.	D-1
Size and Distance.	D-1
Orbital Elements	D-3
Rotation Rate and Pole Position.	D-3
Radar Contributions to Planetary Surfaces	D-6
Venus	D-6
Surface Material.	D-6
Surface Roughness	D-8
Surface Features.	D-11
Mars	D-17
Surface Material.	D-17
Surface Roughness	D-19
Surface Features.	D-19
Radar Contributions to Planetary Atmospheres.	D-23
Venus	D-23
Cross Section vs Wavelength	D-23
Atmospheric Scattering.	D-25
Limb Darkening	D-27
Mars	D-33
Discussion	D-33
Surface Material of Venus	D-33
Surface Material of Mars	D-34
Atmosphere of Venus	D-34
Future Work	D-35
Venus.	D-35
Mars	D-36
Bibliography	D-37

TABLE OF CONTENTS (continued)

LIST OF ILLUSTRATIONS

<u>Figure</u>	<u>Title</u>	<u>Page</u>
1	The radar cross section of Venus	D-7
2	The echo power vs delay observed for Venus at 23 cm wavelength	D-9
3	Comparison of the echo power vs delay for Venus at three wavelengths	D-10
4	Anomalous scattering regions on the surface of Venus as seen in an echo power vs delay plot . . .	D-12
5	Anomalous scattering regions on the surface of Venus as seen in echo power frequency spectra at 12.5 and 3.8 cm wavelength.	D-13
6	The doppler vs date histories of the features recognized by Carpenter (1966) and listed in Table 4.	D-14
7	The variation of the radar cross section of Mars at 70 cm and at 12.5 cm during the opposition of 1965 as a function of the central meridian of the visible disk (after Dyce, Pettengill and Sanchez, 1967).	D-18
8	Martian height profile at 21°N obtained from vertical incidence radar ranging at 3.8 cm wavelength (G. H. Pettengill, private communication)	D-21
9	The radar cross section of Venus and theoret- ical curves predicted by two simple models described in the text.	D-24
10	A spectrum of echo power for Venus at 3.8 cm wavelength	D-26
11	The echo power vs delay observed for the initial part of the return from Venus at two wavelengths .	D-28
12	Comparison of echo power vs delay at 3.8 and 23 cm wavelength	D-30
13	The mean echo power spectrum derived by Evans et al. (1966b) for 3.8 cm.	D-31
14	Comparison of the curve of Figure 13 (labelled X-band) with that obtained by Muhleman (1965) at 12.5 cm (S-band).	D-32

TABLE OF CONTENTS (continued)

LIST OF TABLES

<u>Table</u>	<u>Title</u>	<u>Page</u>
1	The Astronomical Unit and Planetary Radii . . .	D-2
2	Inverse Masses of Inner Planets and Earth-Moon Mass Ratio	D-3
3	Osculating Elliptic Orbital Elements at JED 2439340.5 Referred to Mean Equinox and Equator of 1950.0	D-4
4	Location of Anomalous Scatterers on the Surface of Venus.	D-15

RADAR OBSERVATIONS OF VENUS AND MARS

J. V. Evans*

Lincoln Laboratory#

Massachusetts Institute of Technology

July 1967

INTRODUCTION

It is the purpose of this paper to review the status of recent radar observations of the planets Venus and Mars and to point out some of the logical extensions of these radar investigations. Further experimental data and its interpretation for the planet Venus is contained in a companion paper (See Appendix C Evans, J. V., "Variations in the radar cross section of Venus" July 1967). The support of the staff of the Haystack Microwave Facility in the work described here is gratefully acknowledged. We are also indebted to Dr. Irwin Shapiro of Lincoln Laboratory whose staff kindly supplied us with the working ephemerides necessary for the taking of radar data. The work of preparing this review was performed during the course of the "TYCHO" Study Group meeting, Dartmouth College, Hanover, New Hampshire, June - July, 1967.

RADAR CONTRIBUTIONS TO PLANETARY SIZES AND MOTIONS

Size and Distance

Precise radar distance and velocity measurements have been made by a number of observers (e.g. Evans et al. 1965, 1966a Pettengill et al. 1962, 1967). These have been reduced in conjunction with appropriate optical observations of the planets (by the U. S. Naval Observatory) to yield revisions for the orbital elements of Earth, Venus and Mercury, the Earth-Moon mass ratio, the radii of Venus and Mercury and the astronomical unit

* Presently Visiting Professor, University of Illinois, Urbana, Ill.

Operated with support from the U. S. Air Force.

(Ash, Shapiro, and Smith 1967).

The methods of making precise delay and velocity measurements have been well documented by the above observers, as has the procedure by which these data have been reduced. Thus, we will merely summarize the conclusions reached in the form of Tables. Table 1 presents the most recent value for the astronomical unit (presented in light seconds) together with values for the radii of the planets Mercury and Venus.

TABLE 1 (After Ash et al. 1967)
THE ASTRONOMICAL UNIT AND PLANETARY RADII

	Newtonian	General Relativity	Formal Standard Error
A. U. (light-sec)	499.004785	499.004786	5×10^{-6}
Mercury Radius (km)	2440.0	2434.0	2.2
Venus Radius (km)	6055.5	6055.8	1.2

Two estimates are presented for two hypotheses concerning the nature of the universe. In the first it is assumed that the motion of the planets proceeds according to the laws of Newtonian gravitation, and that light propagates always as in flat space, whereas in the second the consequences of general relativity on both the motion of the planets and the interaction of the electromagnetic probing signal with the gravitational field of the sun are assumed to hold. Table 2 presents the inverse masses of the inner planets and the earth-moon mass ratio also based upon the combined radar and optical data as processed by Ash et al (1967). In both tables the formal standard errors quoted represent the internal consistency of the results, and undetected systematic errors may exist which are significantly larger.

TABLE 2 (After Ash et al. 1967)

INVERSE MASSES OF INNER PLANETS AND EARTH-MOON MASS RATIO

	Newtonian	General Relativity	Formal Standard Error
Mercury	6029000	6021000	53000
Venus	408450	408250	120
Earth and Moon	328950	328900	60
Mars	3106700	3111200	9000
Earth-Moon mass ratio	81.3024	81.3030	0.005

Orbital Elements

Although 15 years of optical data were employed in this study (Ash et al, 1967) and only a few years of radar data, the latter serve to improve the initial mean anomaly, and the orbital eccentricity, and to redetermine the semimajor axis for each planet with comparable accuracy. These results are summarized in Table 3, where only the "relativity fit" is given. Since only a few precise distance determinations of Mars have been made thus far, no results have been published for radar/optical determinations of the orbital elements of that planet.

Rotation Rate and Pole Position

The rotation rate of Mars is well known from optical observations and radar is unlikely to make any significant improvement. In the case of Venus, however, radar provides the only reliable Earth-based technique for determining the sense and rate of rotation. For this purpose several different radar techniques have been employed. Goldstein (1964) and Carpenter (1964) attempted to recognize the echo power in the frequency spectrum associated with the planet's limbs and thus obtain directly the maximum doppler broadening. This so-called "base-bandwidth" technique led to a value of 250 ± 40 days retrograde, which was later refined to 250 ± 9 days (Goldstein 1965a). A second method which takes advantage of radar "features" which are seen in the

TABLE 3 (After Ash et al. 1967)

OSCILLATING ELLIPTIC ORBITAL ELEMENTS AT JED 2439340.5
 REFERRED TO MEAN EQUINOX AND EQUATOR OF 1950.0

Orbital Element	Mercury	Venus	Earth-Moon Barycenter
Semi-major axis (a.u.)	0.387098414951 ± 1.0 x 10 ⁻⁹	0.723329859677 ± 2.1 x 10 ⁻⁹	1.000003794771 ± 7.4 x 10 ⁻⁹
Eccentricity	0.2056252616 ± 2.2 x 10 ⁻⁸	0.0067893036 ± 1.7 x 10 ⁻⁸	0.0166821414 ± 1.9 x 10 ⁻⁸
Inclination	28.6032349° ± 0.000011°	24.4665152° ± 0.0000055°	23.4435741° ± 0.0000055°
Right Ascension of Ascending Node	10.8601939° ± 0.000028°	7.9788228° ± 0.000022°	0.0004358° ± 0.000019°
Argument of Perihelion	66.9333922° ± 0.000028°	123.3336740° ± 0.00011°	102.1909785° ± 0.000039°
Initial Mean Anomaly	269.8930787° ± 0.0000083°	297.4517291° ± 0.00011°	208.7069368° ± 0.000033°

doppler broadened power spectra and which correspond to regions on the surface that reflect anomalously. Because Venus presents approximately the same face towards Earth at successive inferior conjunctions, these tend to reappear from conjunction to conjunction. Employing this "feature method" Carpenter (1966) concluded that the period lay between 244 and 254 days. Subsequently, Evans et al. (1966b) and Carpenter employed the method over two successive conjunctions to obtain a period of 244 days, to within an error of only about 1%. The most recent determination reported in the literature (Dyce et al. 1967a) is based upon combined delay-doppler mapping and yields a value of 244.3 ± 2 days (retrograde). The pole position is at declination $-66.4^\circ \pm 1^\circ$ and right ascension $90.9^\circ \pm 1^\circ$ (1960 epoch). The inclination of the axis is about 87° with respect to the orbital plane of Venus and approximately 90° with respect to the plane of the Earth's orbit (i.e., the ecliptic). The coincidence of these results (i.e., the axis inclination and rotational period) with the theoretical orientation and period (of 243.16 days) which would result were the Earth's orbit to control the rotation of Venus through an interaction with a permanent dipole moment of that planet is remarkable. In the event this locking proves to exist, Venus would, on average, just complete 4 axial rotations between inferior conjunctions as seen by a terrestrial observer. The length of a Venus "day," i.e., the rotation period with respect to the Sun, corresponds to about 177 Earth days.

The rotation period of Mercury was long thought to be close to 88 days, i.e., equal to its orbital period. Delay-doppler measurements (Pettengill and Dyce, 1965), however, showed that the period is more nearly $59 (\pm 3)$ days, and that Mercury, therefore, executes $3/2$ axial rotations in each orbital revolution (Colombo and Shapiro, 1965). This revision is now supported by recent optical evidence (see Dyce et al., 1967a). All that can be said concerning the tilt of the pole is that it appears to be normal to the plane of Mercury's orbit to within 62° . If the planet is

truly locked, as seems highly probable, the solar day on Mercury would be 176 Earth days (i.e., just twice the orbital period, since the 3/2 resonance requires that the planet present alternate faces to the sun at successive perihelion passages).

RADAR CONTRIBUTIONS TO PLANETARY SURFACES

Venus

Surface material.- The radar cross section of Venus has been obtained at a number of wavelengths and is plotted in Fig. 1 (Evans et al. 1966b). The dotted curve has merely been put in by eye. For comparison the moon exhibits no clear wavelength dependence but has a cross section $\sigma = 7\%$ over the range $1 \text{ cm} < \lambda < 10 \text{ m}$. It is tempting to conclude that the marked dependence shown in Fig. 1 results from atmospheric attenuation (next section) though it is not impossible to construct a surface having reflection properties which would give rise to the reflection law indicated. Such a surface would, however, require careful control of the dielectric constant (both real and imaginary parts) as a function of depth, and would require a remarkable degree of horizontal uniformity, such that it seems it can be discounted as being exceedingly artificial. We cannot discount, however, the possibility that the trend shown in Fig. 1 results from a combination of atmospheric attenuation and reflection coefficient changes occurring with wavelength.

The mean of the long wave ($\lambda \geq 23 \text{ cm}$) measurements is $\sigma = 16\%$, which corresponds to a dielectric constant of $\epsilon \sim 5.5$. This value would be consistent with dry compact rocklike material and definitely excludes water as the surface covering. It is interesting to note that the reflection coefficients of the Moon, Mercury and Mars on average lie between 6% and 8%. It seems unlikely (though of course not impossible) that the surface material on Venus is entirely unlike that on the other three bodies. A more plausible argument is that Venus is distinguished by having more compact surface material than the other three. That is, it may be supposed that

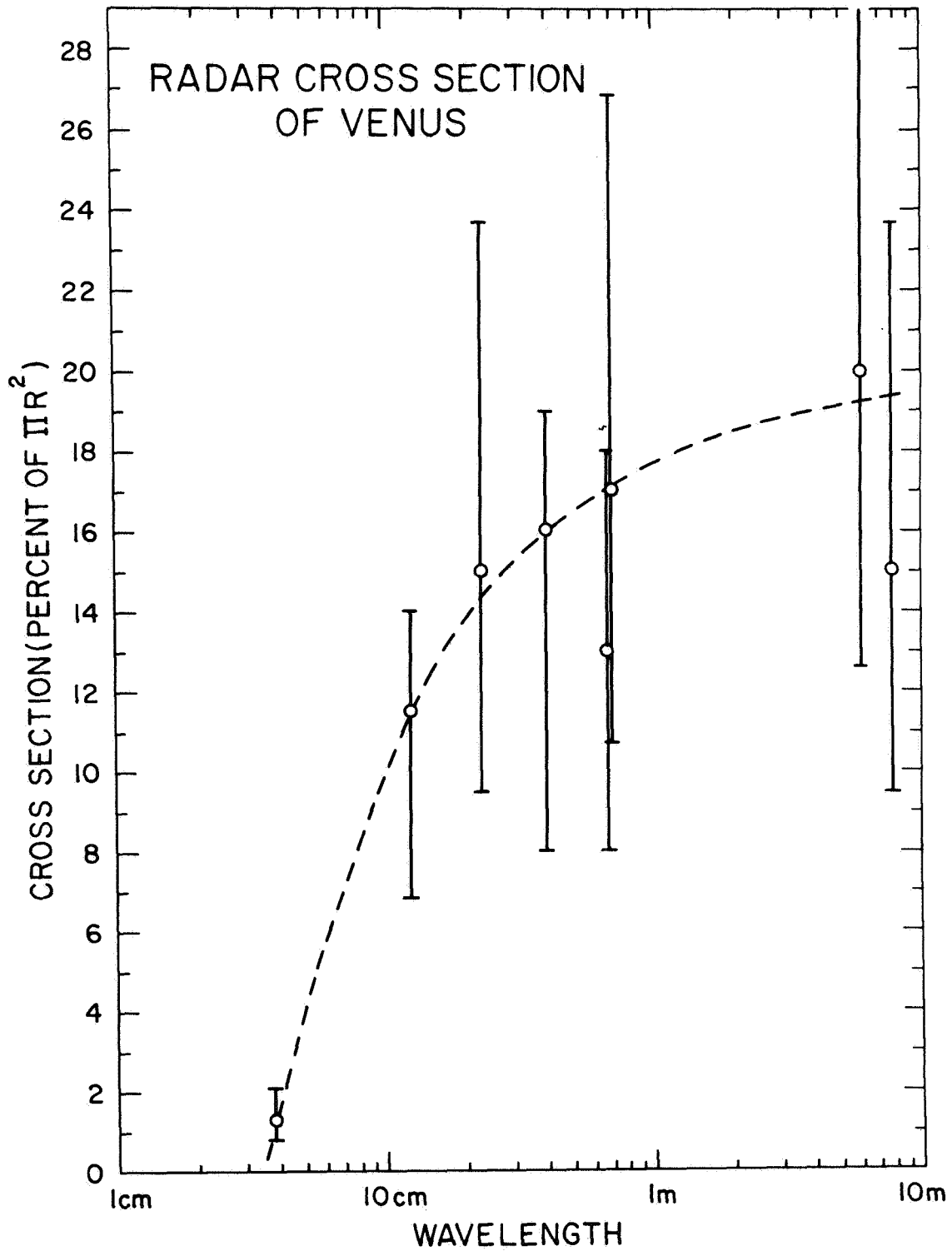


Figure 1. The radar cross section of Venus (Evans, et al. 1966b).

the surfaces of the Moon, Mercury, and Mars have been eroded (we have evidence of this in the case of the Moon and Mars) such that the surface rocks have been ground to particulate matter with a porosity of 50% or more for some considerable depth (centimeters). A corollary is that on Venus such processes are not at work or that the surface rocks melted and resolidified in the not too distant past.

Surface roughness.- The angular scattering law for Venus has been determined in different ways by a number of observers. As an example, Fig. 2 shows that the mean echo power vs delay obtained by Evans et al. (1966a). The measurements show a fall off in echo power with delay which is more rapid than that from the moon. Since the delay is related to the cosine of the angle of incidence ϕ , it is possible to replot Fig. 2 as echo power vs ϕ and regard such a plot as a spectrum of surface slopes (at least for $\phi < 30^\circ$). On this basis the mean slope obtained for Venus when averaging over-all azimuthal planes is 8.2° . The corresponding value for the moon at $\lambda = 23$ cm is 10.2° . These slopes probably correspond to intervals over the surface of the order of 10λ , or say 2 meters. When sampled over smaller intervals, the mean surface slope for the moon is found to increase and conversely when the wavelength is increased the mean slope decreases. No such clear-cut effect exists for Venus. Fig. 3 presents echo power vs delay curves similar to that of Fig. 2 obtained at 70 cm (Pettengill, 1965), 23 cm (Evans et al. 1965) and 12.5 cm (Muhleman, 1965). The observations at 70 cm and 23 cm were made directly using short pulses, whereas the 12.5 cm curve was obtained from the mean echo power frequency spectrum by an appropriate transformation (Evans et al. 1965). This difference, together with variations in the pulse lengths employed (in the case of the pulse radars) caused the resolution achieved in the region ≤ 1.0 m sec delay to differ between the three experiments. This probably accounts for most of the divergence between the curves near the origin (Fig. 3). Another factor that enters is that the scattering law actually

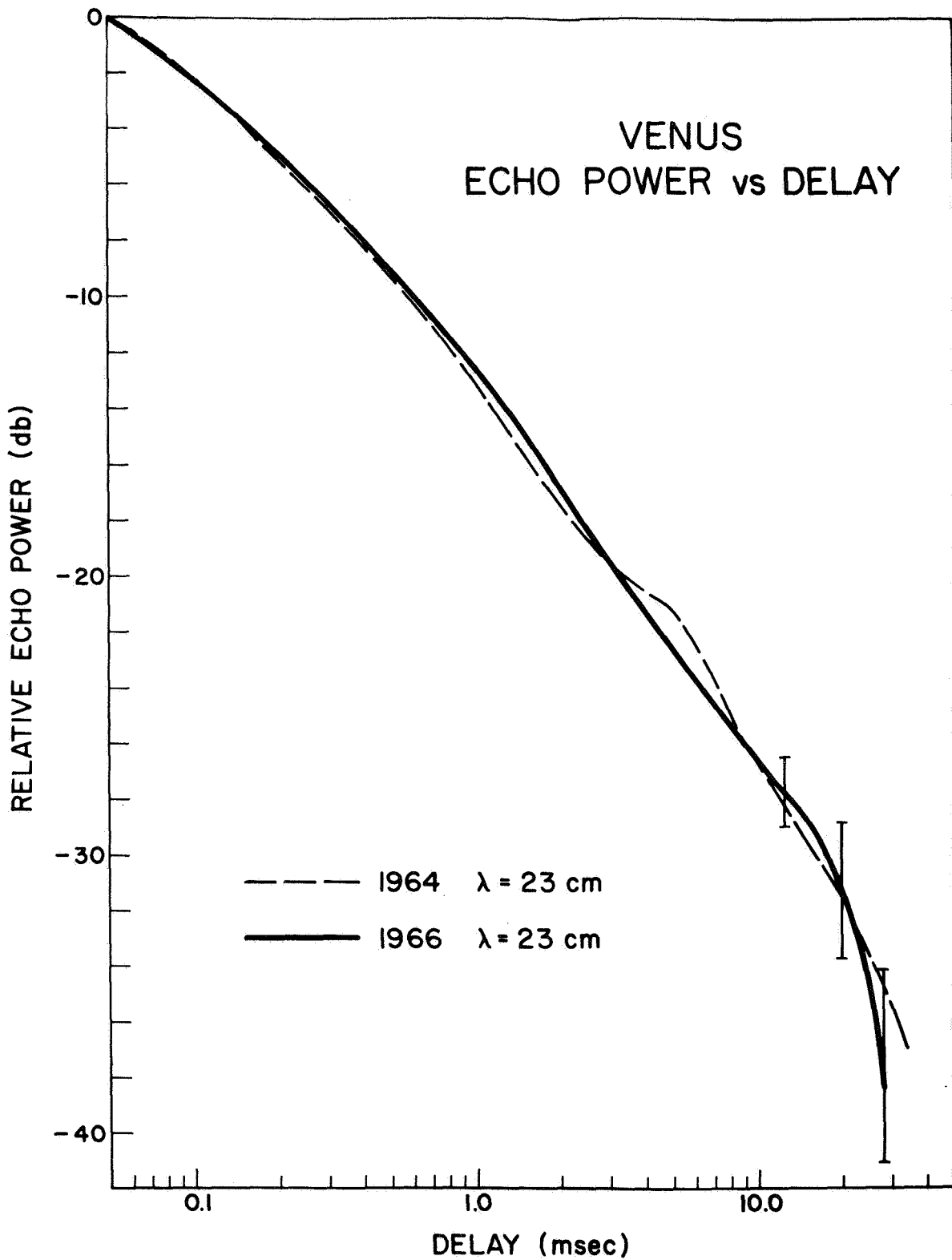


Figure 2. The echo power vs delay observed for Venus at 23 cm wavelength (Evans, et al. 1966a).

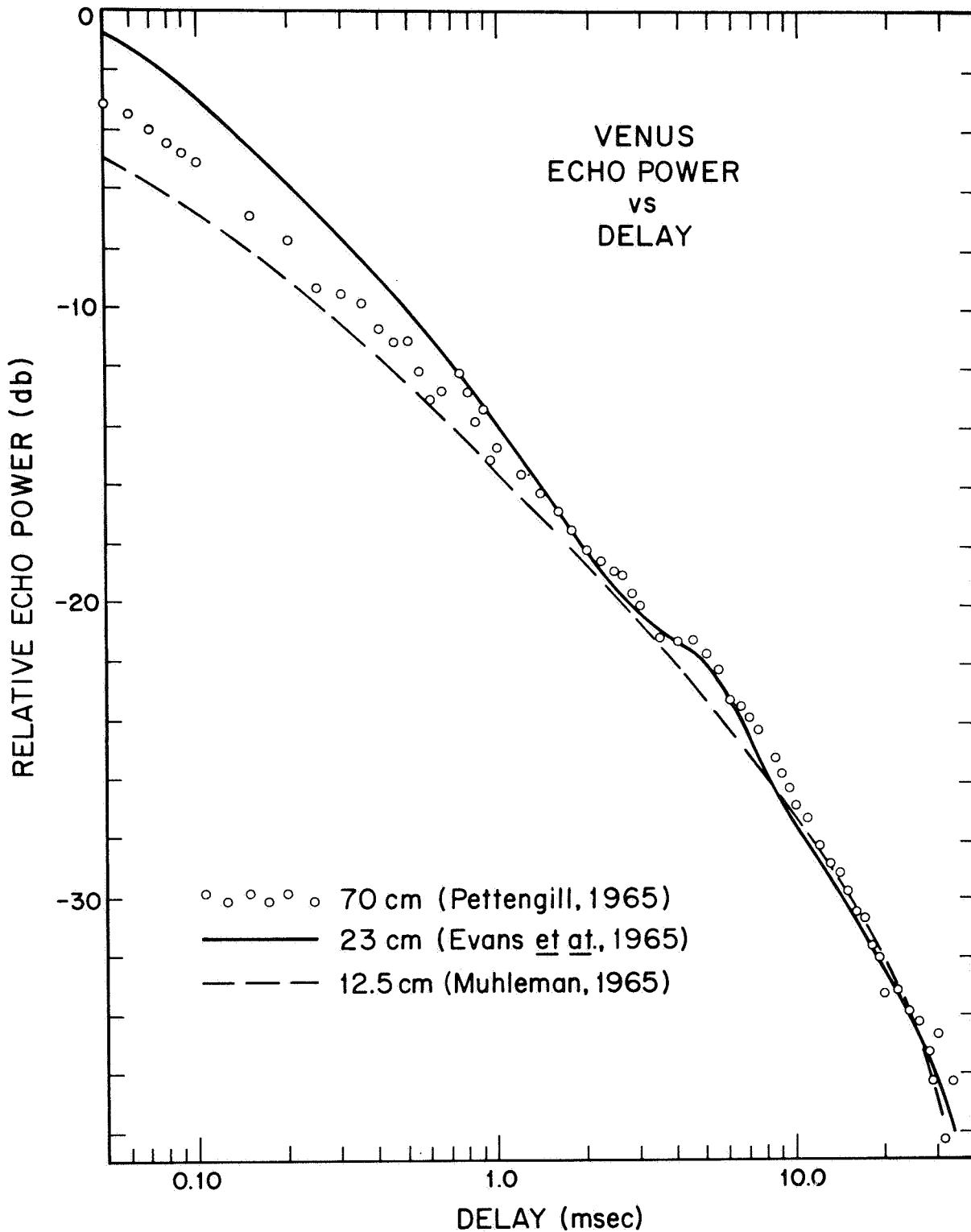


Figure 3. Comparison of the echo power vs delay for Venus at three wavelengths. The divergence of the curves for delays of less than 1 msec is believed in part to be due to differences in the range resolution achieved at the three wavelengths and in part to differences in the nature of the terrain near the subradar point when the three sets of measurements were made (Evans, et al. 1966b).

changes with time depending upon the nature of the terrain at the subradar point, and none of the curves shown in Fig. 3 represents a long-term average. Thus, it is concluded that no systematic variation of scattering has yet been established for Venus, and hence the spectrum of surface roughness (or the number or different types of surface feature) must be less than for the Moon.

At large angles ($\phi \geq 60^\circ$) the echo power has been attributed solely to surface structure having horizontal and vertical dimensions comparable with the wavelength. As such this structure can scatter into wide angles and provides the predominant scattering mechanism at grazing angles, because then so few large surface elements are tilted normal to the ray. In the case of Venus at 23 cm wavelength about 11% of the echo power is associated with these scatterers. For the moon at the same wavelength the corresponding figure is twice as much. Thus not merely are the surface elements of Venus more gently undulating than those on the Moon, they are covered to a lesser extent by boulders, small craters or comparable structure.

Surface features.— Regions on the moon--such as the rayed craters--are known to be anomalously scattering in that they are considerably brighter than their environs. Similar regions, though of unknown character, are visible in the radar returns from Venus. Figure 4 shows three such regions visible in an echo power vs delay plot such as was presented in Fig. 2. The greatest amount of attention to these features has been provided by the Jet Propulsion Laboratory (J.P.L.) group (e.g. Carpenter 1966) who have observed them as departures from the mean echo power vs frequency spectra (e.g. Fig. 5). In the early J.P.L. observations (Goldstein 1965a) only two features (named α and β) were resolved. Carpenter (1966) subsequently showed that the region β was complex and contained at least 3 revolvable features (seen on the lefthand side of Fig. 5). In all, Carpenter was able to identify some seven scattering centers and by plotting their doppler shifts vs time (Fig. 6) was able to locate them on the planetary surface (albeit with ambiguity in some cases). Table 4 presents the positions deduced for these features in a coordinate system defined by Goldstein (1965a).

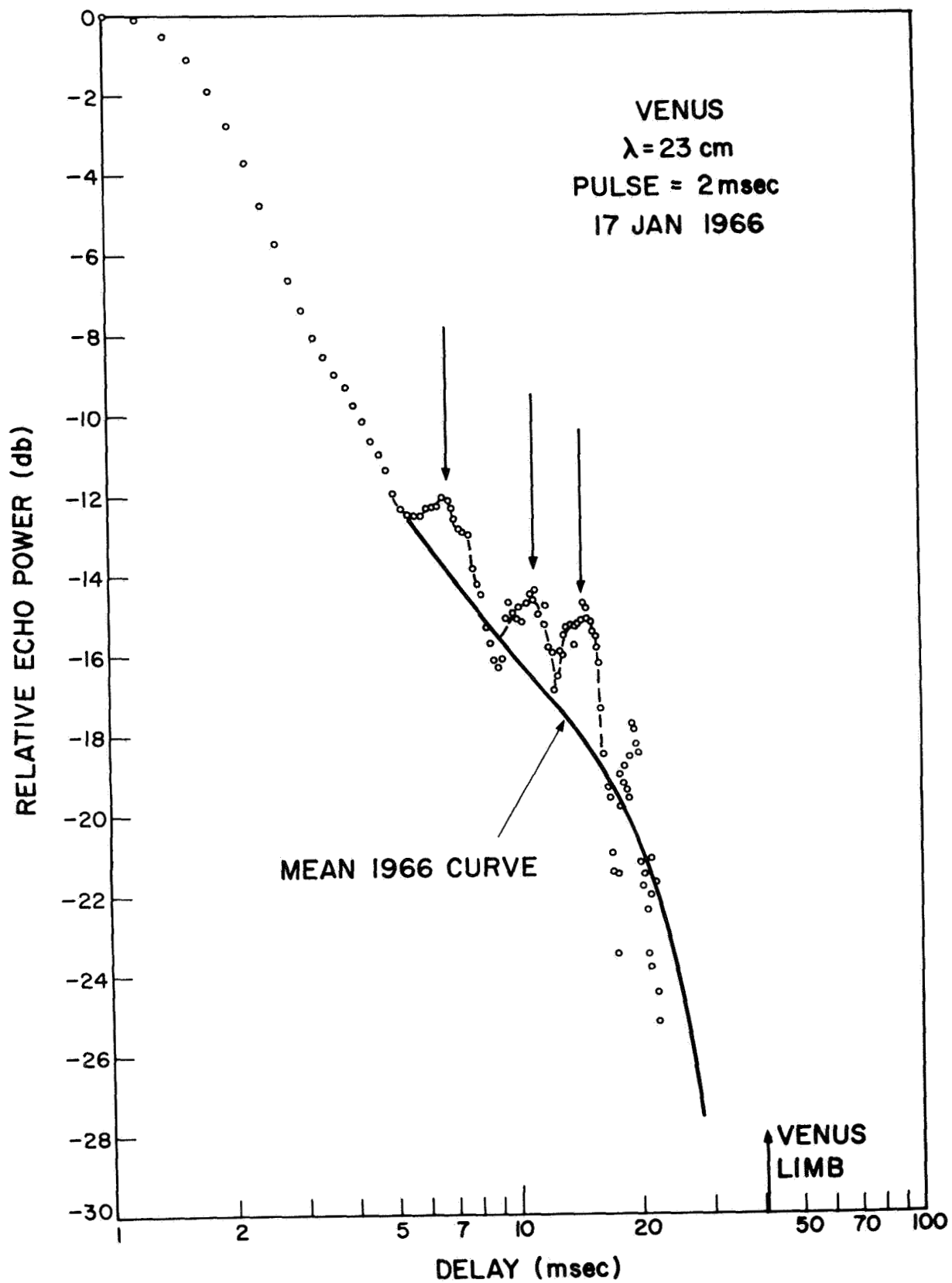


Figure 4. Anomalous scattering regions on the surface of Venus as seen in an echo power vs delay plot (Evans, et al. 1966a).

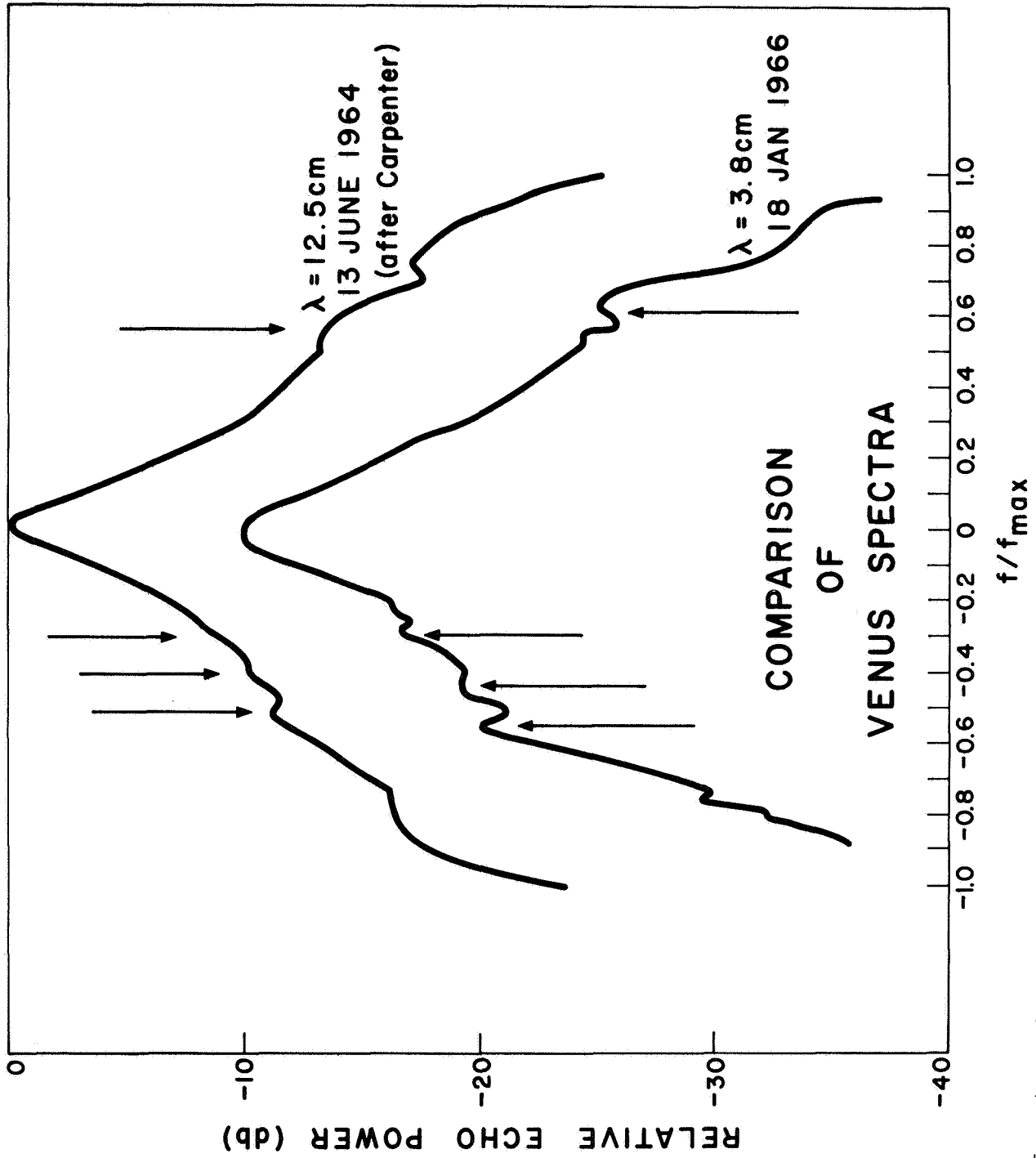


Figure 5. Anomalous scattering regions on the surface of Venus as seen in echo power frequency spectra at 12.5 and 3.8 cm wavelength. Note the near identical location of these features seen on the disk at an interval of one synodic year (Carpenter 1966a, Evans, et al. 1966b).

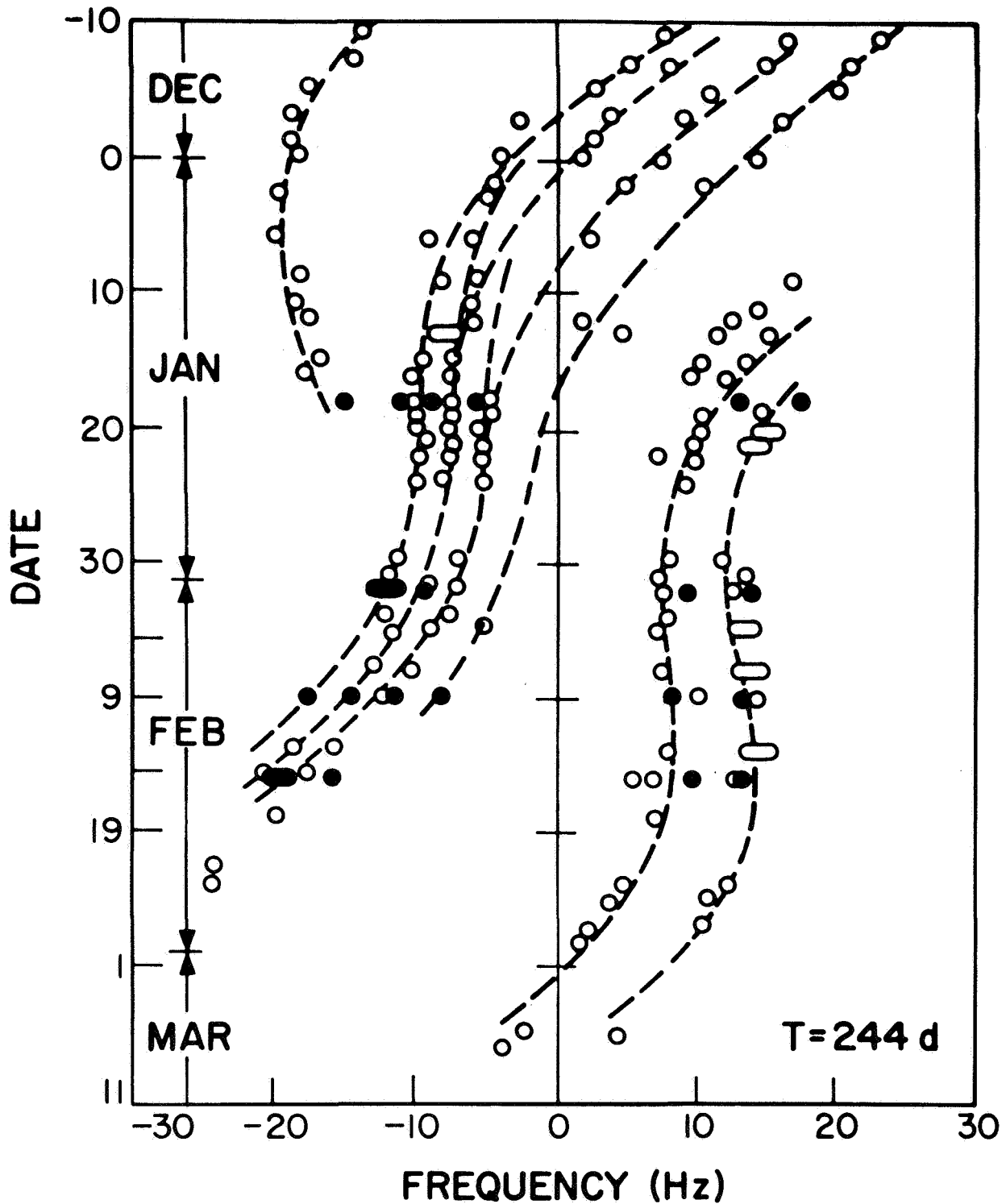


Figure 6. The doppler vs date histories of the features recognized by Carpenter (1966) and listed in Table 4. Reading from left to right at about January 18 these are A through G. Ambiguity is introduced by the blanding of the features in early January which prevents precise locations being assigned to features B through D (Carpenter 1966).

TABLE 4 (After Carpenter 1966)

LOCATION OF ANOMALOUS SCATTERERS ON THE SURFACE OF VENUS

Feature Designation		Longitude	Latitude
Goldstein (1965)	Carpenter (1966)		
	A	-108.6 ± .44	+ 6.3 ± 2.3
	B	- 78.1 ± 2.6	- 3.3 ± 8.7
	B1	- 75.8 ± .62	+11.9 ± 4.4
	C	- 68.9 ± 1.3	- 6.8 ± 5.8
β-----	C1	- 76.8 ± .63	+16.7 ± 2.1
	C2	- 70.0 ± .65	- 2.5 ± 3.7
	D	- 61.0 ± 1.8	- 1.7 ± 7.1
	D2	- 70.0 ± .65	+22.7 ± 1.7
	D3	- 60.5 ± .67	- 2.5 ± 4.1
	E	- 49.3 ± .92	+ 6.4 ± 8.5
α-----	F	00.0 ± .69	-26.7 ± 1.8
	G	+ 15.7 ± .83	-12.4 ± 2.1

In this coordinate system the prime meridian (zero longitude) was defined as the central meridian as seen on 23 July 1964, when it then passed through α . The features seen in Fig. 4 are believed to be (from left to right) F, G, and A. Those in Fig. 5 are B, C, D, and F (again reading from left to right). The feature to the right of F in Fig. 5 that is not marked with an arrow is thought to be G. It is interesting that the features are more readily observable in the depolarized echo component. This indicates that (like Tycho in the case of the moon) they cannot be explained as merely regions of anomalously high reflecting material but must also be rougher. That they seem more prominent in the 3.8 cm wavelength spectrum than 12.5 cm (Fig. 5) would be consistent with this, but one could also explain this as a consequence of a height difference between these regions and their environs. If the anomalous regions were mountains then the lower atmospheric absorption to the mountain tops would

render them brighter than their environs by a larger amount at 3.8 cm than at 12.5 cm where little absorption may be presumed to take place.

The similarity of the spectra shown in Fig. 5 is one argument to discount the possibility that the 3.8 cm echo arises from scatterers in the atmosphere. Since features are seen in the spectra at both wavelengths and these move across the disc as the planet rotates we have strong evidence that both reflections are from a solid surface.

In Fig. 5 the dotted lines represent the locus of the doppler shift (measured with respect to the center of the spectrum) of each feature as a function of date. Reading across at Jan. 18 the lines correspond to the features A through G (Table 4). The features blend between January 10 and 20 making it impossible to determine the locations of B through D unambiguously and several alternate positions are listed in Table 4. Similar work at the Arecibo Ionospheric Observatory (A.I.O.) (Dyce et al. 1967a) suggests that the feature α (Feature F of Table 4) is probably less than 900 Km in extent E-W and in excess of 3800 Km N-S and confirms that region β is complex.

In the companion paper the discovery of a major new feature is presented which is larger in longitudinal extent ($\sim 40^\circ$) than any hitherto observed. This feature lies approximately 60° to the west of feature G (i.e. at about $+76^\circ$ longitude) and hence is not observable until about 50 days following inferior conjunction. As such it has not been reported previously. This new result depends upon a more careful examination of spectra obtained by Evans et al. (1966b) and 3.8 cm wavelength using the Massachusetts Institute of Technology Lincoln Laboratory Haystack microwave facility. In the case of this extended feature there is reason to believe that it is elevated with respect to the surrounding terrain.

Mars

Surface material.-- Mars has been observed by radar at a variety of wavelengths since 1963: 70 cm by Dyce et al. (1967b), 40 cm by Kotelnikov et al. (1963), 23 cm by Evans et al. (1965), 12.5 cm by Goldstein and Gillmore (1963) and by Goldstein (1965) and at 3.8 cm by G. H. Pettengill (private communication). Unfortunately, in some of these detections the signal to noise ratio was too poor to permit a reliable cross section determination and as yet it is not possible to construct a meaningful cross section vs wavelength curve (cf. Fig 1 for Venus) for Mars. As far as can be determined the average cross section is of the order of 7 - 8% at all wavelengths--a result akin to that for the moon. This cross section implies a dielectric constant of the order of 3 suggesting that the Martian soil is unconsolidated and fairly dry.

Variations of the reflection coefficient are found at different Martian longitudes (Goldstein and Gillmore 1963, Goldstein 1965b and Dyce et al. 1967b). Fig. 7 shows a comparison of the reflectivity observed by the Arecibo (70 cm) and J.P.L. (12.5 cm) groups respectively during the 1965 opposition. The J.P.L. data have been averaged over 10° intervals of longitude, whereas the A.I.O. data have been plotted individually and then the shaded region drawn to encompass all the points.

Fig. 7 shows that there are variations in cross section of the order of 3:1. The lowest values ($\sim 3\%$) are lower than encountered for the Moon while the highest ($\sim 13\%$) are about twice that of the Moon and approach the high average value for Venus discussed above. The exact reason for these variations is not known, but the correlation of the peaks with the dark markings (Fig. 6) is conducive to speculation (e.g. Sagan et al. 1967). The different optical albedo suggests changes in surface material and hence in the intrinsic reflection coefficient. However, changes in surface roughness are also believed responsible (see below).

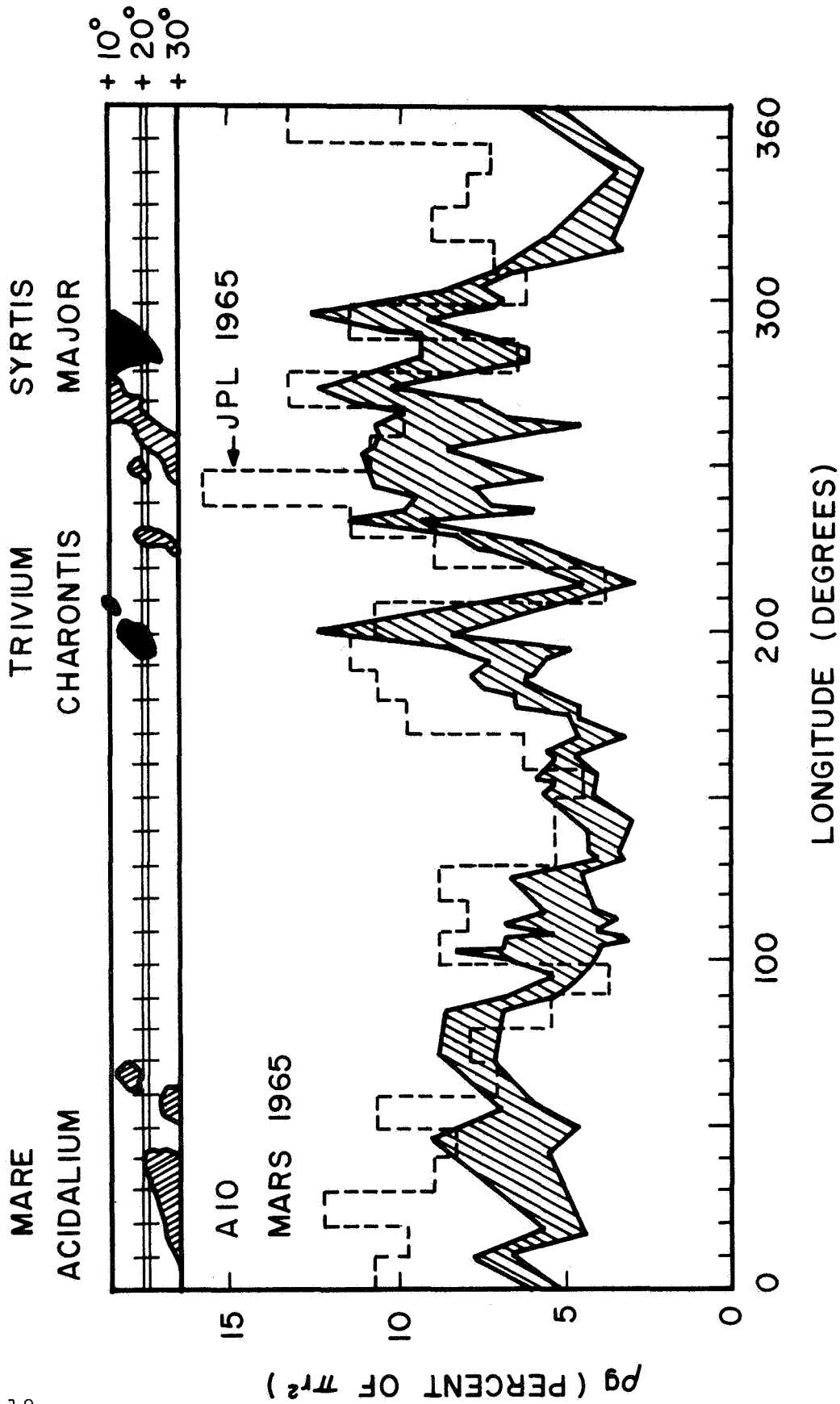


Figure 7. The variation of the radar cross section of Mars at 70 cm (Arecibo Ionospheric Observatory, shaded region) and at 12.5 cm (Jet Propulsion Laboratory, dotted line) during the opposition of 1965 as a function of the central meridian of the visible disk. A strip map appears across the top showing the principle optical features of Mars near the sub-radar latitude of 20°N. (After Dyce, Pettengill, Sanchez, 1967)

Surface roughness.- The average angular scattering law (cf. Fig. 2 for Venus) has not yet been obtained for Mars. The smaller size and higher spin rate of Mars (compared with Venus) render it a much more difficult object to study. Thus there has been adequate signal-to-noise ratio in existing experiments to examine the power spectrum (cf. Fig. 5 for Venus) of the echoes only around the peak. It is found that the spectral width is narrowest when the echo intensity is high suggesting that, in part, the increase in cross section arises as the result of an unusually smooth region occupying the subradar point. At these times the width of the spectrum indicates that the rms surface slope is of the order of only one or two degrees. This suggests reflection from a surface that has been leveled in some fashion as a salt-flat has on earth.

The average spectrum (i.e. averaging over all longitudes) is somewhat broader, but still indicates that the surface of Mars contains fewer elements than the Moon with slopes $\geq 5^\circ$. Beyond this qualitative statement little else can be said at present, and we need considerably greater sensitivity in order to measure the angular scattering law over a wider range of angles.

Surface features.- Beginning in early April, 1967, short-pulse (60 microsecond) echoes were obtained from Mars using the Haystack microwave facility at 3.8 cm wavelength (G. H. Pettengill, private communication). With this system direct measurement of the Martian topography at about 21° North latitude was possible as the planet rotated under the radar beam. The planetary rotation was sufficiently rapid that errors in the planetary ephemeris did not affect the determination of the relative heights of the distant surface. In a given night about 100° of longitude could be observed in this way. Observations spaced a week apart gave an overlap of about 40° and in every case the results from the overlapping region for the two nights agreed well.

Although the resolution offered by the use of a pulse length of 60 microseconds might appear at first glance to be only about

8 km, in most cases the bulk of the echo could be shown (from the narrowness of the early maximum) to occupy a very much smaller interval. The accuracy of the measurement was better than 1 km in almost all cases. Both the accuracy and resolution are obviously better where the signal was strong.

Figure 8 shows the results obtained (G. H. Pettengill private communication). The heights plotted are relative, of course, and the zero height is arbitrary. Eventual reductions involving an improvement in the full orbit using the methods described by Ash et al. (1967) should yield an accurate radius for Mars at the zero reference level shown here. The relative intensity of the initial echo maximum, whose location in delay yields the height information, is also indicated on the diagram by the thickness of the line traced through the observational points. The locations of the more prominent dark features at the observed latitude (21°N) are given as well as some of the traditional names for others.

Perhaps the most obvious conclusion that can be drawn immediately is that the dark regions do not correspond uniquely to elevated nor to depressed areas, at least at this latitude. This is in contrast to the conclusions reached by Sagan et al. (1967) on the basis of the J.P.L. cross section and spectral results alone. In their model the dark regions of Mars are highland areas. Such a model was originally proposed by Wells (1965) on the assumption that the lighter areas of Mars result from a layer of fine dust and that these particles preferentially settle in the lowlands. Reasoning from the slight displacements between the longitudes of the radar maxima and nearby visually dark regions, Sagan et al. (1967) conclude that the dark areas correspond to regions of the Martian surface which are elevated by some 5 to 15 km above the lighter areas. Such is not the case apparently.

It is also evident from Fig. 8 that the signal maxima occur not precisely but only approximately when the dark areas lie under the subradar point. The steepest slopes that may be

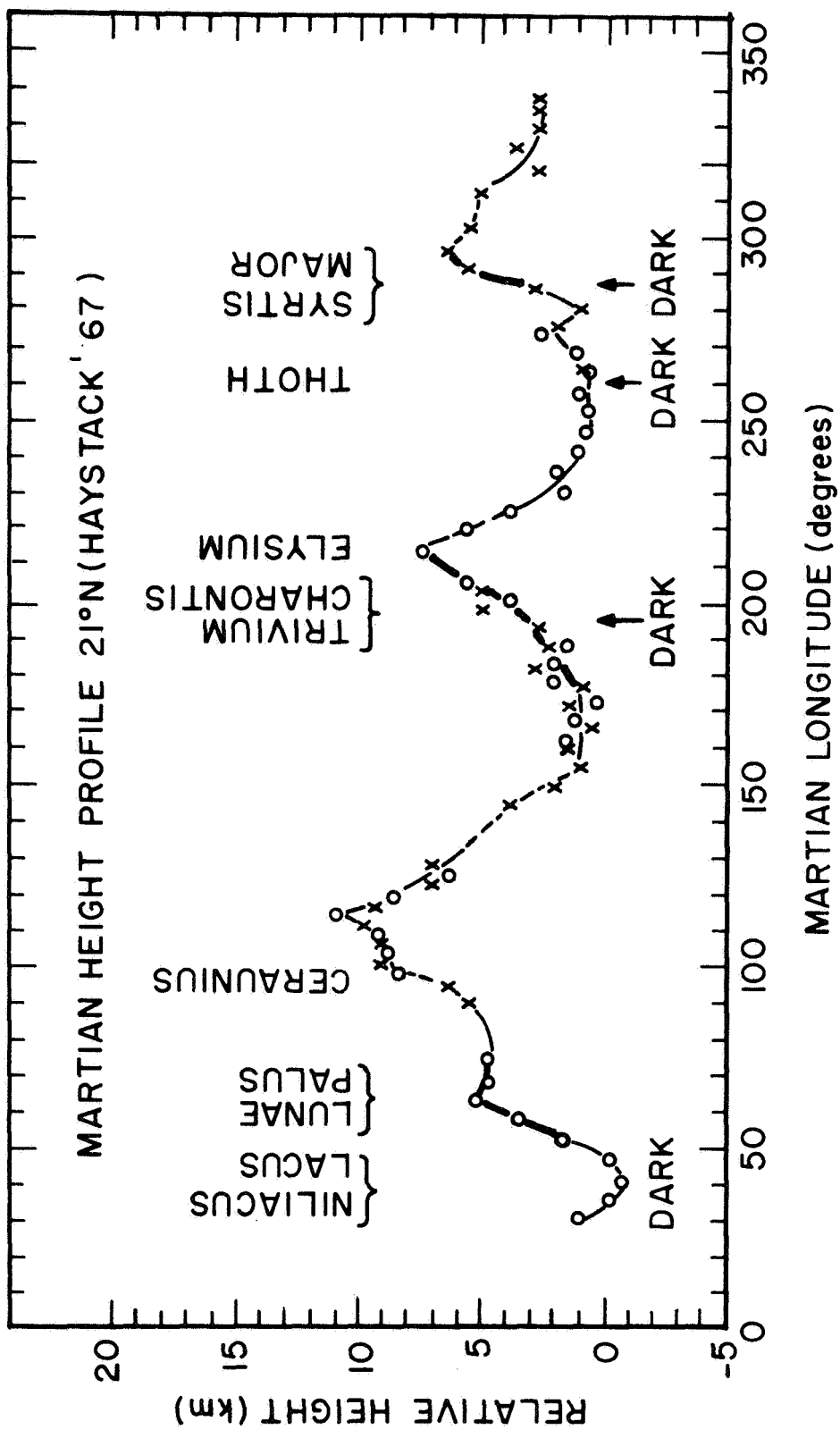


Figure 8. Martian height profile at 21°N obtained from vertical incidence radar ranging at 3.8 cm wavelength. The zero reference height level is arbitrary. Data from 4 different runs taken at weekly intervals 7 through 29 April, 1967, are shown; circles and crosses distinguish between overlapping segments of adjacent runs. Line thickness is sized according to strength of echo (dotted line weakest). Some features are listed as well as the positions of the major visually dark areas at 21°N latitude. (G. H. Pettengill, private communication)

derived from the data in Fig. 8 are in the vicinity of Syrtis Major and Lunae Palus and are approximately 0.5° with respect to a smooth sphere. It may be significant that these slopes occur in conjunction with relatively strong echoes, and also in approximate coincidence with dark areas. If one draws a parallel with the distribution of snow in wintry regions of the earth (ignoring the temperature variation with altitude), it is neither the flat uplands nor the flat lowlands that are barren, it is the steep sides of mountains. Thus, G. H. Pettengill (private communication) has suggested that it may be the relative absence of dust that causes a higher radar reflection efficiency as well as the darker visual appearance.

It should be remembered in this discussion that both the cross section and the height represent an average over a region of about 100 km in radius (1.7° arc on the surface). This estimate of the size of the effective scattering region has been established from spectral observations by earlier workers and is confirmed by spectral data obtained in the measurements reported above as well. Thus the mean heights and slopes determined by Pettengill are large-scale averages and may hide substantially larger local variations.

In comparison with the earth the sample of Mars at 21°N that has been studied during the opposition of 1967, displays far greater height dispersion. If the terrestrial ocean floors are included, this is no longer true. However, since Mars has only half the radius of the earth, the fractional large-scale height variation remains considerably larger. With only slightly more than one-third the surface gravity of earth and with considerably less erosion, Mars' greater relative surface relief may be understood.

RADAR CONTRIBUTIONS TO PLANETARY ATMOSPHERES

Venus

Cross section vs wavelength.- The suggestion has been made (see previous section) that the variation of the radar cross section of Venus with wavelength (Fig. 1) can be accounted for in terms of atmospheric absorption. Since the largest part of the echo is returned from a region around the subradar point where the rays penetrate the atmosphere nearly vertically we may neglect the curvature of the surface and to a first approximation write

$$\sigma = \sigma_0 \exp(-2\tau) \quad (1)$$

where σ_0 is the intrinsic cross section (observable in the absence of an atmosphere) and τ the "optical depth" defined in

$$\tau = \int_0^{\infty} K \, dh \quad (2)$$

where K is the absorption coefficient per vertical height element dh . Evans et al. (1966b) suggested that the wavelength dependence of the absorption coefficient might be of the form $K \propto 1/\lambda$ leading to a law of the form

$$\sigma = \sigma_0 \exp(-a/\lambda) \quad (3)$$

and B. Lax in a companion paper (see Appendix H,) has examined a law of the type $K \propto 1/\lambda^2$ leading to

$$\sigma = \sigma_0 \exp(-b/\lambda^2). \quad (4)$$

These two laws are compared in Fig. 9. This figure differs from Fig. 1 in that in order to test these two laws (Equation 3 and Equation 4) to the fullest we have reduced the error bars associated with the $\lambda = 12.5$ cm measurement to the +1% value given by Carpenter (1966) in his most recent paper. The error associated with the 23 cm point has been reduced from +2 db to +1 db on the basis of a subsequent radar calibration using the Lincoln Calibration Sphere (a perfectly round machined metal sphere placed in earth orbit as a standard radar target). This later calibration confirmed the earlier cross section measurement but reduced its associated uncertainty. The 70 cm point has been replaced by a revised value reported by Pettengill et al. (1967), viz. 14 + 7%.

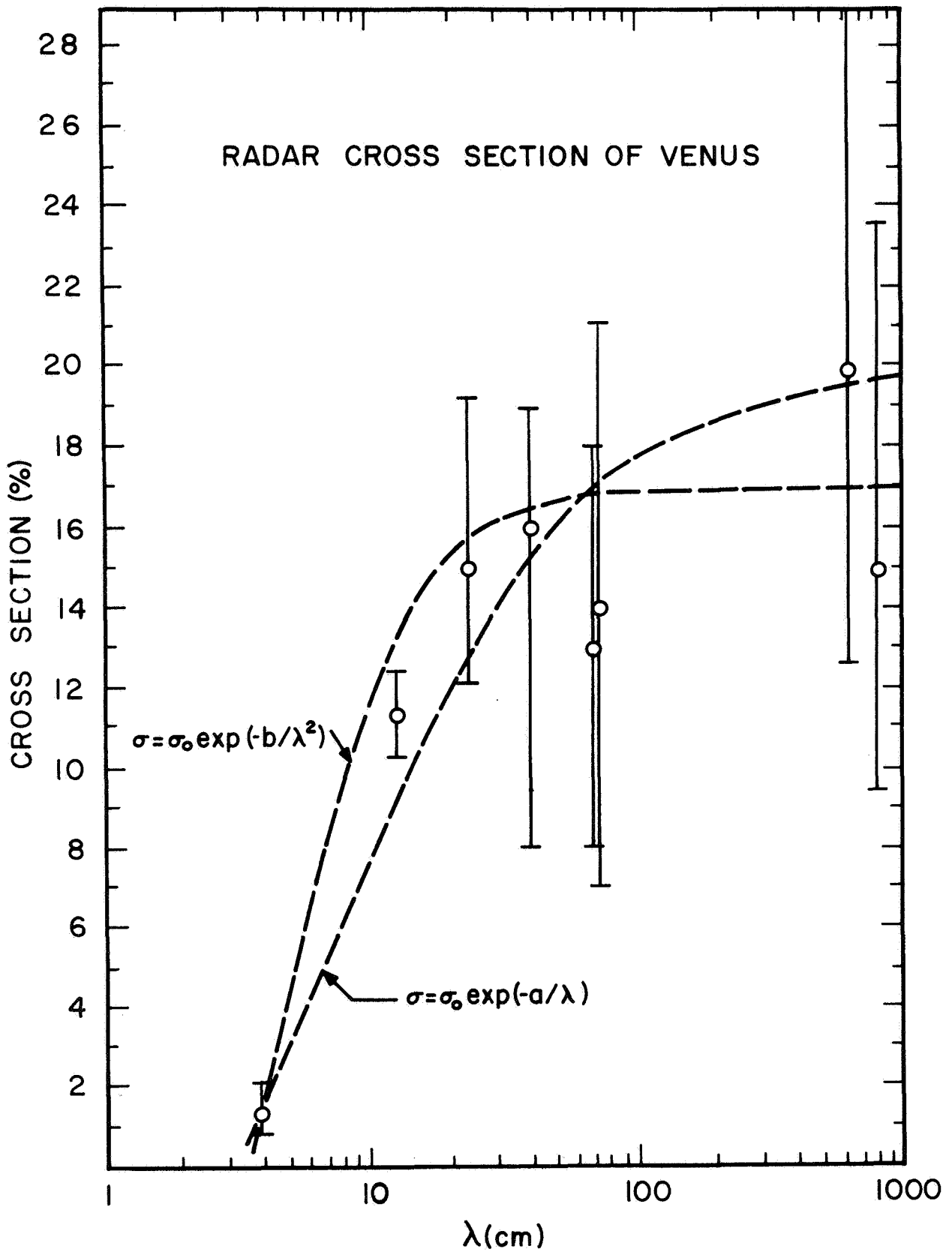


Figure 9 The radar cross section of Venus and the curves predicted by two simple models described in the text. The error bars shown in this plot have been refined over those given in Fig. 1 by the use of more recent values.

The curves drawn in Fig. 9 have been forced to pass through the value $\sigma = 1.2\%$ reported by Evans et al. (1966) at $\lambda = 3.8$ cm. By allowing a change in the value of σ at this wavelength, yet remaining within the error bars shown, either curve could be made to pass through the error bars of the $\lambda = 12.5$ cm point.

In sum the present cross section measurements are incapable of distinguishing between the two most elementary wavelength dependencies for the absorption coefficient. It is possible that the wavelength dependence of the absorption is compounded with variations in the intrinsic cross section σ_0 with wavelength due to different penetration depths of the signals. Little can be said about this possibility other than to point out that in the case of the moon (where it is known to occur) the intrinsic cross section is lower at all wavelengths. This suggests, as noted before, that Venus has a more compact surface and therefore that this is not an important effect. Such a conclusion is, however, little more than surmise at present.

Atmospheric scattering.- It is possible to argue that the low value for the cross section observed at 3.8 cm arises because the signals are no longer being scattered from the surface but from particles (e.g. rain or ice) in the atmosphere. Four arguments can be advanced against this hypothesis:

1. The absolute doppler shift agrees with that predicted for the planetary surface to the limit of the experimental accuracy. Thus the particles would have to have equal upward and downward velocities with respect to the surface (or none at all) to be seen at the same velocity as the planet.

2. The overall doppler width of the signals (Fig. 10) is precisely that computed from the known size and rotation rate of the planet. No signals are seen at frequencies outside this band that could be attributed to particles in turbulent motion.

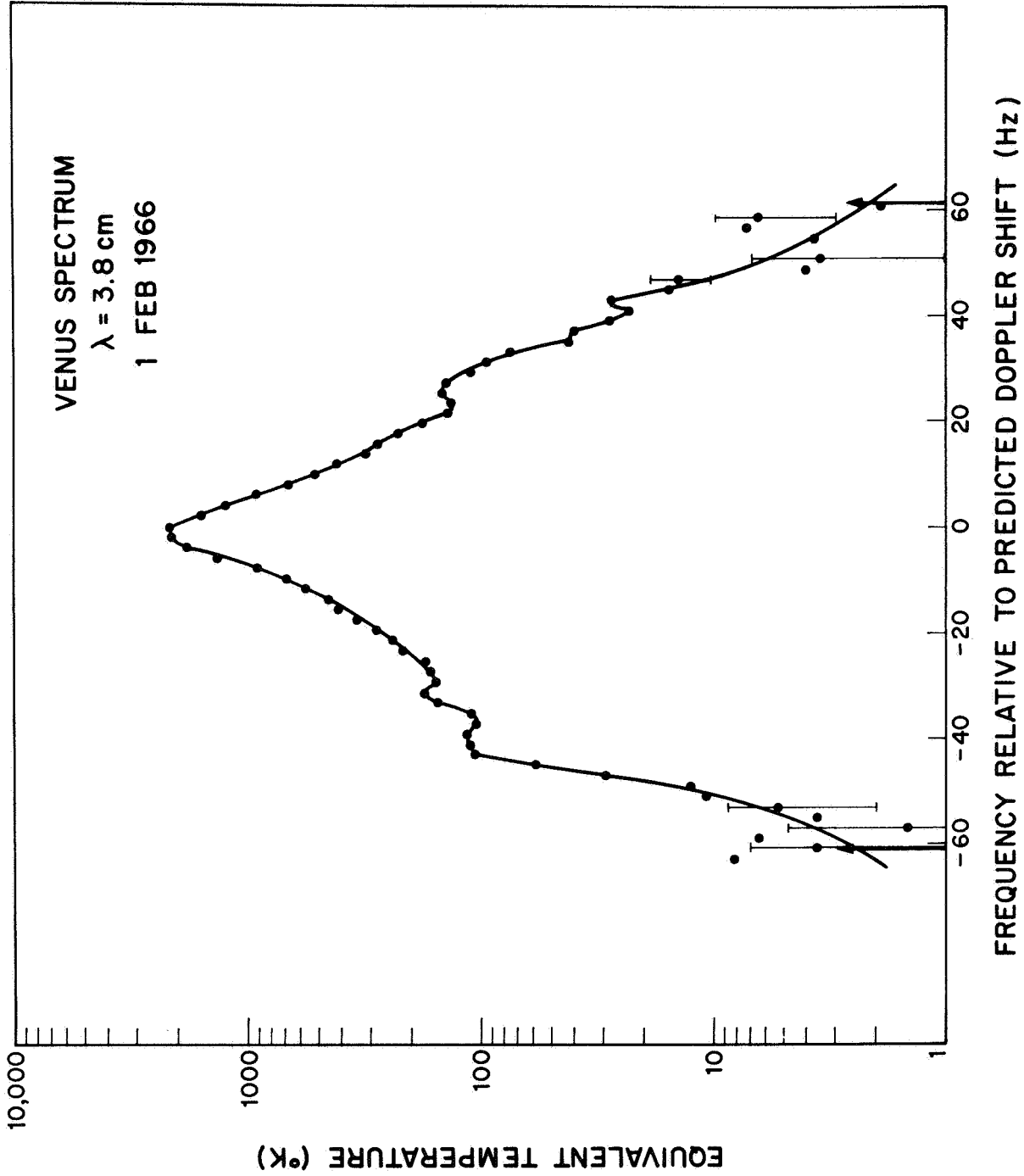


Figure 10. A spectrum of echo power for Venus at 3.8 cm wavelength. Note that the peak echo occurs at the predicted doppler shift and all the power is contained between the two arrows which indicate the computed positions of the limbs (Evans, et al. 1966b).

3. The features are seen in the spectra (e.g. Fig. 10) and these move in position within the spectrum in a systematic manner consistent with their being attached to the planetary surface. These features appear to be the same as those seen at longer wavelengths (see Fig. 5).

4. Short pulse range measurements have been made essentially simultaneously (Evans et al. 1966b) at wavelengths of 3.8 and 23 cm (Fig. 11). The results show that the nearest reflection point for the two frequencies is at the same range to within the experimental accuracy (± 1 km).

In conclusion, if any scattering does occur in the atmosphere of Venus, existing experiments have failed to detect it. A radar operating at a frequency of 1 cm or less would be better suited to such a task because a) the atmospheric absorption to the surface would presumably be higher thus reducing the background "glare" of the planet, and b) the particle cross section would be increased by 200 times assuming that the particle radius is small compared with the wavelength.

Limb darkening.- If the reduced cross section at 3.8 cm is to be accounted for in terms of atmospheric absorption, we would expect the absorption to be most severe near the limbs of the planet where the rays must penetrate the atmosphere obliquely. This would serve to steepen the angular scattering law $\bar{P}(\phi)_{3.8}$ over that which would be seen in the absence of an atmosphere. If the one-way attenuation were A db, this modification can be expressed in:

$$10 \log_{10} \bar{P}(\phi) - 10 \log_{10} \bar{P}(\phi)_{3.8} = 2 A \sec \phi \text{ db} \quad (5)$$

Thus, given some independent means of measuring $\bar{P}(\phi)$, it would be possible to deduce A directly. It should be noted that Eq. (5) is based on the premise of rectilinear propagation, thin atmosphere (i.e. scale height \ll planetary radius) and uniform absorption over the disc. A number of these assumptions can be questioned and in particular the last. If the poles are colder than the

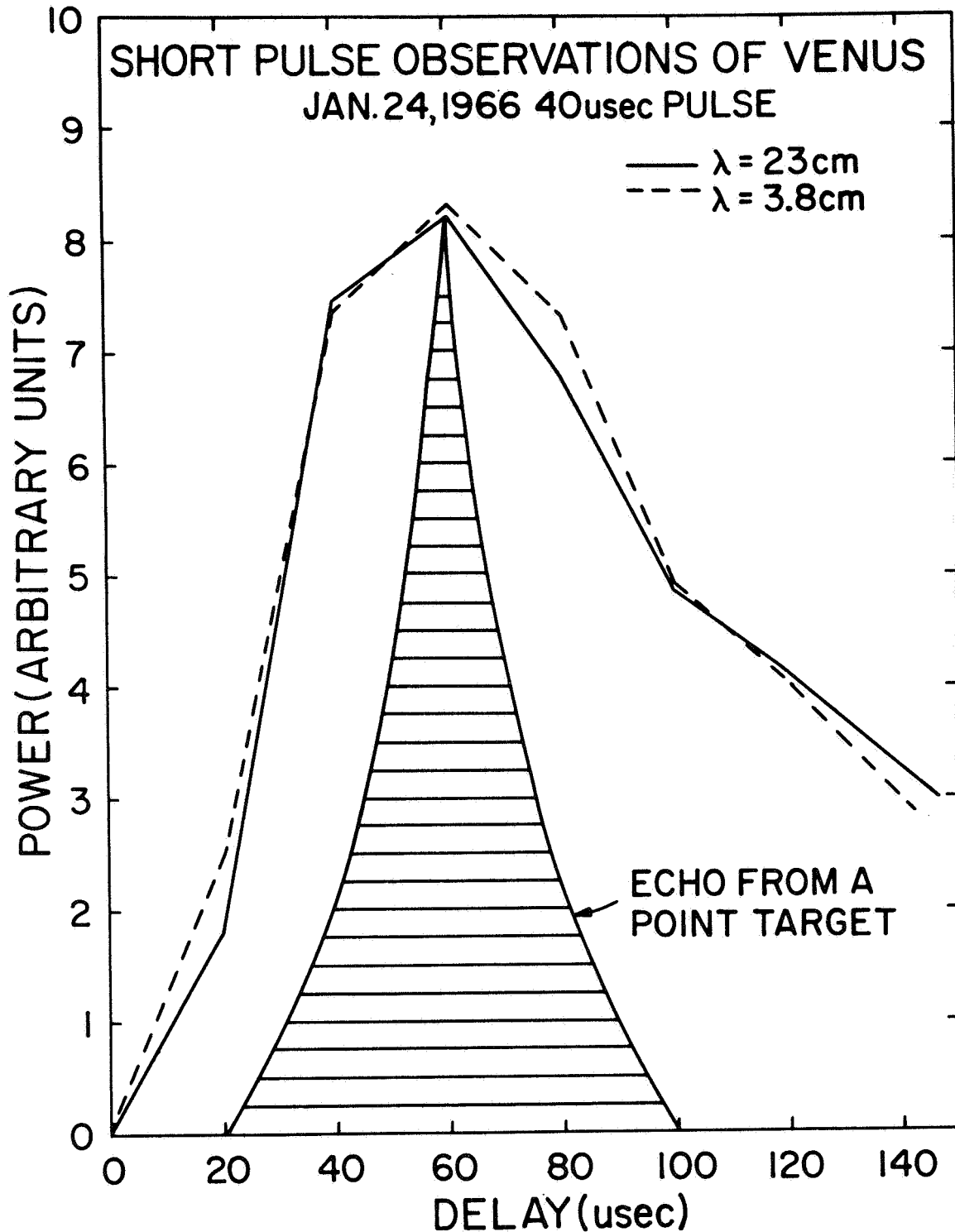


Figure 11. The echo power vs delay observed for the initial part of the return from Venus at two wavelengths. The delay to the reflecting surface is the same at both wavelengths to the limits of the experimental accuracy (± 1 km). Further the shapes of the echoes are nearly identical. These results show beyond doubt that it is the surface and not the atmosphere that gives rise to the 3.8 cm echo (Evans, et al., 1966b).

equator, then the total absorption there might be different. For example, for a dense $\text{CO}_2 - \text{N}_2$ atmosphere (Barrett 1961) in which the absorption is produced by collision-induced dipole moments (Barrett and Staelin 1964):

$$A \propto (1/T^{4.6}) \text{ db} \quad (6)$$

Accepting the limitations of this model, Evans et al. (1966b) searched for a limb darkening effect. In the absence of any way of measuring $\bar{P}(\phi)$ (i.e., the scattering behavior with the atmosphere removed) they were obliged to adopt as a model for $\bar{P}(\phi)$ the curve observed at some longer wavelength, and then assume that this did not differ from the one that would be obtained at 3.8 cm. In the case of the moon such an assumption would be invalid. However, no systematic wavelength dependence in $\bar{P}(\phi)$ for Venus has yet been found (see preceding section). Two experiments were tried. In one, an echo power vs delay curve was constructed using pulses of various lengths, and is compared with the 23 cm results (Fig. 2) in Fig. 12. In the second, a mean echo power spectrum was constructed by normalizing the four best frequency spectra to a common relative scale (Fig. 13) and this was then compared with a similar mean spectrum obtained at 12.5 cm at J.P.L. (Muhleman 1965) in Fig. 14. In both cases the effects of limb darkening are evident.

From the pulse measurement (Fig. 12) a value of $2A = 5.5 \pm 2$ db was obtained, and from the spectrum (Fig. 14) $2A = 3.5 \pm 2$ db. Thus in neither case was the limb darkening observed consistent with the amount required ($2A \sim 10$ db) to reduce the cross section to the low value observed. This discrepancy can result from a number of causes such as: a) the model may be oversimplified (as noted above), b) the intrinsic cross section σ_0 may be lower at 3.8 cm, and c) the angular scattering law $\bar{P}(\phi)$ may change with wavelength for Venus as it does for the Moon. This last eventuality is capable of introducing the entire discrepancy. In all probability, however, the true

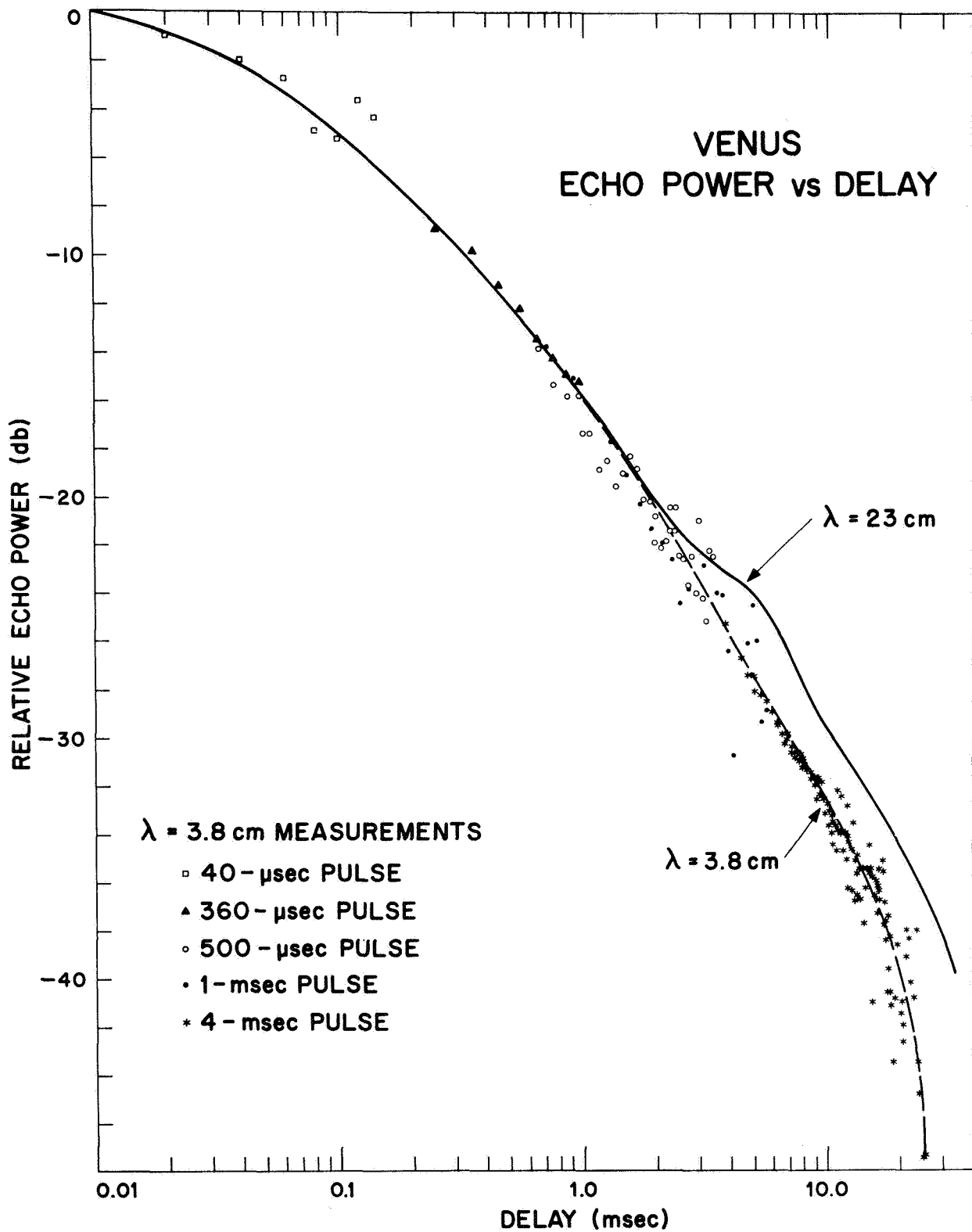


Figure 12. Comparison of echo power vs delay at 3.8 and 23 cm wavelength. The divergence at delays >1 m sec is thought to indicate limb darkening caused by the atmosphere of Venus (Evans, et al. 1966b).

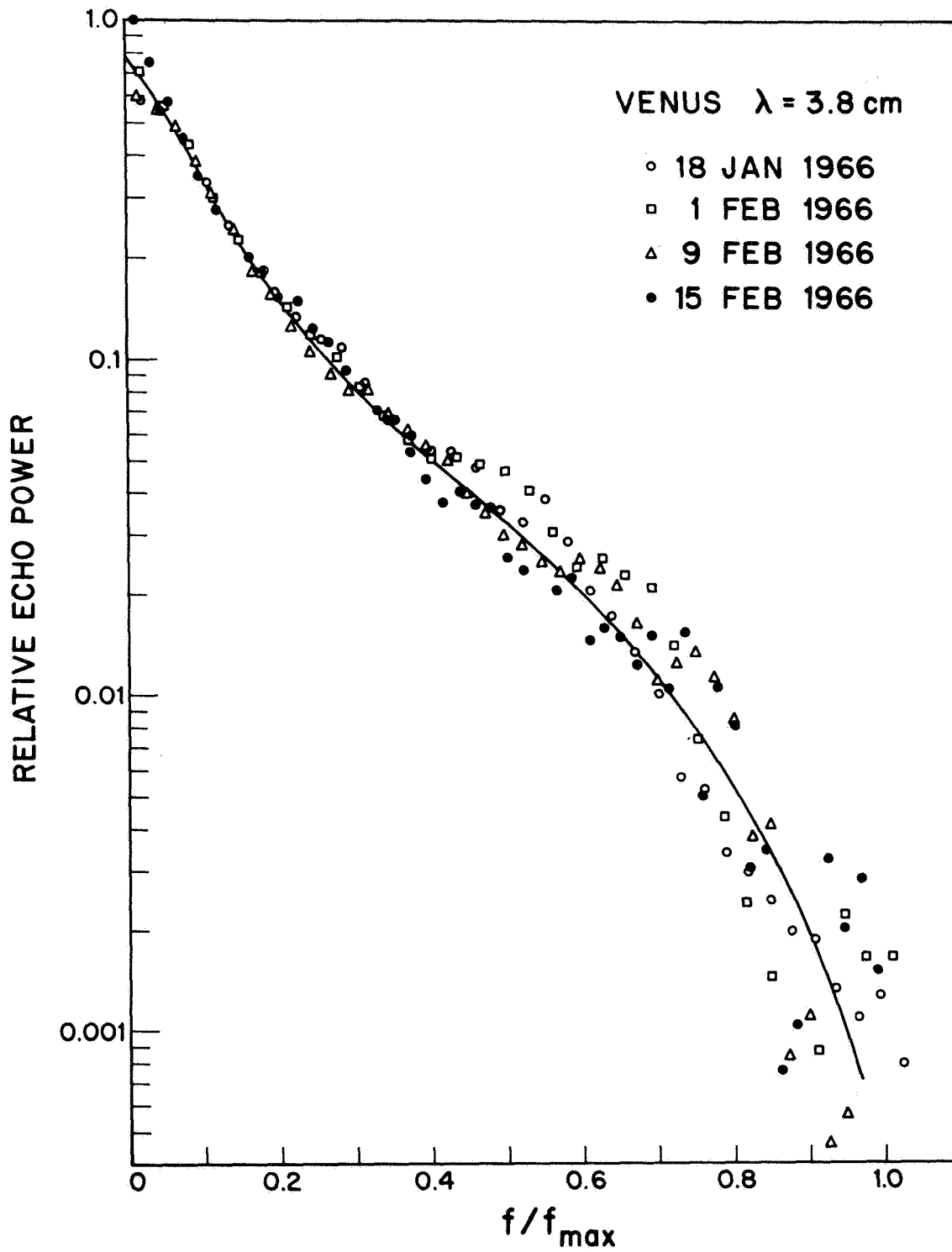


Figure 13. The mean echo power spectrum derived by Evans, et al. (1966b) for 3.8 cm.

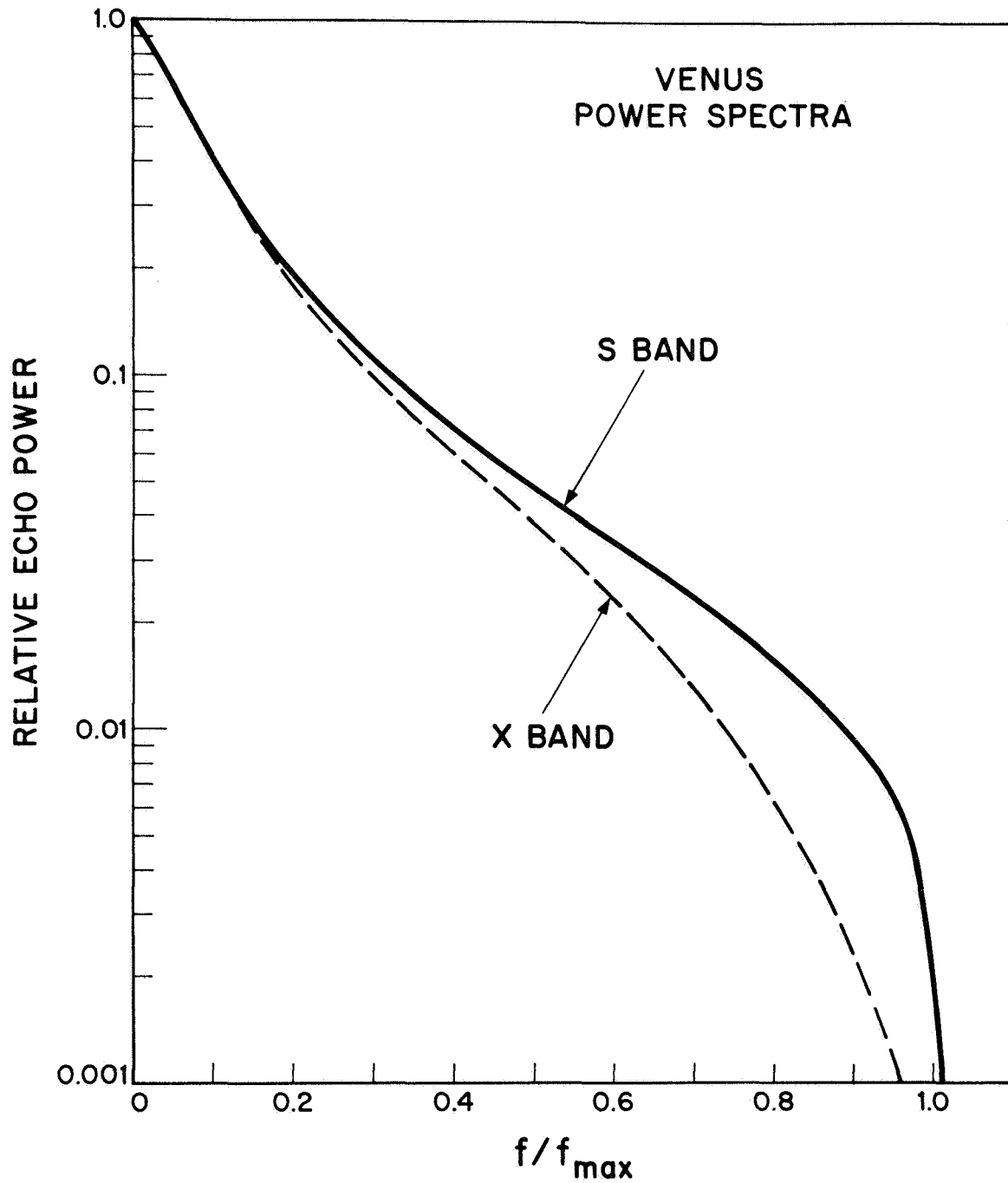


Figure 14. Comparison of the curve of Fig. 13 (labelled X-band) with that obtained by Muhleman (1965) at 12.5 cm (S-band). The divergence is again thought to indicate limb darkening (Evans, et al. 1966b).

explanation probably lies in a combination of all three effects.

In conclusion this experiment would indicate that the one-way zenithal absorption of 3.8 wavelength signals is probably not less than 2 db while the cross section measurements (see above) imply that it cannot be more than 6 db. Refinements in these conclusions can be expected from further observations at 3.8 cm wavelength using the improved Haystack radar. Very desirable also would be new measurements at say $\lambda = 1, 2,$ and 6 cm.

Mars

Radar experiments on Mars have, as yet, yielded no information concerning its atmosphere.

DISCUSSION

Surface Material of Venus

The long-wave radar measurements suggest a dielectric constant of the order of 5 - 6 (see above). The value of $\epsilon = 3.5$ reported by Carpenter (1966) should be regarded as suspect in view of the possible atmospheric attenuation at this wavelength (Fig. 9). The value $\epsilon = 2.2$ reported by Clark and Kuzmin (1965) from radio interferometer polarization measurements at 10.6 cm is likewise suspect. The curves of Fig. 9 imply the existence of between 1.25 and 2.25 db zenithal absorption (one-way) at this wavelength. Thus at a position on the disc where the emission would appear polarized ($\phi \geq 60^\circ$) the one-way absorption will be between 2.5 and 4.5 db. That is at least half the emission will be from the atmosphere and will be unpolarized.

If correct, this argument serves to resolve the discrepancy between the radar and radiometric values for the dielectric constant, and incidentally argues against the cloud-greenhouse model of Sagan and Pollack (1965, 1967) which predicts essentially no absorption of 10.6 cm wavelength radio signals. This conclusion was reached

earlier by Hansen and Matsuchima (1967) who show rigorously that a surface dielectric constant of $\epsilon = 6$ is compatible with the fringe visibility observed by Clark and Kuzmin (1965) given an atmospheric attenuation as large as the values suggested above.

Surface Material of Mars

Strongest reflections from Mars are apparently associated with sloping terrain, and such terrain tends to be dark, though here the correspondence is less than perfect (Fig. 8). G. H. Pettengill (private communication) has suggested a model to account for this behavior in which it is supposed that the dark regions having high radar reflectivity are the sloping surfaces which are less densely covered in eroded material or debris. On the other hand, B. Murray (private communication) has suggested that the strong radar returns are from subsurface water or ice tables. This might then account for the extremely smooth appearance of these regions and at the same time account for an albedo difference--the soil above being damp. Apart from the obvious comment that such regions might be expected to occupy the lowland ground rather than the slopes little more can be said, and it seems profitless to speculate further until more data is available.

Atmosphere of Venus

We believe that the atmosphere of Venus gives rise to between 2 and 6 db atmospheric attenuation one-way at the zenith. Of the eight models for the atmosphere of Venus proposed by Barrett and Staelin (1964) to account for the microwave emission spectrum only 3 can give rise to this much absorption. These are: a) the $\text{CO}_2 - \text{N}_2$ model with a pressure of several hundred atmospheres, b) the water vapor cloud model--6 km thick with 1 gm/meter^3 water vapor in equilibrium with liquid water at the cloud bottom, and c) the lossy (and therefore absorbing) dust model.

Sagan and Pollack (1965, 1967) favor a cloud-greenhouse model for the atmosphere in which CO₂ largely provides the infrared opacity and is enhanced by cloud particles, and the latter provide the microwave opacity. This may be regarded as a combination of models a) and c) and has been criticized by Hansen and Matsushima (1967) on the grounds that the radar reflectivity and differential polarization of 10.6 cm emission (see above) indicate that the microwave opacity is concentrated most heavily near the planetary surface; and not in a low temperature cloud region. As an alternative they propose a variant of model c) in which the heat input is solely that of the internal heat of the planet. The amount of dust required in the atmosphere above each cm² of surface is then of the order of 10 gm. Despite these somewhat bizarre propositions, the model is capable of matching both the microwave emission and radar reflectivity data.

A major obstacle to this last model is the variability in the 3.8 cm cross section of Venus observed by Evans et al. (1966b) who suggested that there might be "clearings" in the atmosphere, i.e. regions in which the abundance of the microwave absorbing agent is substantially lower than the average. Such clearings would destroy the effectiveness of the dust blanket and would in any event be difficult to generate in an atmosphere where surface temperature differences (and therefore winds) must be largely absent.

In the companion paper we examine the evidence for variations in the radar cross section of Venus and conclude that, in large measure, these can be accounted for by variations in the height and roughness of the terrain at the subradar point.

FUTURE WORK

Venus

Important new results can be expected from a continuation

of existing programs--in particular the 12.6 cm J.P.L. observations (hopefully with the 210 ft. antenna) and the 3.8 cm measurements at Haystack. Yet measurements at new wavelengths almost anywhere in the range $\leq 1 - 10$ cm are urgently required. These offer the promise of determining the absorption coefficient vs radio wavelength for the Venus atmosphere and consequently will constrain the number of models that can be invoked to account for the microwave emission spectrum. In addition, observations at the shortest of these wavelengths could yield direct evidence of particulate matter in the atmosphere. Accurate observations at long wavelengths ($\lambda \geq 2$ m) are required in order to provide a reliable value for the intrinsic reflection coefficient of the surface.

The new measurements at 70 cm, 12.6 cm and 3.8 cm promise to provide additional information on the location and nature of the anomalously bright scattering regions. Plans to employ a radar interferometer at 3.8 cm hold the possibility of providing a crude though useful radar map.

Mars

The extension of the height contour measurements (Fig. 8) to other regions promises to yield the first contour map for Mars. The variation of cross section with surface height and the associations of these two with surface markings are exciting results. With added data the meaning of these associations may be made clear.

Long wave measurements ($\lambda \sim 2$ m) would be extremely useful in conjunction with the 3.8 cm measurements. They might show for instance that the longer wavelength penetrates to a greater depth and encounters ice or water (as proposed by Murray above and Smoluchowski in Appendix J).

BIBLIOGRAPHY

- Ash, M. E., Shapiro, I. I., Smith, W. B., "Astronomical Constants and Planetary Ephemerides Deduced from Radar and Optical Observations," 1967 *Astron. J.* 72, pp. 338-350.
- Barrett, A. H., "Microwave Absorption and Emission in the Atmosphere of Venus," 1961 *Astrophys. J.* 133, pp. 281-293.
- Barrett, A. H., and Staelin, D. H., "Radio Observations of Venus and the Interpretations," 1964 *Space Sci. Revs.* 3, pp. 109-135.
- Carpenter, R. L., "Study of Venus by CW Radar," 1964 *Astron. J.* 69, pp. 2-11.
- Carpenter, R. L., "Study of Venus by cw Radar--1964 Results," *ibid* 71, pp. 142-152.
- Clark, B. G., and Kuzmin, A. D., "The Measurement of the Polarization and Brightness Distribution of Venus at 10.6-cm wavelength," 1965 *Astrophys. J.* 142, pp. 23-45.
- Colombo, G., and Shapiro, I. I., "The Rotation of the Planet Mercury," 1965 *Smithsonian Astrophys. Obs. Spec. Report No. 188*, also 1966 *Astrophys. J.* 145, pp. 296-307.
- Dyce, R. B., Pettengill, G. H., and Shapiro, I. I., "Radar Determinations of the Rotations of Venus and Mercury," 1967a *Astron. J.* 72, pp. 351-359.
- Dyce, R. B., Pettengill, G. H., and Sanchez, A. D., "Radar Observations of Mars and Jupiter at 70 cm," 1967b *ibid* 72, pp. 771-777.
- Evans, J. V., Brockelman, R. A., Henry, J. C., Hyde, G. M., Kraft, L. G., Reid, W. A., and Smith, W. W., "Radar Echo Observations of Venus and Mars at 23 cm Wavelength," 1965 *ibid* 70, pp. 486-501.
- Evans, J. V., Brockelman, R. A., Dupont, E. N., Hanson, L. B., and Reid, W. A., "Radar Observations of Venus at 23 cm in 1965/1966," 1966a *ibid* 71, pp. 897-901.

BIBLIOGRAPHY (continued)

- Evans, J. V., Ingalls, R. P., Rainville, L. P., and Silva, R. R.,
"Radar Observations of Venus at 3.8 cm Wavelength," 1966b
ibid 71, pp. 902-915.
- Goldstein, R. M., "Venus Characteristics by Earth-Based Radar,"
1964 ibid 69, pp. 12-18.
- Goldstein, R. M., "Preliminary Venus Radar Results," 1965a
J. Res. Nat. Bur. Stds., Radio Sci. 69D, pp. 1623-1625.
- Goldstein, R. M., "Preliminary Mars Radar Results," 1965b,
J. Res. Nat. Bur. Stds., Radio Sci. 69D, pp. 1625-1627.
- Goldstein, R. M., and Gillmore, W. F., "Radar Observations of
Mars," 1963 Astron. J. 141, pp. 1171-1172.
- Hansen, J. E. and Matsushima, S., "The Atmosphere and Surface
Temperature of Venus: A Dust Insulation Model," 1967,
to be published.
- Kotelnikov, et al., (9 authors), "Radar Detection of the Planet
Mars in the Soviet Union," 1963 Dokl. Akad. Nauk. 151,
pp. 811-814.
- Muhleman, D. O., "Radar Scattering From Venus and Mercury at
12.5 cm," 1965 J. Res. Nat. Bur. Stds. 69D, pp. 1630-1631.
- Pettengill, G. H., "Radar Observations of the Planets," 1965
J. Res. Nat. Bur. Stds. 69D, pp. 1617-1623.
- Pettengill, G. H., Briscoe, H. W., Evans, J. V., Gehrels, E.,
Hyde, G. M., Kraft, L. G., Price, R., and Smith, W. B.,
"A Radar Investigation of Venus," 1962 Astron. J. 67,
pp. 181-190.
- Pettengill, G. H., and Dyce, R. B., "A Radar Determination of the
Rotation of the Planet Mercury," 1965 Nature 206, p. 1240.
- Pettengill, G. H., Dyce, R. B., and Campbell, D., "Radar Measure-
ments at 70 cm of Venus and Mercury," 1967 Astron. J. 72,
pp. 330-337.
- Sagan, C., and Pollack, J. B., "An Analysis of Microwave
Observations of Venus," 1965 J. Res. Nat. Bur. Stds. 69D,
pp. 1583-1584.

BIBLIOGRAPHY (continued)

- Sagan, C., and Pollack, J. B. 1967. To be published.
- Sagan, C., and Pollack, J. B., "Radar Doppler Spectroscopy of Mars: I. Elevation Differences Between Bright and Dark Areas," 1967 Astron. J. 72, pp. 20-34.
- Wells, R. A., "Evidence that Dark Areas on Mars are Elevated Mountain Ranges," 1965 Nature 207, pp. 735-736.

APPENDIX E
(Report of 1967 Summer "TYCHO" Meeting, TG # 31)

REFLECTION AND DIFFRACTION IN A
BISTATIC RADAR OCCULTATION EXPERIMENT

T. Hagfors

July, 1967

Contract No: NSR-24-005-047

Prepared by

UNIVERSITY OF MINNESOTA
Minneapolis, Minnesota

For

HEADQUARTERS, NATIONAL AERONAUTICS & SPACE ADMINISTRATION
Washington, D. C. 20546

REFLECTION AND DIFFRACTION IN A BISTATIC
RADAR OCCULTATION EXPERIMENT

ABSTRACT

The strength of the field reflected obliquely from a planet in an occultation experiment is computed for a number of parameters. It is shown that a study of the reflected signal component can provide information about the electrical properties of the planetary surface. Possible distortions of the diffraction pattern caused by surface roughness are also investigated and it is found that the likelihood of occurrence of surface undulations large enough to be observable is very small.

TABLE OF CONTENTS

<u>Title</u>	<u>Page</u>
Introduction	E-1
Evaluation of Reflection from the Surface.	E-2
The Diffracted Field	E-7
Conclusions	E-10
Reference	E-11
Appendix	E-12

LIST OF ILLUSTRATIONS

<u>Figure</u>	<u>Title</u>	<u>Page</u>
1	Spacecraft in Relation to the Planet	E-3
2a	Relative Reflected Field due to Reflection from Dielectric Planet as a Function of Position when Spacecraft is at Height $1.0 \cdot a$ Above Surface	E-5
2b	Relative Reflected Field due to Reflection from Dielectric Planet as a Function of Position when Spacecraft is at a Height $0.3 \cdot a$ Above Surface	E-6
3	Definition of Quantities Required to Compute Diffracted Fields	E-7
4	Effect of Uneven Edge on Diffraction Pattern	E-9

REFLECTION AND DIFFRACTION IN A BISTATIC
RADAR OCCULTATION EXPERIMENT

T. Hagfors

Lincoln Laboratory*, Massachusetts Institute of Technology
July, 1967

INTRODUCTION

G. Fjeldbo and V. R. Eshleman (1965) have described methods whereby atmospheric properties can be derived by careful studies of phase and frequency of a signal received by a spacecraft being occulted by a planet. The method has been applied to studies of the atmosphere of Mars with considerable success.

In that work little consideration was given to the possibility of deriving information about surface properties. The surface properties are indeed not of great importance in determining the signal properties as long as the spacecraft is at a large distance from the planet at the time of occultation. However, future occultation experiments both on Mars and Venus will employ spacecrafts which approach the planetary surface quite closely, and it is felt that an analysis of the amplitude pattern of the signal near occultation could well supply valuable information concerning surface material and possibly structure.

To evaluate these possibilities some numerical calculations are carried out in this report in order to evaluate the relative

*Operated with support from the National Aeronautics and Space Administration under Contract No. NSR-22-009-106.

strength of a direct and a reflected signal when the planet is smooth. Little progress has so far been made in evaluating the effect of surface roughness on the reflected signal but it is believed that the total strength is not strongly dependent on the roughness. With substantial surface undulations the occultation diffraction pattern will be affected. The conditions for this to occur are also worked out in some detail.

In the process of this work, inspired by several good suggestions from D. L. Anderson, California Institute of Technology, an exact method was developed to determine the refractivity profile of an atmosphere from the Doppler-offset versus time behavior of the signal. The method apparently is well known in seismic sounding techniques.

EVALUATION OF REFLECTION FROM THE SURFACE

The geometry of the spacecraft in relation to the occulting planet is shown in Fig. 1. The spacecraft is assumed to move in the xy plane and to have coordinates R, ϕ as shown. The direction to the observer (at infinity) is taken to be along the negative y -axis. We shall assume that the spacecraft is transmitting. The signal at the observer can be considered to consist of two parts, one derivable from the free space field on the plane $y = 0$ exterior to the planet and another derived from the field distribution set up on the planetary surface. When the distance R is much larger than the planetary radius a the former is dominant, but for smaller R the reflected component may become appreciable. In order to assess the importance of this component we compute the reflected signal strength by Huygens' principle:

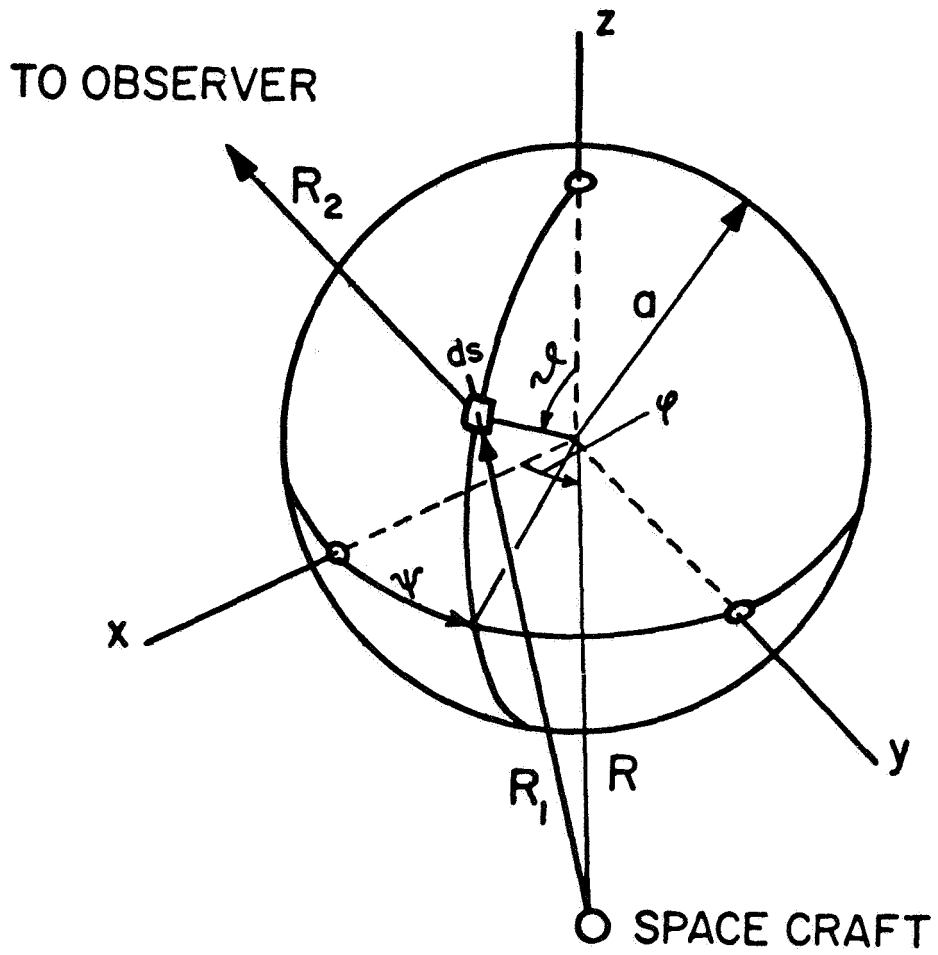


Fig. 1 Spacecraft in Relation to the Planet.

$$\psi_r = \frac{iE_o}{2\pi} \int d\vec{S} \cdot \vec{n} R \left(\frac{\vec{k}_i \cdot \vec{n}}{k} \right) e^{-ik(R_1+R_2)} / R_1 R_2 \quad (1)$$

where

E_o/R_1 = free space field strength at distance R_1

$d\vec{S}$ = surface element = $a^2 d\psi \sin\theta d\theta$

\vec{n} = surface normal

$R(\cos\alpha)$ = reflection coefficient at an angle of incidence α

$k = 2\pi/\lambda$

$R_1 = \sqrt{(R \sin\phi - a \sin\psi \sin\theta)^2 + (R \cos\phi - a \cos\psi \sin\theta)^2 + a^2 \cos^2\theta}$

$R_2 = R_o + a \sin\psi \sin\theta$

R_o = distance from center of planet to observer

The stationary phase point $\psi_s \theta_s$ is found by equating the partial derivatives of $(R_1 + R_2)$ with respect to ψ and θ to zero. It is found that:

$$\theta_s = 90^\circ \quad \text{and} \quad \frac{a}{R} \cos\psi_s = \cos(\theta - 2\psi_s) \quad (2)$$

In terms of θ_s and ψ_s the field at the receiver becomes:

$$\psi_r = \frac{E_o}{R_2} \cdot \frac{a}{R} \frac{\sin\psi_s \cos\psi_s R(-\sin\psi_s)}{\cos\psi_s \sqrt{1 - \frac{a}{R} \cos^3\psi_s / \cos\phi}} e^{-ik(R_1+R_2)} \quad (3)$$

Expression (3) was evaluated on a digital computer for ϕ ranging from -90° to $\phi = \text{Arc cos}(a/R)$ at which point geometric occultation occurs. The calculations were carried out for a dielectric planet with dielectric constants of 4.0 and 6.0, and for values (R/a) of 1.1, 1.3, 1.5, 1.8 and 2.0. Some of the results of the calculations are plotted in Figs. 2a and 2b. As can be seen the reflected signal may well be appreciable. The very different behavior of the two principal linear polarizations

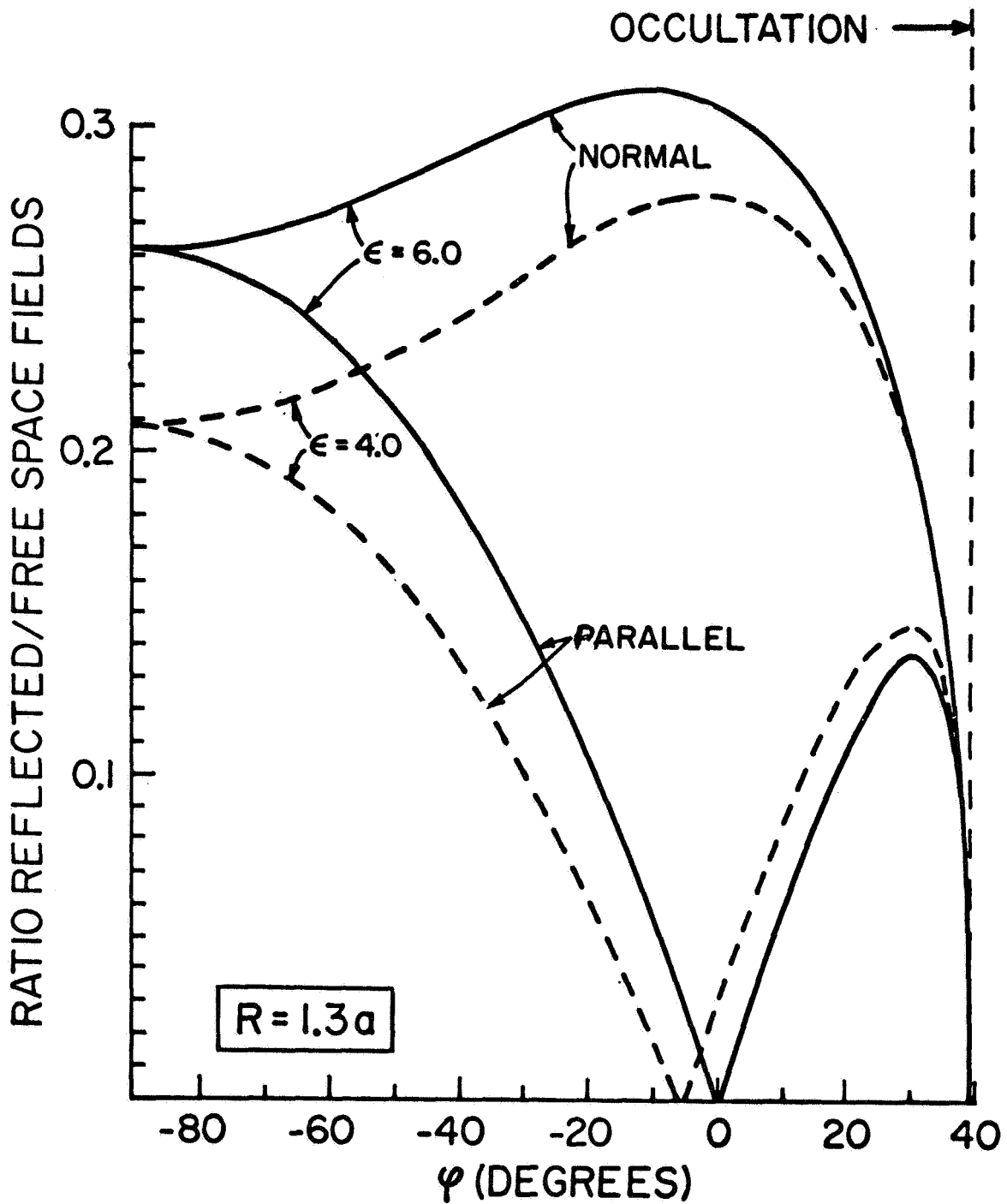


Fig. 2a Relative Reflected Field due to Reflection from Dielectric Planet as a Function of Position when Spacecraft is at Height $1.0 \cdot a$ Above Surface.

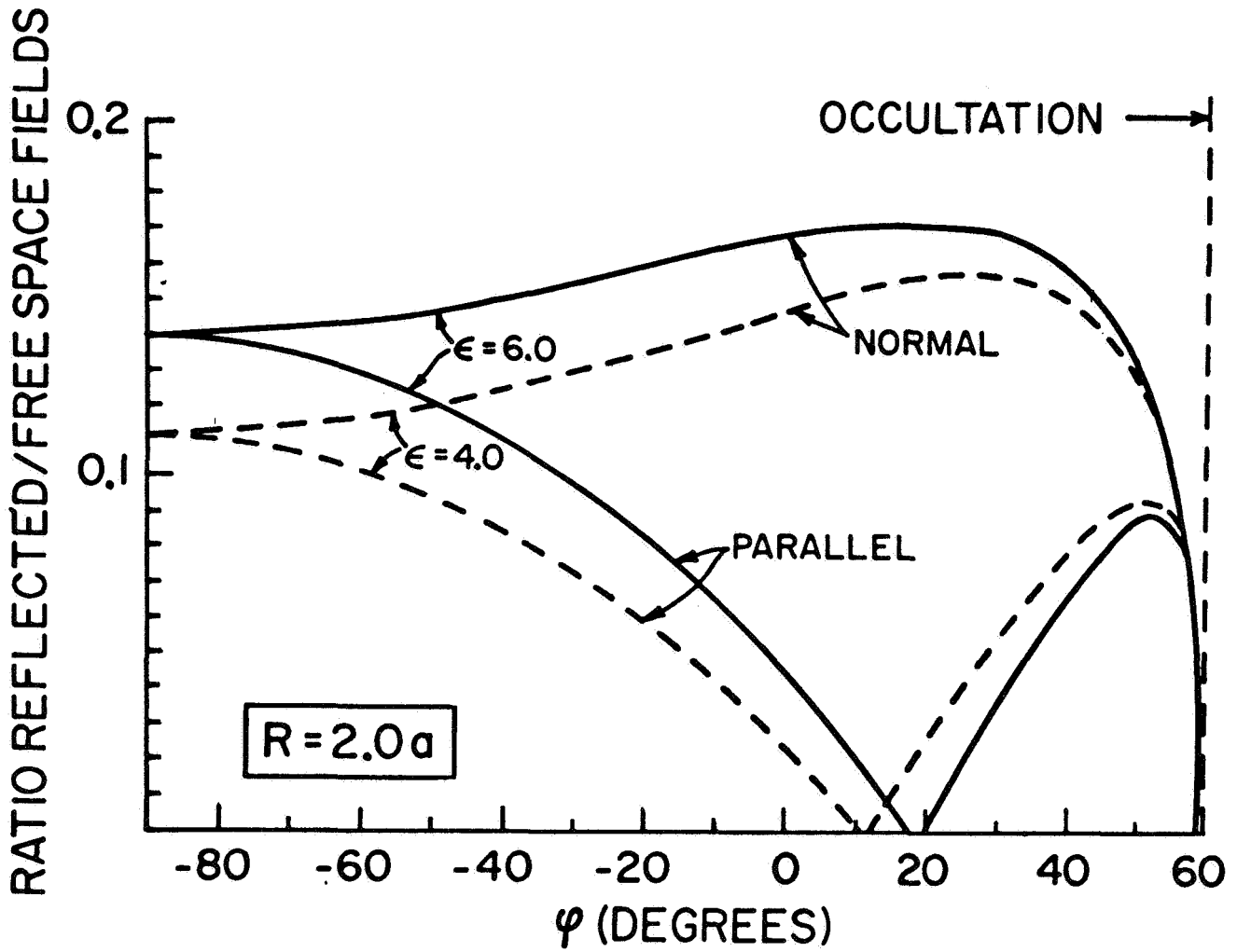


Fig. 2b Relative Reflected Field due to Reflection from Dielectric Planet as a Function of Position when Spacecraft is at a Height $0.3 \cdot a$ Above Surface.

should also be observed. Given enough signal strength a close study of the modulation as well as the polarization of the received signal hence can provide valuable information on the dielectric properties of the planetary surface.

THE DIFFRACTED FIELD

In addition to the reflected field evaluated in the preceding section there is a diffracted field which can be determined approximately from Huygens' principle by integrating the free-space fields set up by the transmitter over the plane $y = 0$ exterior to the planetary body, see Fig. 3.

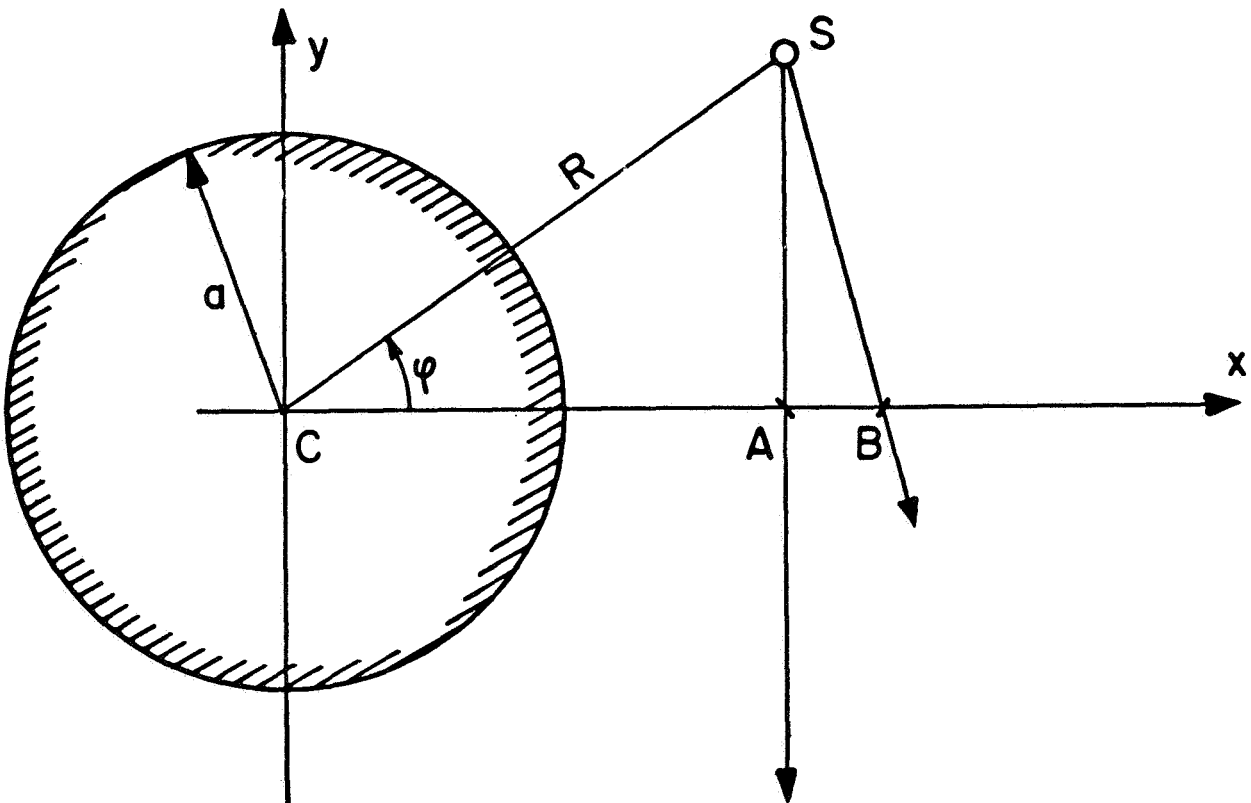


Fig. 3 Definition of Quantities Required to Compute Diffracted Fields.

The free-space field over the plane $y = 0$ is:

$$\psi_0(x, z) = \frac{E_0}{\sqrt{(x-R \cos\phi)^2 + R^2 \sin^2\phi + z^2}} e^{-ik\sqrt{(x-R \cos\phi)^2 + R^2 \sin^2\phi + z^2}} \quad (4)$$

As long as $a \gg \sqrt{\lambda R \sin\phi}$ we may regard the limb of the planet as a straight edge normal to the xy plane at $y = 0$, $x = R \cos\phi - a$. In terms of the Fresnel integrals one finds for the field at the observer:

$$\psi_0 = \frac{E_0}{2R_0} (1-i) e^{-ik(R_0 + R \sin\phi)} \left\{ \frac{1}{2}(1-i) + C(A) - iS(A) \right\} \quad (5)$$

where:

$$A = \sqrt{2} (R \cos\phi - a) / \sqrt{R\lambda \sin\phi}$$

and where the Fresnel integrals are defined by:

$$C(x) = \int_0^x \cos\left(\frac{\pi}{2} \phi^2\right) d\phi \quad S(x) = \int_0^x \sin\left(\frac{\pi}{2} \phi^2\right) d\phi$$

Expression (5) which is well known from previous work is to be combined with (3) to give the total received field at the observer.

We next investigate the possibility that surface roughness may play a significant part in determining the properties of the diffracted field. To simplify matters we consider the edge to be straight in the mean and to have random deviations superimposed according to:

$$x = a + f(z) \quad (6)$$

where $f(z)$ is a zero-mean random function of z , see Fig. 4.

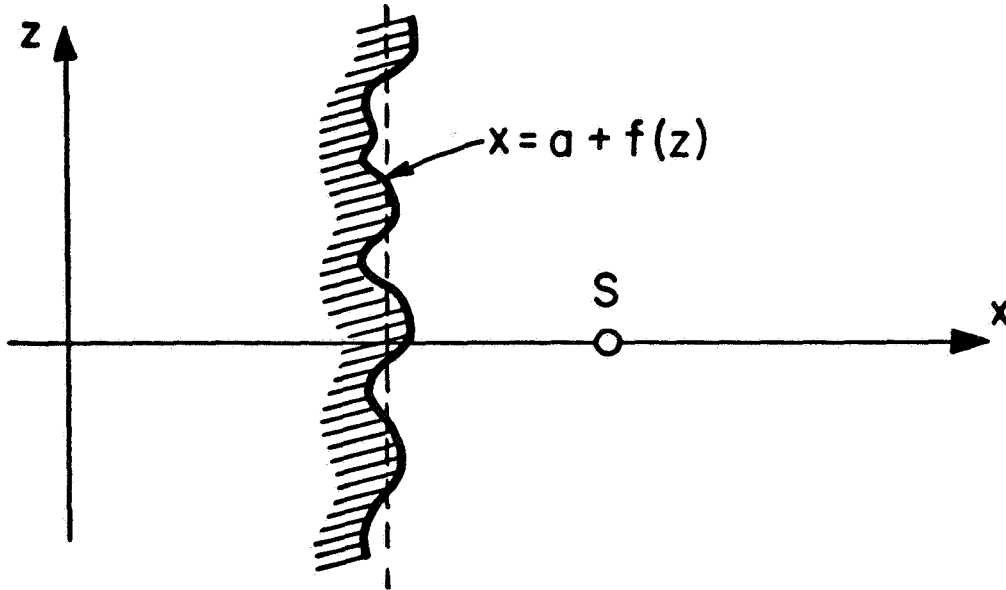


Fig. 4 Effect of Uneven Edge on Diffraction Pattern.

Using the same approximations and notations as before we obtain:

$$\psi_0 = \frac{ie^{-ik(R_0 + R \sin\phi)}}{\lambda R_0 R \sin\phi} E_0 \sqrt{\frac{\pi R \sin\phi}{k}} \int_{-\infty}^{+\infty} dz \exp(-i k z^2 / 2 R \sin\phi) \cdot \left\{ \frac{1}{2} (1-i) + C(A(z)) - i S(A(z)) \right\} \quad (7)$$

where now:

$$A(z) = \sqrt{2} \left(R \cos\phi - a - f(z) \right) = A - \sqrt{2} f(z)$$

Expanding the Fresnel integrals about $A(z) = A$ for reasonably small values of $f(z)$ (see Appendix) one obtains from (7):

$$\psi_0 = \frac{E_0}{2R_0} (1-i) e^{-i k(R_0 + R \sin\phi)} \left\{ \frac{1}{2} (1-i) + C(A) - i S(A) + \right. \\ \left. + \frac{2 \cdot e^{-i\pi A^2/2}}{(1/A) + i\pi A} \left(1 - \sqrt{i/\lambda R \sin\phi} \int_{-\infty}^{+\infty} dz e^{-ikz^2/2R} - \frac{f(z)^2}{\lambda R \sin\phi} (1/A^2 + i\pi) \right) \right\} \quad (8)$$

Little further progress can be made here unless a specific functional dependence $f(z)$ is assumed. However, a crude general conclusion can be drawn. Appreciable corrections to the straight edge result can only appear when $f(z)$ is of the same order of magnitude as $\sqrt{\lambda R \sin\phi}$, i.e. the extent of the central Fresnel zone, and this variation of $f(z)$ must occur in a distance of order $\sim \sqrt{\lambda R \sin\phi}$. Numerical estimates indicate that even at the shortest wavelengths such variations are quite unlikely to occur. Therefore, information about surface roughness does not seem to be readily available from studies of distortions of the diffraction pattern.

CONCLUSIONS

The present note has shown that the signal component which is reflected from the planetary surface may be appreciable and that it can be used to derive information about planetary surface properties of considerable interest.

The note has also shown that distortions in the diffracted field caused by surface roughness are very unlikely to be observable under conditions expected to prevail on planetary surfaces.

REFERENCE

Fjeldbo, G., and Eshleman, V. R., "The Bistatic Radar-Occultation Method for the Study of Planetary Atmospheres," J. Geophys. Res., pp. 3217-3225, 70; (1965).

APPENDIX

NOTE ON AN APPROXIMATION RELATING TO FRESNEL INTEGRALS

Let us define the function $F(x)$ by:

$$F(x) = C(x) - i S(x) = \int_0^x \exp \left(-i \frac{\pi}{2} \phi^2 \right) d\phi \quad (9)$$

We would like to derive a simple approximation to $F(x+\Delta x)$ in terms of $F(x)$ and elementary functions of Δx . To do this we first write $F(x)$ as:

$$\begin{aligned} F(x) &= \frac{1}{2} \int_0^{x^2} \exp \left(-i \frac{\pi}{2} t \right) dt / \sqrt{t} = \\ &= \frac{1}{2} \int_0^{x^2} dt \exp \left(-i \frac{\pi}{2} t - \frac{1}{2} \log t \right) \end{aligned} \quad (10)$$

Hence:

$$\begin{aligned} F(x+\Delta x) - F(x) &= \frac{1}{2} \int_{x^2}^{(x+\Delta x)^2} dt \exp \left(-i \frac{\pi}{2} t - \frac{1}{2} \log t \right) = \\ &= \frac{1}{2} \exp \left(-i \frac{\pi}{2} x^2 - \frac{1}{2} \log x^2 \right) \int_0^{\Delta x^2} dt' \exp \left(-t' \left(i \frac{\pi}{2} + 1/2 x^2 \right) \right) = \\ &= e^{-i \frac{\pi}{2} x^2} \left(1 - e^{-\Delta x^2 \left(i \frac{\pi}{2} + 1/2 x^2 \right)} \right) (1/x) + i \pi x \end{aligned} \quad (11)$$

This expression is valid over a region considerably greater than that of a Taylor expansion of $F(x)$ about the same point.

TG #37

APPENDIX F
(Report of 1967 Summer "TYCHO" Meeting, TG # 31)

WATER VAPOR AND ICE IN THE
MARTIAN ATMOSPHERE

H. Heffner

July, 1967

Contract No: NSR-24-005-047

Prepared by

UNIVERSITY OF MINNESOTA
Minneapolis, Minnesota

For



HEADQUARTERS, NATIONAL AERONAUTICS & SPACE ADMINISTRATION
Washington, D. C. 20546

WATER VAPOR AND ICE IN THE MARTIAN ATMOSPHERE

ABSTRACT

The infrared measurements of water vapor content in the Martian atmosphere together with the atmospheric temperatures inferred from the Mariner IV occultation experiment seem to indicate that the atmosphere is saturated with water vapor. Since winds and clouds have been observed on Mars, it is reasonable to assume that there is considerable vertical mixing in the lower atmosphere. Moreover, the warmer Martian surface will act as a reservoir to maintain a saturated or slightly supersaturated water vapor content in the atmosphere above it. Thus the model for water vapor content is one in which the lower atmosphere is saturated with water up to a height of some tens of kilometers. In this region water ice crystals will form whose size is dependent on temperature and height. The existence of these ice crystals can perhaps explain the blue haze, diurnal clearings of haze, the white clouds, blue clearings, and the clouds observed on the limb in the Mariner photographs and in other earth-based photographs. Water ice crystals cannot be invoked to explain the yellow clouds or the polar caps.

TABLE OF CONTENTS

<u>Title</u>	<u>Page</u>
Introduction	F-1
The Model for Atmospheric Water Vapor.	F-2
Particle Sizes in the Martian Atmosphere	F-3
Ice, Haze and Clouds	F-10
References	F-12

LIST OF ILLUSTRATIONS

<u>Figure</u>	<u>Page</u>
1 The Geometric Reflectivity of Mars	F-5
2 Gradual Variation of the Extinction Curve if the Imaginary Part of the Refractive Index is Varied, according to Computation by Johnson, Eldridge, and Terrell for $m = 1.29 (1-ik)$	F-6

LIST OF TABLES

<u>Table</u>	<u>Page</u>
1 Transmission Coefficient (p) and Specific Scattering of the Martian Atmosphere (a) and Reflectivity of the Surface (s).	F-4

WATER VAPOR AND ICE IN THE MARTIAN ATMOSPHERE

H. Heffner

July, 1967

INTRODUCTION

The existence of particulate material in the Martian atmosphere is attested to by a wide range of visible phenomena. They include the almost constant presence of "blue haze" and the formation, movement, and dissipation of several types of clouds. These clouds fall into classes termed: yellow clouds, white clouds, and blue clouds depending upon the optical wavelength where greatest contrast is observed. The blue haze refers to the obscuration of surface detail when the planet is photographed over a wavelength range in the blue and ultraviolet.

Many explanations have been tendered to account for the various types of clouds and for the blue haze. They have included hypotheses of great dust storms, of particles of water ice, and of particles of solid CO_2 . Each of these hypotheses was put forth before the 1965 Mariner IV occultation experiment revealed the pressure and temperature profile of the Martian atmosphere, and little re-examination of the models in the light of this new information has been carried out.

As a result of the occultation experiment¹, we now believe the Martian atmosphere is almost wholly composed of CO_2 with a surface pressure 4.1 to 5.7 mb. at the immersion point and a scale height of 8.5 to 9 km. The experiment seems to indicate an isothermal atmosphere to some 20 km or so above the immersion point having a temperature of 160°K (Fjeldbo, private communication). Since the surface temperature is some 60° to 90°K higher than this, we expect a thin atmospheric boundary layer where the temperature varies rapidly from perhaps 250°K at the surface to 160°K and then remains essentially constant with

height for perhaps the next 20 km. At the point of immersion (local summer night time) the surface pressure was approximately 9 mb with a scale height of 10.5 to 14.2 km. The atmospheric temperature was estimated to be 250°K to perhaps as low as 220°K.

Observations of water vapor absorption lines in the Martian atmosphere are rendered difficult by the Earth's own atmosphere, however, the experiment of Kaplan, Munch, and Spinrad² was sensitive enough to yield an estimate of the precipitable water above the Martian surface of $(14 \pm 7) \times 10^{-4}$ gm cm⁻². If one assumed a constant mixing ratio in the Martian atmosphere, then the scale height of 9 km would imply a surface density of H₂O molecules of $(2.75 \pm 1.37) \times 10^{13}$ cm⁻³ and for a temperature of 175°K, a surface pressure of 0.663 ± 0.332 microbars.

At this temperature, the saturation vapor pressure for ice is about .08 microbars, or almost an order of magnitude less than the pressure derived. Johnson³ has cited this discrepancy to question the accuracy of the measurement. It is reasonable to believe, however, that the summer hemisphere exhibits higher temperatures so that an integrated disc average would yield the amount of water vapor measured.

The value is sufficiently close to the saturated value that it suggests further investigation of the implications of a model Martian atmosphere which is saturated with water vapor and which contains ice crystals in a variety of sizes and numbers to account for most of the clouds and haze observed.

THE MODEL FOR ATMOSPHERIC WATER VAPOR

If our experience of Earth conditions is any judge, the outgassing of the Martian surface must have released immense amounts of water, yet very small amounts are observed in the atmosphere. The explanation probably lies not only in the fact that great amounts of water vapor probably escaped, but because

of the low temperature of the planet a considerable amount of ice exists on and below the surface. Even though this ice is likely to be in capillary fissures or covered with sandy material, it can act as a reservoir for water vapor to be given off to the even colder Martian atmosphere. Because the temperature declines rapidly with height in the narrow boundary layer just above the surface, the vertical mixing action of wind will attempt to keep the water vapor pressure above the saturation value for some distance up. The atmosphere of course cannot remain appreciably supersaturated for long until ice crystals begin to form and to grow in sufficient size and number that the partial pressure of H_2O is reduced to nearly the saturated value. As a result, we expect the partial pressure of water vapor to stay essentially constant at approximately the saturation value for a region extending perhaps to 25 km above the boundary layer. Mixed in will be small ice crystals of sufficient size and number to keep the partial pressure of H_2O near the saturation pressure in the face of vertical mixing from the boundary layer with its relatively high water vapor content. The value of 25 km is taken for the extent of this region principally because the Mariner IV data show this to be the region of constant temperature. Moreover, Leighton⁴ has interpreted a light area on the limb in a Mariner IV photograph as being a cloud with its top at 25 km.

It should be noted that even at saturation, water vapor would make up an almost negligibly small fraction of the total atmosphere. With the above model, even at 25 km the density ratio of water vapor to CO_2 is less than 10^{-6} at $160^\circ K$ and at the surface is less than 10^{-7} .

PARTICLE SIZES IN THE MARTIAN ATMOSPHERE

From extensive Russian observations of limb darkening, Opik⁵ quotes the following table of optical characteristics of the Martian atmosphere and surface.

TABLE 1
TRANSMISSION COEFFICIENT (p) AND SPECIFIC SCATTERING OF THE
MARTIAN ATMOSPHERE (a) AND REFLECTIVITY OF THE SURFACE (s).

Wavelength (A°)	p	a	s
4600 (Blue)	0.33	0.20	0.25
5200 (Green)	.54	.22	.29
5430 (Green-Yellow)	.60	.23	.34
5800 (Yellow)	.69	.24	.40
6400 (Red)	.74	.20	.53

Brooks⁶ plots the curve shown in Fig. 1 for the total albedo or geometric reflectivity of Mars showing a minimum in the vicinity of 3500 A°.

From these data we can gain some rough ideas concerning the size of the particles and their density. The intensity in a scattering atmosphere goes as

$$I = I_0 e^{-N\pi a^2 Q_{\text{ext}} \ell} \quad (1)$$

where N is the volume density of the particles, a their radius and Q_{ext} is the coefficient of extinction. Figure 2, taken from van de Hulst⁷ shows computed values of Q_{ext} for spheres with index of refraction of 1.29. The curve peaks for k near zero at a value of $2\pi a/\lambda \approx 6.5$. Taking this point to be the minimum reflectance point of Fig. 1 at 3500 A°, we find a particle diameter of $2a = 0.7$ microns. By matching the attenuation to the value given by Opik⁷ for 4600 A° we obtain $N\ell = 2.2 \times 10^7$ particles per square centimeter. This number is lower by an order of magnitude than that of Greenspan and Owen⁸ who derive a particle density required to bring into agreement pressures derived from both visible and ultraviolet measurements. Assuming the particles are ice with diameter of .7 microns, we

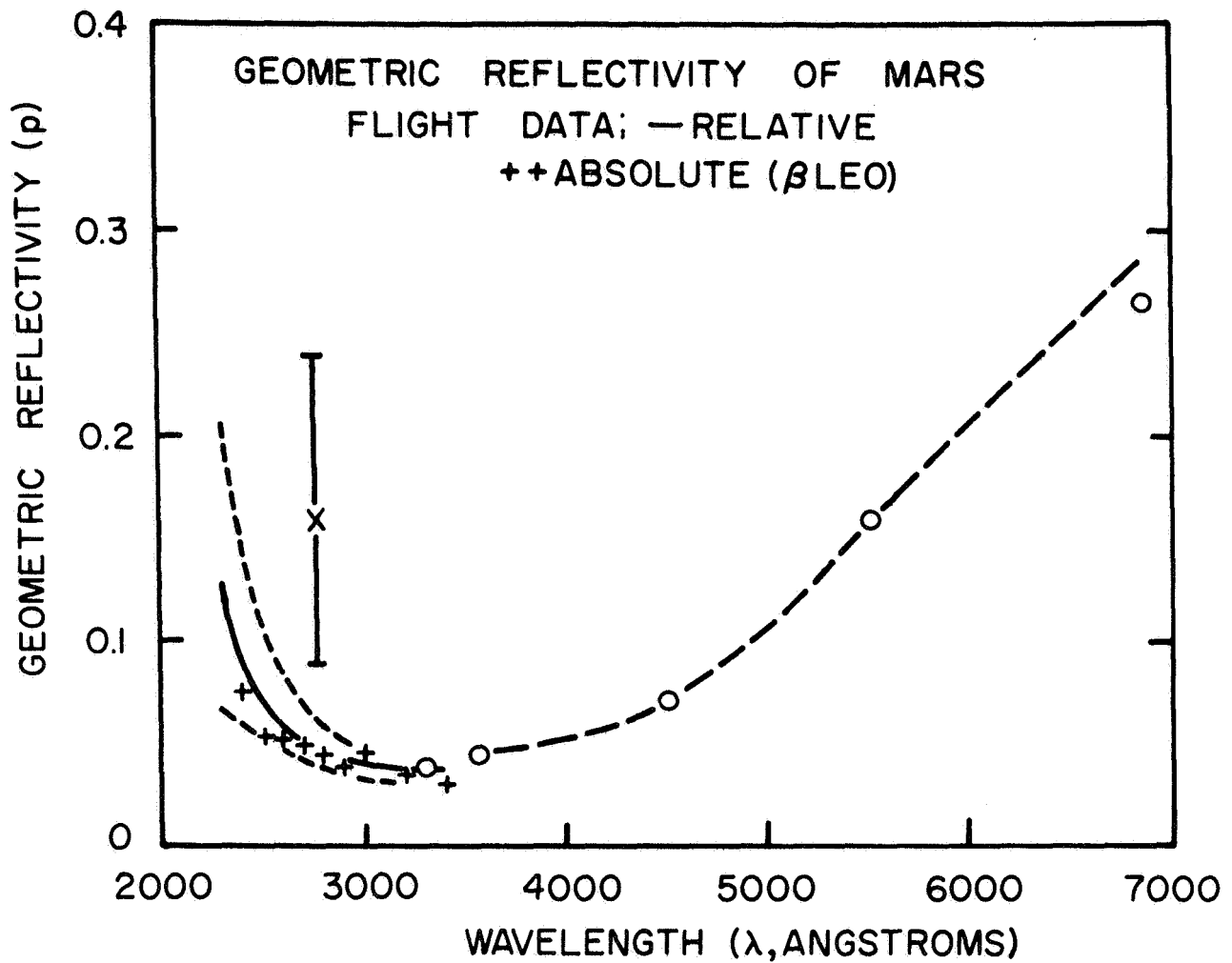


Figure 1 The geometric reflectivity of Mars. Solid line, relative data adjusted to 0.04 at 3400 Å; +, absolute reflectivity determined by comparison with β Leo, plotted independently. The dashed lines below 3400 Å represent the error range applied to the relative data.

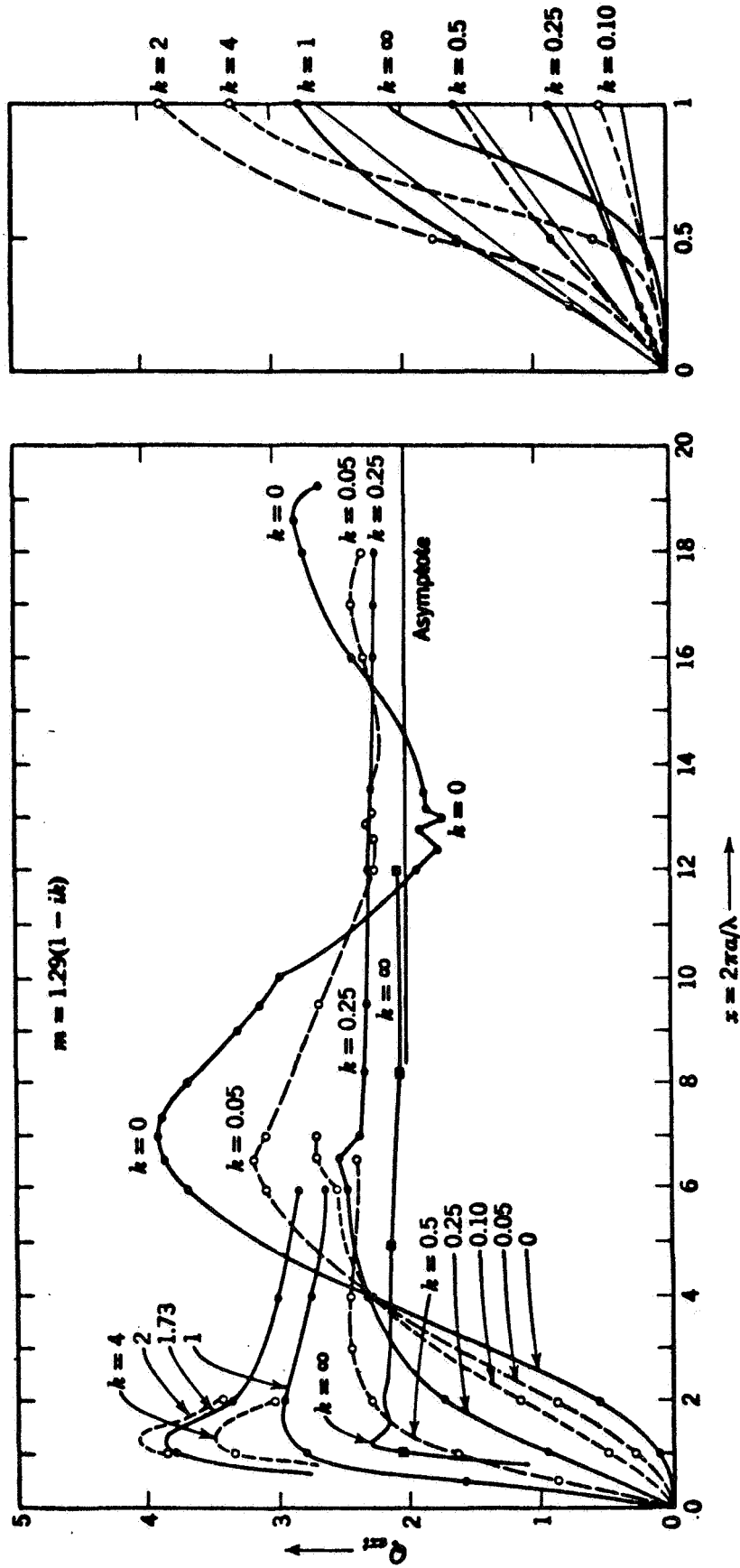


Figure 2 Gradual variation of the extinction curve if the imaginary part of the refractive index is varied, according to computations by Johnson, Eldridge, and Terrell for $m = 1.29(1 - ik)$.

find their total mass to be 4×10^{-6} gm/cm². This value is less than one hundredth of the observed amount of precipitable water vapor.

Ice crystals of this small size will stay suspended indefinitely. Being much smaller than a mean free path, their fall rate is governed not by Stoke's Law but rather by non-viscous flow considerations. The terminal velocity for these particles of radius a smaller than a mean free path is given by

$$v = \frac{4\rho ga}{3m'nv_a} \quad (2)$$

where ρ is the density of the particle, g is the acceleration due to gravity and m' , n and v_a are respectively the mass, number density, and average thermal velocity of the surrounding gas molecules. For particles of 0.7 microns diameter in the Martian atmosphere, the fall rate is approximately 0.04 cm/sec and is thus negligible in comparison to effects of winds.

The growth of the ice crystals is governed by diffusion. Thus, the rate of growth is given by

$$\frac{da}{dt} = \frac{1}{4\pi a^2 \rho} \quad \frac{dm}{dt} = \frac{D(p_w - p_i)}{\rho R_w T_a} \quad (3)$$

where D is the diffusion constant for water vapor, p_w and p_i are the ambient water vapor pressure and the vapor pressure of the ice crystal respectively, ρ the density of ice, T the ambient temperature, and R_w the specific gas constant for water vapor.

The vapor pressure of the ice crystal will be determined by its temperature according to:

$$p_i = Ke^{-L/R_w T_i} \quad (4)$$

where L is the heat of sublimation of water (2834×10^7 erg/gm), T_i is the temperature of the ice crystal, and K is a constant of

proportionality. Numerically, this equation becomes

$$P_i = (3.63 \times 10^7) 10^{-2670/T_i} \quad (5)$$

The temperature of the ice crystal is determined by the rate at which heat is transferred to or away from it. There are four main effects. First, heat is absorbed from the Sun at a rate which is determined by the solar constant on Mars, S the size of the crystal, and its absorption coefficient. If we consider a spherical crystal of radius a with an average coefficient of extinction in the visible due to absorption of Q_{abs} , then the rate of solar energy absorbed is

$$\frac{dH_1}{dt} = \pi a^2 Q_{abs} S \quad (6)$$

Heat is also radiated, primarily in the infrared and so there is a heat loss term of

$$\frac{dH_2}{dt} = 4\pi a^2 Q'_{abs} \sigma (T_i^4 - T^4) \quad (7)$$

In general, we expect Q'_{abs} to be smaller than Q_{abs} since the particle size is smaller compared to the wavelength in the infrared than in the visible region. However, the emissivity of ice is much greater in the infrared than in the visible region, so that the net effect is probably one of increasing the value of Q'_{abs} over Q_{abs} .

Heat is also gained or lost through sublimation or evaporation. This heat flow rate is

$$\frac{dH_3}{dt} = L \frac{dm}{dt} = \frac{4\pi a LD(p_w - p_i)}{R_w T} \quad (8)$$

Finally, heat is lost through convective cooling by the predominantly CO_2 molecules striking the crystal. Assuming the accommodation coefficient to be unity, this rate is

$$\frac{dH_4}{dt} = -\frac{3}{2} \pi a^2 P_{CO_2}(T) v_a(T) \left(\frac{T_i}{T} - 1 \right) \quad (9)$$

where $P_{CO_2}(T)$ is the pressure of CO_2 at the ambient temperature and height of the particle.

At equilibrium, we expect both $\frac{dm}{dt}$ and $\frac{dH}{dt}$ to be zero. Since cooling by thermal radiation is negligible compared to convective cooling, these two conditions yield $P_i = P_w$ and

$$\frac{T_i - T}{T} = \frac{\Delta T}{T} = \frac{2Q_{abs}S}{3P_{CO_2}(T)v_a(T)} \quad (10)$$

Using the vapor pressure-temperature relation, we find

$$\frac{P_w}{P_{sat}} = e^{\frac{2L}{R_w T} \frac{\Delta T}{T}} = e^{\left[\frac{4LQ_{abs}S}{3R_w T P_{CO_2}(T)v_a(T)} \right]} \quad (11)$$

Here p_{sat} is the saturation vapor pressure of water vapor at the ambient temperature and p_w is its actual ambient partial pressure.

The extinction coefficient due to absorption, Q_{abs} , for small particles is proportional to the radius⁹. For ice crystals such that $2\pi a/\lambda$ is small

$$Q_{abs} \cong -\frac{16\pi a}{\lambda} \text{Im}(m-1) \quad (12)$$

where m is the complex dielectric constant. Thus, if one knows the spectral variation of absorption of ice and the degree of supersaturation, (P_w/P_{sat}) , then he can compute the equilibrium radius of the ice crystals which are formed.

Several qualitative inferences can be drawn from the above relations. First, the crystal size should decrease with height. This effect results from the slower cooling due to reduced CO_2 pressure and the correspondingly smaller radius which the particle reaches before its temperature rises sufficiently for

its vapor pressure to equal the ambient value. Further, we expect that as the atmospheric temperature rises, the degree of supersaturation decreases and so does the particle size. Conversely, a decrease of atmospheric temperature causes crystal sizes to increase.

ICE, HAZE AND CLOUDS

This model of the Martian atmosphere is appealing since it can explain many of the visible features of Mars. As has been mentioned, the attenuation of the atmosphere can be attributed to the almost continual presence of minute ice crystal less than one micron in diameter. This blue haze is occasionally observed to clear over large areas in a matter of a few hours only to reform after a period of hours or days. This phenomenon seems impossible to explain if one assumes the scattering particles are dust and that clearings simply represent a settling of the windborne dust on the surface. Settling times for particles small enough to have the proper scattering characteristics are far too long to allow such rapid clearings. The model which accounts for the blue haze by ice crystals can allow for rapid clearings simply by atmospheric temperature increases which act to reduce the crystal size or conceivably, to cause them to disappear completely.

In addition to the blue haze there is a generally whitish haze which varies diurnally, tending to clear off by Martian noon and to reform in late afternoon¹⁰. Such a characteristic is precisely what one would expect were somewhat larger ice crystals responsible. Relatively large crystals would form in the cold atmosphere toward late afternoon and dissipate as the sun heats the atmosphere each noon.

Additional evidence tending to confirm the water vapor model arises from the polarization measurements of the white

clouds made by Dollfus¹¹. From his studies, Dollfus identified these clouds as being ice crystal mists.

Water ice cannot explain either the polar caps or the yellow clouds. Because of the very small amount of water vapor present even at saturation, unreasonably high wind velocities would have to be invoked in order to account for the transfer of water from pole to pole as the seasons change. It is much more reasonable to believe that the polar caps are composed of solid CO₂ and that the clouds observed immediately over them are CO₂ crystals rather than H₂O.

The yellow clouds must be composed of considerably larger particles than those responsible for the blue haze and white clouds. This fact can be inferred in part from the characteristic yellow color which would be difficult or impossible to obtain from Rayleigh or Mie scattering, and in part from the settling time determined by the cloud durations. The particles must be 10 microns or more in diameter¹² and the color must be characteristic of their composition. The standard explanation suggests they are dust particles transported upward by winds, by volcanic activity or by meteoric impact. It appears to be impossible to raise sufficient dust by meteor impact to account for the extent of the clouds observed if one assumes a meteor size-frequency distribution compatible with the crater counts made on the Martian surface¹³. One is then left with the hypothesis of volcanic origin--for which there is no evidence--or of wind. The latter seems more probable.

REFERENCES

1. Kliore, A., D. L. Cain, G. S. Levy, V. R. Eshleman, G. Fjeldbo, and F. D. Drake, "Occultation Experiment: Results of the First Direct Measurement of Mars' Atmosphere and Ionosphere," Science, 149, pp. 1243-1248, (1965).
2. Kaplan, L. D., G. Münch, and H. Spinrad, "An Analysis of the Spectrum of Mars," Astrophysics J., 139, pp. 1-15, (1964).
3. Johnson, F. S., "Atmosphere of Mars," Science, 150, pp. 1445-1448 (1965)
4. Leighton, R. B., and B. C. Murray, "Behavior of CO₂ and Other Volatiles on Mars," Science, 153, pp. 136-144, (1966).
5. "Opik, E. J., "The Martian Surface," Science, 153, pp. 255-265, (1966).
6. Brooks, E. M., "Comprehensive Summary of Available Knowledge of the Meteorology of Mars and Venus," GCA Corp. NASA CR-786, p. 30, (May, 1967).
7. van de Hulst, H. C., Light Scattering by Small Particles, John Wiley and Sons, New York, 1957.
8. Cann, M. W. P., W. O. Davis, J. A. Greenspan, and T. C. Owen, "A Review of Recent Determinations of the Composition and Surface Pressure of the Atmosphere of Mars," I.I.T. Res. Inst. under Contract NAS 5-9037, NASA CR-298, (1965).
9. van de Hulst, op. cit. p. 70.
10. Robinson, J. C., "Ground-Based Photography of the Mariner IV Region of Mars," Icarus, 5, pp. 245-247, (1966).
11. Dollfus, A., "Study of the Planet Mars, 1954-58," Annales d'Astrophysique, 28, pp. 722-747, (1965).
12. "Opik, E. J. op. cit.
13. Collins, R. J., private communication

APPENDIX G
(Report of 1967 Summer "TYCHO" Meeting, TG # 31)

THE VENUS ATMOSPHERE:
FUTURE EXPERIMENTS
AND PRESENT KNOWLEDGE

J. J. Hopfield and R. A. Phinney

July, 1967


Contract No. NSR-24-005-047

Prepared by

UNIVERSITY OF MINNESOTA
Minneapolis, Minnesota

For

HEADQUARTERS, NATIONAL AERONAUTICS & SPACE ADMINISTRATION
Washington, D. C. 20546



THE VENUS ATMOSPHERE:
FUTURE EXPERIMENTS AND PRESENT KNOWLEDGE

ABSTRACT

A review of present knowledge of the parameters most important to an understanding of Venus stimulates vital questions about the systematics of the lower atmosphere and its interaction with the surface. An atmospheric sounder (or entry probe) is proposed as a logical initial investigation to help satisfy most of these questions. General requirements for sensors and other devices to sample various characteristics of the atmosphere during the probe are included. The paper is concluded with a series of recommendations concerning the composition, design development, and operation of the proposed entry probe that are hoped will be helpful to planners considering further investigations of the planet Venus.

TABLE OF CONTENTS

<u>Title</u>	<u>Page</u>
Introduction	G-1
Present Knowledge.	G-2
Atmospheric Sounder.	G-7
Engineering Sensors	G-8
Thermodynamic Sensors	G-9
Composition of the Atmosphere	G-10
Radiation Environment	G-11
Composition of the Clouds	G-13
Discussion and Recommendations	G-13

THE VENUS ATMOSPHERE: FUTURE EXPERIMENTS AND PRESENT KNOWLEDGE

J. J. Hopfield and R. A. Phinney

July, 1967

INTRODUCTION

This paper begins with a brief review of the present knowledge of the parameters most important to an understanding of Venus. The principle thesis of this paper is that in view of this knowledge the most crucial questions about Venus concern the systematics of the lower atmosphere and its interactions with the surface. The answering of the question "what is the physical and chemical nature of the atmosphere, clouds, and surface of Venus" should motivate the planning of missions to Venus in the immediate future. Recommendations arising out of this paper are given in the discussion section.

In planning missions to the neighborhood of Venus it is essential to emphasize the great importance of an atmospheric sounder relative to a fly-by or an orbiter. Admittedly, any Venus probe which uses the "bus" method will have available a relatively large spacecraft which does not enter the atmosphere. We do not quarrel with using the bus as an experimental platform, but feel that first priority should be given to making it as effective as possible in support of the drop-sonde. We want to deliberately contrast this paper, with its strong emphasis on priorities, with other documents which regard all potential experiments as being equal in some sense, subject only to engineering constraints. (Reference JPL reports). In spirit, we follow the approach of the 1965 Space Science Board summer study, (Space Research: Directions for the Future; NAS-NRC publication 1403; 1966), but hope in addition to add to the general priorities stated therein by specific consideration of the most crucial experiments.

The experiments on a Venus mission can be divided into two broad classes. One is concerned with the physics of a tenuous atmosphere and ionosphere and its responses to the solar radiation and particle flux environments. The second is concerned with the lower atmosphere and its relation to the solid planet. There is extremely little which can be conclusively derived of fundamental interest to the second set of experiments from the first set. In addressing ourselves to the logical next step of this second problem, of interest to geology, astronomy, cosmology, and biology, we can virtually ignore the state of knowledge of the upper atmosphere.

The only experiment likely to give further information on the basic atmospheric problem of Venus before the 1972 Mariner flight is the S-band occultation experiment on the current Venus probe. Even if successful, it cannot represent the major breakthrough for Venus that it did for Mars. While many detailed observations can be made on the ground, their nature has not and will not permit a decisive breakthrough on the Venus atmosphere problem.

The first part of the following material discusses the state of knowledge of the physics and chemistry of the Venus atmosphere as an aid to understanding:

- a) why the atmospheric problem is not solvable from remote sensing;
- b) why the atmospheric question is at present the important question on Venus; and
- c) what parameters are of relevance.

The second part discusses the instrumentation of a sub-sonic atmospheric sounder designed to answer the most relevant questions.

PRESENT KNOWLEDGE

The gamut of conventional photographic, spectrometric, and radio and radar astronomy studies have been performed on Venus.

The most important conclusions of these studies are:

1) Venus is covered by "clouds" at an altitude of about 35 kilometers above the surface. This cloud cover has structure, but the surface of the planet has never been observed through rifts in the clouds.

2) The cloud-top temperatures are of the order of 250°K. The cloud-top pressure is in the .05 - 1 atmosphere range. There are several independent methods of determining these "pressures" and "temperatures" from ground-based astronomy. (These methods do not directly measure temperature and pressure. Differences between the results obtained by different methods are expected and do occur.) There are observed (and probably real) temporal variations of the deduced temperatures and pressures.

3) The combination of radar and radio astronomy show that the mean surface temperature of the planet is about 620°K, with a 150° day-night difference, and a relatively small north-south difference.

4) CO₂ is a sizable constituent of the atmosphere, although it is probably diluted by a major and yet unidentified component such as N₂ or A.

These important questions arise from the observations:

a) What is the physical, chemical, and geological nature of the atmosphere, clouds, and surface?

b) Is this nature of the planetary surface a logical consequence of minor differences between the initial conditions of Earth and Venus, or were there important differences in the initial conditions at the time and place of the formation of Earth and of Venus?

c) Has (or will) Venus go through a thermal and chemical configuration hospitable to the development of life?

Much speculation has been written on these three questions. In spite of this, the questions are far from being satisfactorily answered. The logical dependencies of these questions necessitate

answering the first one first. The Venus space missions in the near future should be designed for the explicit purpose of answering this question.

The Venus atmosphere keeps the planetary surface at a temperature almost twice that to be expected from an atmosphere-free planet the same distance from the sun. The origin of this "greenhouse" effect is a major puzzle.¹

Super-adiabatic lapse rates (vertical temperature gradients) in an atmosphere are not stable. As a result, there is an upper limit on the mean temperature gradient in an atmosphere. For all likely gasses, this puts an upper limit of $7^{\circ} - 10^{\circ}$ /kilometer on the Venus atmospheric temperature gradient. This lapse rate is consistent with estimates of the thickness of the atmosphere. It immediately leads to an estimate of the surface pressure of the order of 10-20 times the cloud-top pressure, i.e. $\sim 1-20$ atmospheres. The uncertainty in thickness and lapse rates lead to a large uncertainty in the surface pressure--a design range of 1 - 100 atmospheres should be allowed. A common feature of all models (in order to fit the observed data) is a thick, quasiadiabatic atmosphere.

Cooling of the lower atmosphere (and surface) by radiation (and convection) tend to reduce the temperature gradient in the lower atmosphere. A high infrared opacity is essential to avoiding such radiative cooling. The three model mechanisms which have

¹Throughout this paper we will presume the surface temperature is $\sim 650^{\circ}\text{K}$. Although this is by far the most likely interpretation of the relevant data, there is in an indirect line of argument always some small possibility of gross misinterpretation. This possibility seems small enough that it need not be discussed here. On the other hand, it would be both scientific and engineering folly not to design experiments with sufficient dynamic range to cope with a possible lower surface temperature and much lower greenhouse effect.

been proposed for such opacity are:

- 1) gaseous CO_2 and H_2O at reasonable (1 - 10 atm) pressures.
- 2) Pure CO_2 with a high pressure atmosphere.
- 3) Dense clouds of particulate matter having appropriate particle sizes and opacities.

With a planetary surface temperature of 650° and a cold top of its upper atmosphere, general heat conduction processes will necessarily result in some upward heat flow by convection, radiative conduction, and/or precipitation and evaporation. For heat balance a source of heat at the surface is required. The models proposed for this heat source include

- 1) penetration of solar radiation in the visible
- 2) internal heat release
- 3) frictional heating of the surface by high velocity winds
- 4) a "thermal engine" driving adiabatic compression.

The first of these is the mechanism by which the "greenhouse" is driven on the earth. The second is feasible if Venus is at present passing through a period of intense volcanism. The third and fourth note that the winds produced by insolation differences will drive circulation patterns which themselves can be used to heat the surface. The third mechanism uses frictional heating from these winds, while the fourth uses this circulation to adiabatically compress high altitude air (raising its temperature) while carrying it downward toward the surface.

All models take into account some form of cloud cover. The three cloud materials most seriously suggested are CO_2 (solid), H_2O (solid or liquid), and non-volatile inorganic solid dust particles. The presumed role of the clouds ranges in models from 1) transparent in IR; barely opaque in visible to 2) very dense and opaque at all wavelengths. The observed albedo of Venus is explicitly due to the cloud cover and determines the heat balance and "infrared temperatures" of the outer atmosphere.

The present atmosphere can be regarded to be in (perhaps evolving) equilibrium. On a short time scale, the atmosphere must by some mechanism maintain its heat balance, cloud cover, and a stable composition in spite of perturbations. (There is such a stabilization, for example, in the earth cloud cover.) The partial pressures of some of the constituents are also likely to be quantitatively understandable from the appropriate equilibrium. For example, the O_2/CO_2 ratio on the earth is maintained by plant life. The CO_2 pressure on Mars is probably regulated by the temperature of its north polar cap. On the high temperature Venusian surface, carbonate-silicate reactions are likely to buffer the CO_2 partial pressure. The relation between the surface, cloud, and gaseous atmospheric components is thus a problem any atmospheric model must try to understand.

The variety and cleverness of ground-based observations of Venus have yielded an incredible amount of detailed information on Venus. The interpretations of this information are chiefly indirect. The great diversity of models now still "in agreement" with the observational data is a consequence of this indirect relation between theory and experiment. At this point, it is not likely that a few more years of conventional observations will produce any definitive progress in the understanding of the Venus atmosphere. When, on the other hand, a correct zero-order model for the atmosphere is given, presently available data will add much to the understanding of this atmosphere.

In the period of time between now and the sending of the next interplanetary mission to Venus (Mariner 1972 or Voyager 1973) the following fundamentally new information is likely to be added to our knowledge of Venus.

- 1) An S-band occultation experiment yielding the atmospheric number density and temperature profile in the upper atmosphere. Interpretational problems and atmospheric attenuation are unlikely to allow the extension of the altitude of this profile below an

altitude of 5 - 20 kilometers, or to pressures over 2 - 3 atmospheres.

2) A map of the radar reflectivity with a resolution of the order 1/40th of the planetary diameter will be made.

3) The atmospheric attenuation of Venus at radar wavelengths will be known at several more wavelengths and with greater precision.

In addition, much more information on the spectroscopy of the cloud top layer and its variability, the distribution of surface heights and surface slopes, the surface distribution of radio emission, and the physics of the Venus ionosphere will be available. Only the S-band occultation, however, makes any real progress toward a detailed understanding of the bottleneck in the scientific study of Venus, namely the understanding of the general atmospheric problem.

ATMOSPHERIC SOUNDER

For the sake of this discussion, we will posit an entry probe whose experiments weigh a few tens of pounds, and which is slowed to subsonic fall at an atmospheric pressure of about 5 millibars. It is possible to design a group of experiments which will answer the present major questions about the atmosphere. The probe will require at least two minutes to pass to the 1 atmosphere level, and several minutes more to reach the solid surface, depending on the drag coefficient of the probe and the atmospheric pressure profile. No special provision is made for these experiments to be usable at ionospheric or supersonic altitudes. It is assumed that the data will be telemetered essentially in real time, and that the probe will land "hard." (It would be desirable for the probe to survive landing as a working device, but this must be given low priority at this time.) The (probable) high surface temperatures present obstacles to the survival of conventional instrumentation; the short-term viability of the package at high temperatures is essential,

however, since the most important single objective is to determine the position, pressure, density, and temperature within a kilometer of an identifiable solid surface.

Engineering Sensors

We now discuss the following engineering sensors which are required more or less independent of other experiments.

1) Accelerometer. - To be integrated to give the position of the probe. If the dynamic response of the probe is well enough known, then an effective density can be inferred. With another instrument to measure density, the accelerometer data can be used to infer vertical winds. Only an x axial (z) component is needed for the important altitude determination; the other two would give horizontal winds, and can probably be justified only for their diagnostic engineering value.

2) Radar Altimeter. - This is needed to fix the relative position of the probe and the planetary surface.

3) Communication Link. - It is possible to phase lock the carrier to an oscillator at the master station (bus or ground station). Integration of the doppler shift gives an optical path distance to the probe. It is not clear that this data adds anything essential to the information from the accelerometer and altimeter, although redundance may be desired. There seems to be no real reason to want to measure refractivity of the atmosphere if the variables of real interest are to be determined directly.

4) Thermal Sensors. - Thermal regulation of the probe is required both to cool the infrared sensors and to preserve the electronics at the high near-surface temperatures. The necessity of having engineering thermal data suggests that all thermal sensors be designed as a compatible system, including those sensors designated specifically to measure the local atmospheric temperature.

Thermodynamic Sensors

We next describe the group of sensors for determining the local thermodynamic properties of the atmosphere. Little elaboration is needed; the instrumentation is well understood.

1) Atmospheric Temperature. - One or more temperature sensors for determining the kinetic temperature of the atmosphere, appropriately shielded from radiation and appropriately placed so that the heating produced by the probe can be determined.

2) Atmospheric Pressure. - One or more pressure sensors. By situating one at a point where the relative motion of probe and atmosphere are small, and one directly in the airstream for a dynamic measurement, both pressure and airspeed would be obtained.

3) Atmospheric Density. - Direct density measurement. This can be done easily by measuring the beta absorption of a short column of "air". In conjunction with P and T, this gives a mean molecular weight (M).

4) Velocity of Sound. - A measurement of the acoustic resonant frequency of a short open column or enclosure will give c. Since $c = (\gamma RT/M)^{1/2}$, the quantity inferred is γ , which implies a weighted measure of the polyatomicity of the atmosphere.

In principle, the determination of M and γ is made redundant by the presence of a mass spectrometer experiment. This redundancy is probably worth having for various reasons: (1) Both sensors are extremely simple; (2) For a mass spectrometer of limited resolution and dynamic range, various isotopes of C, O, and N will complicate the interpretation; (3) Strong inferences can still be made about the major atmospheric constituents even if the mass spectrometer fails to operate or is deleted from the mission.

The entire group of sensors should be interrogated at a rate which will produce data at least once every kilometer...at least once in three seconds. Of particular note is the need for dynamic range in the pressure and density experiments; P will range from about .005 to possibly 100 atmospheres and n from .01

to $120 \times 10^{19} \text{ cm}^{-3}$. If necessary, multiple sensors with different sensitivities and saturation levels must be incorporated.

Composition of the Atmosphere

We now consider the major experiment aimed at determining the composition of the atmosphere...a mass spectrometer. Since 1954 a number of low-weight non-magnetic instruments have been flown on rockets and satellites in the study of the earth's upper atmosphere. The difficulties present in the interpretation of much of this data have not been minor, and the art may be regarded as being possibly in adolescence at this time. Although the lower atmosphere of Venus might be thought to be an easier experimental subject, by analogy with the Earth's lower atmosphere, no experience exists, to our knowledge, in the mass analysis of the troposphere and lower stratosphere from drop-sondes. We recommend that the ability of a mass analyzer to determine the "exact" atmospheric composition of Venus be regarded very conservatively until suitable instruments have been built, tested, and calibrated under various conditions.

No specific design recommendations are offered for the instrument. Nonmagnetic designs which have been successfully flown in upper atmosphere studies include radio frequency, time-of-flight, and quadrupole mass spectrometers. Typical resolution separates mass numbers up to about 50, and a dynamic range of mass current of about 10^4 is more than adequate to answer the first-order questions about the atmosphere. We do suggest that mechanical moving parts are quite undesirable and that an entrance leak system which takes advantage of the flight profile (into progressively high pressures) is to be desired. It is not clear that the ability to perform at pressures over a few atmospheres would be of any real importance, due to the certainty that the lower atmosphere is well-mixed. (Knowledge of composition in nonequilibrium microenvironments in the tens of meters

immediately above the solid surface is of course desired, but we cannot regard this information as being of very high priority at the present time.)

Radiation Environment

We now consider the class of experiments which measure radiation fluxes in different directions and different wavelength ranges. Since the number of possible measurements and bits of information is very large indeed, selection of a very few experiments must be made on the basis of their pertinence to answering the most important questions. The particular "mix" of sensors suggested here is not in any sense the best that can be proposed, but should be typical of the genre.

Some of the questions which can be answered by photon detection are discussed:

1. Where are the clouds located? - The tops of the clouds would be identified by a detector looking directly at the sun in the visible. The bottom of the clouds would be detected by comparing the outputs of up- and down-looking detectors (assuming an optically transparent atmosphere below a given level and a surface of albedo around 5-30%). The existence of structure, such as well-defined cloud decks or cellularity could be inferred in some vague sense by having for comparison a third detector looking horizontally.

2. What is the water vapor profile in the atmosphere? - This question should be answered by the mass spectrum. Since we are consistently looking for alternative sources of composition data, we will consider a spectroscopic method. The most direct method is to measure the absorption of the solar flux in a water vapor absorption line. The solar flux is strong at 2 microns, but scattering by the clouds hurts the interpretation at a shallow depth in the clouds. A 6 micron experiment would work deeper in the clouds (absorption due to scattering would be down by $3^4 = 81$). At more than one or two optical depths in the clouds, the absorption

measured in a band is determined by the mean photon path in multiple scattering; in principle, one could make an indirect determination of H₂O in the clouds by comparing the 2 and 6 micron absorption with side-looking and solar-looking detectors. The law of diminishing returns has set in, and the mass spectrum is the best bet for measuring water vapor in the lower atmosphere. The independent determination of water in the upper atmosphere is still of real value, since a knowledge of its vapor pressure at the cloud tops should tell whether or not the clouds are ice. A direct measurement of the cloud composition is quite difficult, and redundancy of this sort is highly desirable.

3. What is the radiation balance in the atmosphere? - This question is general, and aimed at the theoretical understanding of the atmospheric dynamics. The measurement appropriate to the usual radiative transfer models is to determine the intensity of the upgoing and downgoing radiation streams throughout the visible and infrared as a function of wavelength. Disregarding this is altogether too grandiose, we suggest experiments in two bands: (1) the broad optical band, to detect the total flux in the solar black body curve, using an ordinary photodetector in the range .35 - 2.0 microns; (2) the broad thermal infrared, to detect the radiation streams due to thermal emission by the planet and the atmosphere, using an ordinary bolometer, in the range 4-20 microns. For each band, an upward looking and a downward looking detector with large solid angles of acceptance (to include the sun), and a side looking narrow-angle detector (to determine scattered photons) are suggested.

If all the above suggestions are brought together, we find that optical band detectors are relevant to both the cloud location and the radiative balance problems. Due to the importance of scattering in determining the radiation field within clouds, side looking sensors are of general use. A fairly simple measurement of absorption in a water band is of real use above the clouds, dubious at lower levels. Detection of CO₂ absorption

above the clouds in the same way is of course possible. Since CO_2 information is implicit in the mass spectrum, the speed of sound, the density, and the infrared balance measurements, we suggest that any additional redundance is probably not worthwhile.

Composition of the Clouds

The clouds are postulated to be water, CO_2 , "dust", and various aerosol mixtures which involve "dust" and other constituents. The lifetimes and falling rates of droplets and particles in the size range .1 - 10 microns are wholly consistent with any composition. Considering the very low particle densities needed to produce opacity on a several km path, it is out of the question to consider a direct sampling. The only technique which has come to our attention that would have any real chance of working involves detection of cloud particles by counting scintillations in a sample tube through which the air is passing. By passing the stream into higher temperatures, a second scintillation count would determine the amount of evaporation. This experiment is specific for H_2O clouds. CO_2 clouds can be inferred if the temperatures are low enough and the H_2O test is negative. With a negative H_2O test and temperatures above 220°K , dust can be inferred. It is evident that careful temperature regulation is needed, and that the experiment is not a very "clean" measurement. Since the cloud composition is an important first-order question, every effort must be made to devise a workable test, of this sort or any other.

DISCUSSION AND RECOMMENDATIONS

The atmospheric entry probe and experiment set discussed here are derived from a "pure" approach, by considering the major questions about Venus and looking for a workable set of crucial experiments. From this point of view our major recommendations are:

(1) The purpose of an entry probe must be the study of the lower atmosphere ($p > 5$ mb) and the clouds. Study of the upper atmosphere and ionosphere, while representing a technology traditionally connected with the space program, implies the measurement of quantities in the Cytherean environment which are at best only imperfectly known for the Earth. A real sense of priorities demands that the spacecraft and probe be designed as far as possible for the prime mission of lower atmosphere study.

(2) Interpretation of data from the probe experiments is an indirect process, and the different results are strongly inter-related, (e.g. mean molecular weight as a clue to major constituents, and water vapor at cloud tops as a clue to cloud composition). The integration and intercalibration of the experiments, and the matching of these to the needed environment (primarily a thermal problem) are a formidable systems design problem.

(3) For this reason the planning of the probe system and the construction and testing of prototype experiments should begin as soon as possible.

(4) Since the probe will be essentially unique, the selection of an integrated science package should precede the specification of a fixed engineering environment, subject to as few constraints as possible (probable ones being weight, general shape, and communication capability).

Our recommendations should be viewed as follows in terms of current plans for planetary exploration:

(1) If a Mariner class of spacecraft can be devised as an entry probe, then we urge consideration of a probe of the sort discussed here. If a Mariner probe is possible only at the expense of many of the proposed experiments, we suggest that the minimum configuration which could be tolerated would do the following:

- a) Determine the pressure, density, and temperature just above the solid surface;

b) Measure the atmospheric mass spectrum just above the clouds.

(2) If the Voyager program goes as scheduled, then an early entry probe along the lines of this report is strongly urged. We recognize that some questions may arise between an early Mariner probe or a somewhat later Voyager probe. The resolution of this question must depend upon specific times, weights, etc.

APPENDIX H
(Report of 1967 "TYCHO" Summer Meeting, TG # 31)

RESONANT AND NONRESONANT
SPECTROSCOPY OF VENUS

B. Lax

November, 1967


Contract No. NSR-24-005-047

Prepared by

UNIVERSITY OF MINNESOTA
Minneapolis, Minnesota

For

HEADQUARTERS, NATIONAL AERONAUTICS & SPACE ADMINISTRATION
Washington, D. C. 20546



RESONANT AND NONRESONANT SPECTROSCOPY OF VENUS

ABSTRACT

The object of microwave, millimeter, and infrared spectroscopy has been to provide information about the atmosphere of Venus. Measurements at microwaves and millimeter radiometry have provided data about the temperature of the surface of Venus of about 600°K . In addition, radar measurements have given the best value of the dielectric constant of approximately $\epsilon = 5 \pm 1$. However, better data can be obtained if further measurements with improved equipment are taken in the wavelength region between 3 and 30 cm. The limit of error can be reduced. The nonresonant character of the microwave radiometric data suggests pressure broadening of the emission lines. However, infrared data at shorter wavelength would show a definite resonance, and in the wavelength range of 1 to 10 microns the quantitative nature of the CO_2 , CO , H_2O , and even other weaker possible components could be determined from orbiting satellites about Venus and Earth-based instruments on high altitude, airborne or near satellite vehicles.

TABLE OF CONTENTS

<u>Section</u>	<u>Page</u>
Introduction	H-1
Microwave Spectroscopy	H-2
Infrared Spectroscopy	H-6
General Comments	H-8
References	H-11

ILLUSTRATIONS

<u>Figure</u>	<u>Title</u>	<u>Page</u>
1	Radar Reflectivity of Venus	H-5
2	The Near-Infrared Solar Spectrum	H-9

RESONANT AND NONRESONANT SPECTROSCOPY OF VENUS

Benjamin Lax

November, 1967

INTRODUCTION

Among our neighboring planets the atmosphere of Venus has been one of the most intriguing puzzles. To date almost all of our information has been obtained from ground-based observations. Unlike Mars, which has now been studied by a fly-by spacecraft whose occultation measurements have confirmed and sharpened the terrestrial data, we still have a great deal of uncertainty concerning the possible constituents in the atmosphere of Venus. Even the magnitude of the total pressure of the components is unknown, much less the partial pressures. Among the likely candidates, which consists of CO_2 , H_2O , N_2 , and CO , in addition to some small concentration of inert gases, only CO_2 is specified with some certainty quantitatively, namely about 10^5 cm atm (NTP) as deduced from spectroscopic observations¹. It is assumed that CO_2 gas is much below the cloud layer, although some investigators have proposed that the clouds may have been CO_2 particles in crystal form. The temperature deduced from radiometric measurements at different regions of the electromagnetic spectrum is too high to substantiate such a hypothesis. In regard to water vapor there is a great deal of controversy as to its presence, although the balloon experiments of Strong and co-workers² in the near infrared indicate traces of water vapor in the Venusian atmosphere. There is less certainty regarding the other two likely candidates, namely N_2 and CO . The problem in each case, therefore, is to devise techniques within the present state of technology to determine (1) the composition of the atmosphere, (2) the quantitative features of the constituent gases,

(3) the structure and distribution of the constituents in the atmosphere. In addition to this type of information, radar and radiometric data can, in principle, determine the dielectric constant and the temperature of the surface of Venus in addition to providing qualitative information about the atmosphere of the planet. However, even the quantitative nature of the dielectric constant is now debated. In analyzing the microwave radiometric studies of Mariner II, Pollack and Sagan³ deduce an absorbing cloud of liquid water droplets as the primary source of capacity. If the dielectric constant is assumed to be $\epsilon = 3.6$ at 19 mm, then they propose an adsorbing and scattering atmosphere containing dust, hailstorms or large raindrops with particle radii of 0.5 mm. The most recent consensus, which is based on the consistence of the microwave and infrared data⁴, favors water vapor and ice clouds as against dust particles as the cause for the opacity of the Venusian atmosphere.

MICROWAVE SPECTROSCOPY

Microwave measurements have been carried out by radar⁴ and radiometric techniques from a few centimeters to about 10 meters with varying degrees of accuracy. The radiometry has actually been performed over a modest band in the 1.35 cm region of the water vapor absorption line without definitively indicating resonances⁵. Thus, to date the microwave measurements have been substantially a method of nonresonant spectroscopy. However, these measurements have been very valuable in defining critical problems which indicate future directions. The radiometry as a function of wavelength has clearly defined two ranges of temperature. At the longer wavelength of several centimeters, the temperature that is deduced is of the order of 600°K and is believed to be that of the surface of Venus. In the region of one centimeter or less the temperature drops to below 400°K. The interpretation of this is that the shorter wavelengths are measuring the temperature of the clouds in the upper atmosphere

of Venus. Another important confirmation is the radar reflection which is substantially higher in the longer wavelength region at 10 cm and above and substantially reduced at 3.8 cm. This is believed to indicate atmospheric absorption by gaseous molecules, although an alternate mechanism of scattering and absorption by particulate material is also a possibility. Much theoretical speculation for resonant and nonresonant absorption has been stimulated by the former. Unfortunately, the radar data has such large limits errors, particularly at long wavelengths, that theoretical analysis will not differentiate between the two types of absorption much less identify the constituents. However, better data may bring about greater consistency with one model of the composition than another and reduce the uncertainty of the total absorption. The same approach may be applied to the determination of dielectric constant which is obtained both from radar data and microwave radiometry. The value of the estimates have varied from about 2 to 7 with the radar favoring a higher value. The uncertainties in the data combined with atmospheric absorption may account for the large discrepancies. Consequently, it is important to refine and extend these measurements since the microwave measurements are the only tools today that can provide information about the solid surface of Venus. Now that the temperature of 600°K has been verified by the successful soft landing of the Russian capsule on the surface of the Moon, ground-based, airborne, and space-borne microwave instrumentation has an excellent opportunity for increasing our qualitative and quantitative knowledge of the Venusian surface and atmosphere.

Let us consider the radar reflectivity data as a function of wavelength. This is shown in Fig. 1 as reproduced from Evans and Pettengill⁶ with their indicated error bars. The data shows that the 3.8 cm measurements in which the reflectivity is small, nevertheless is most accurate. If we then accept this information and postulate that at long wavelengths the radar reflectivity is determined by dielectric constant of the surface which is assumed

to be relatively smooth (the roughness parameter is small), then we can draw horizontal curves at long wavelength. The reflectivity is given by:

$$R_{\infty} = \frac{(\sqrt{\epsilon} - 1)^2}{(\sqrt{\epsilon} + 1)^2} \quad (1)$$

where ϵ is the dielectric constant of the surface. These are indicated on the righthand side of Fig. 1. If we further assume that at shorter wavelengths the absorption is due to the tail end of a Lorentzian resonance associated with rotational transitions of molecular constituents, the absorption is proportional to the square of the frequency. Of the likely constituents the closest resonance is that of water at 1.35 cm all other possible resonances occur in the millimeter and submillimeter range. Hence, the reflectivity can be represented by a simple expression of the form:

$$R = R_{\infty} e^{-\frac{\alpha}{\lambda^2}} \quad (2)$$

The ratio R/R_{∞} is most often written as σ/σ_0 the ratio of the effective radar cross section where the cross section $\sigma_0 = \pi a^2$ is that of a sphere of radius a with a smooth surface. Hence as in the long wavelength limit, in the case of Venus the reflection depends on the dielectric constant as in Eq. (1). At shorter wavelengths the effective radar cross section or reflectivity is reduced by the absorption in accordance with Eq. (2). But we know one point with greater certainty than the others; namely, R at 3.8 cm. If we take this and the value R_{∞} , we can draw a family of curves for different values of the dielectric constant. (These curves do not reflect the uncertainty of the 3.8 cm point.) From the plot it appears that the dielectric constant of 2.2 from the microwave polarization data is outside of the error limits. The radar data would indicate from these curves that a dielectric constant of 4 to 6 would be a reasonable value or $\epsilon = 5.0 \pm 1.0$.

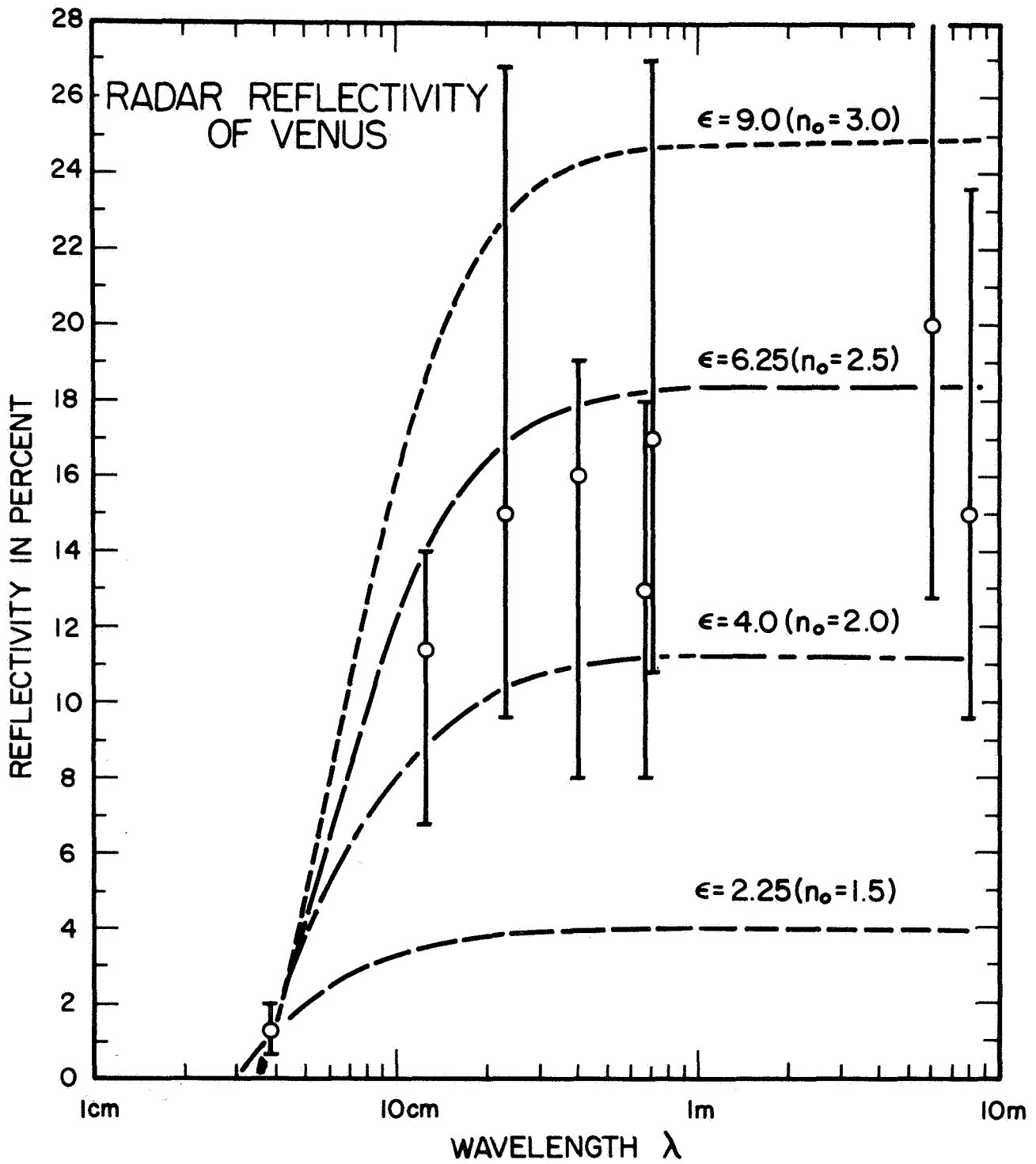


Figure 1. Radar Reflectivity of Venus.

More important, the results indicate that with present techniques data could be obtained which would yield such a curve from about 4 cm to 23 cm with considerably reduced error. This would determine both the dielectric constant and the overall nonresonant absorption within approximately $\pm 10\%$.

It is apparent that neither the microwave radiometry nor the radar are at present able to detect resonant absorption of gases. Barrett and Staelin⁵ searched for the 1.35 cm water vapor line, but were not able to resolve. This could mean that it was not present at the cloud height corresponding to 1 cm emission region or else the line was sufficiently broadened to wash out the resonance. However, such a radiometric experiment at about 1.7 mm and near 0.9 mm would show reasonable resonance emission if such measurements were attempted from an orbiter, a satellite, or airborne radiometer in the millimeter region, and if water vapor were present in the predicted concentration from infrared data. Such a radiometer may also detect presence of O_2 at about 5 mm and 2.5 mm which exhibits sharp rotational lines, although the expected concentration in the atmosphere of Venus is small.

INFRARED SPECTROSCOPY

It is generally accepted that infrared spectroscopy is a more powerful tool than microwave or millimeter spectroscopy for identifying molecular constituents of a planetary atmosphere. Many of the molecules that have been speculated to be present in Venus exhibit strong infrared absorption bands which are quite unique for each of the species. Furthermore, in the wavelength region of about 1 micron to 16 microns, unlike in the microwave region, pressure broadening of these bands will not affect their intrinsic character. Of the various compounds that have been suggested for Venus, only CO_2 has been positively identified primarily from its very strong infrared absorption bands at 2.7 microns and 4.3 microns. Among the other candidates which have

been proposed, H_2O is one that exhibits many resonant bands. Strong and co-workers² have studied the 1.13 micron band and Dollfus⁷ has observed the 1.4 micron band of H_2O . In addition, water vapor shows even stronger and increasingly broader infrared bands centered at 1.8 microns, at about 2.7 microns and a very broad band from 5 to 7 microns. Fortunately it has a window at 4 microns and hence would not obscure the unique band of CO_2 in this region. Another candidate which naturally may accompany the presence of CO_2 is CO . This has a strong identifying band at about 4.7 microns which should be detectable, although the anticipated concentration suggests a weaker absorption. However, with an orbiter or improved ground-based instrumentation this should now be possible. Nitrogen itself, which has been considered, does not possess either a microwave or an infrared spectrum, but its compounds N_2O and NO_2 have both. N_2O can be distinguished from CO in that, in addition to a band at 4.7 microns, it has one at 7.8 microns on either side of the large water vapor band, making its spectrum detectable. O_2 and O_3 both have infrared and microwave resonance spectra. O_2 has weak transitions at 1.06 and 1.27 microns and stronger ones at 0.762 and 0.688 microns. Lastly among the molecules with strong infrared spectra, CH_4 , one of the likely hydrocarbons, does exhibit relatively narrow bands at 3.3 and 7.7 microns again in a fortunate position relative to water vapor.

Recent high resolution measurements by Connes, Benedict, and Kaplan⁸, using a Michelson interferometer, has shown unique spectra of Venus. These were taken at the Observatoire de Saint Michel at high altitudes. The spectra were taken in the three atmospheric windows of water vapor between 1 and 3 microns. The data exhibited distinct lines attributed to HCl and HF , and even distinguished between isotropic species of Cl . This particular result demonstrates the extreme value of high resolution spectroscopy in the infrared. Such an instrument above the Earth's

atmosphere or in a Venus fly-by or preferably an orbiter would uncover other components of the upper atmosphere of Venus.

GENERAL COMMENTS

Among the important major components, N_2 is one of the most difficult to detect because it has no active resonance spectrum either in the infrared or the microwave-millimeter regions because of its symmetrical charge distribution. The inert gases such as argon and neon which may be present are even harder to detect. The only likely possibility will be to look for their natural lines in the ultraviolet. This is a more difficult task and in the presence of either molecules which also absorb in the ultraviolet this becomes even more involved.

In examining Fig. 2, which shows pictorially some of the spectral vibrational-rotational bands of interest, some pertinent observations can be made. The ground-based observations, which have been made with the Mount Palomar telescope and Mariner II for the observation of Venus in the infrared, were made essentially in the 8 to 14 micron window of H_2O . With the exception of O_3 , this does not include spectral lines of importance to us. The negative results may indicate that O_3 is not present at all or not in sufficient quantities to be observed radiometrically. Hence it appears that it would be of greater significance to do measurements in the spectral range of approximately 1 to 10 microns which include the water vapor lines. However, it is necessary to get sufficiently high above the earth's atmosphere to eliminate its water vapor. A limited advantage may be obtained by observations on mountain tops in dry regions, such as Arizona. However, much more can be achieved by the use of high altitude balloons or satellites. The possibility of using high flying airplanes with appropriate large area mirrors is another suitable alternative. Finally, an orbiting radiometric scanning spectrometer about Venus in this region of the infrared would be most desirable.

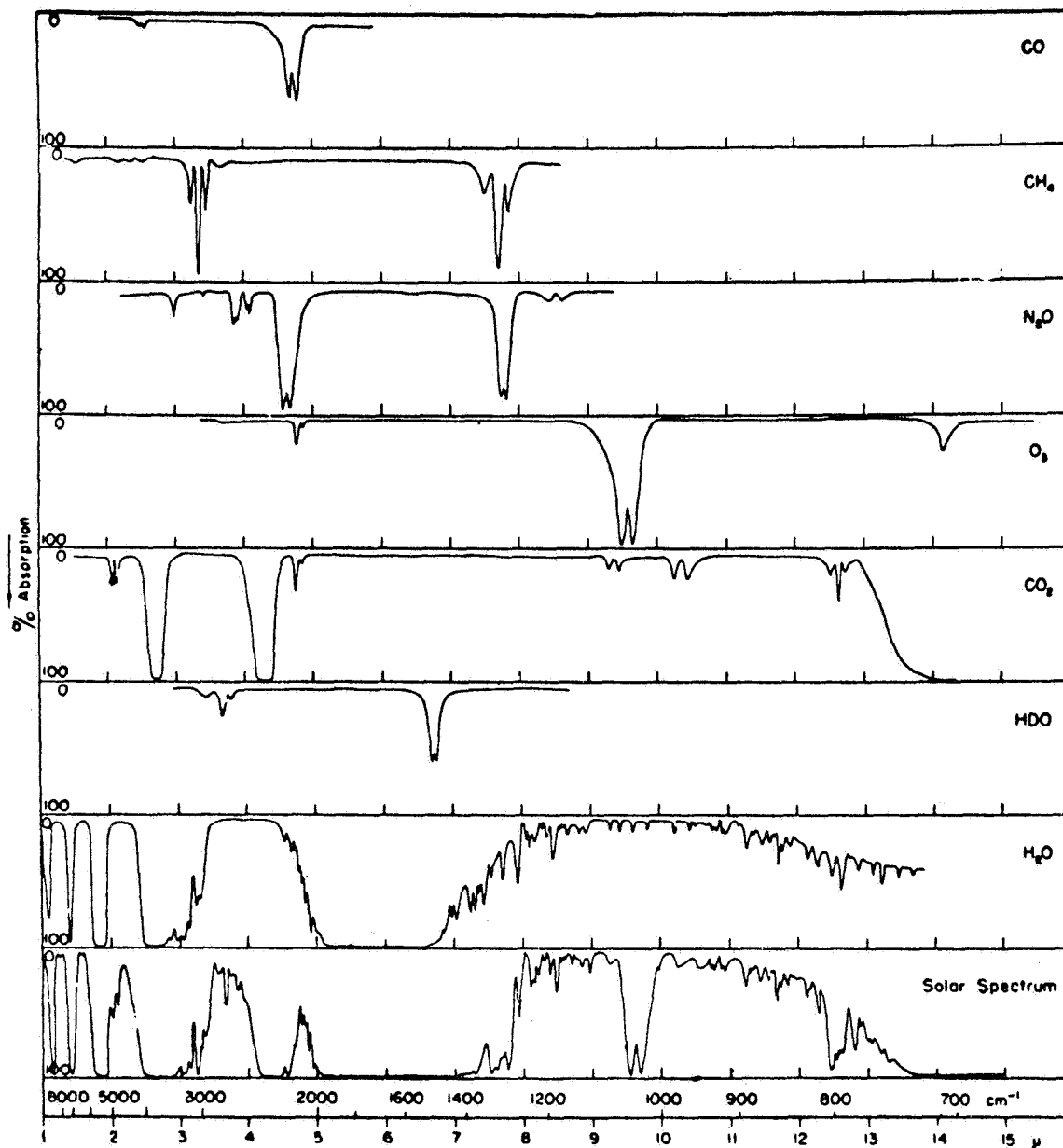


Figure 2. The near-infrared solar spectrum (bottom curve). Other curves are laboratory spectra of the molecule, indicated. The diagram is from J. N. Howard, D. L. Burch, and D. Williams, Geophysical Research Papers (U.S.) 40, Rept. AFCRL-TR-55-213 (1955).

The priority should be in terms of relative cost which would probably be in the order of planes or balloons (or both), then satellites orbiting about the Earth, and finally the Venusian orbiter or fly-by if it precedes an entering capsule which successfully samples the planet's atmosphere.

Greater detail is precluded from this report since its purpose is not to spell out the specific instrumentation, but to point out the fruitful regions of microwave and infrared spectroscopy which can be exploited within the next five or ten years. The recommendations are based upon improved capabilities where some success already has been achieved as in the microwave region. In the infrared region, technology of detection and spectroscopy in the 1 to 10 micron region gives added incentive to try airborne and spaceborne measurements.

Added Note

This report was originally written prior to the successful launching of the Soviet Venus landing probe. This established that CO₂ was the major constituent of Venus and that the surface temperature was very high. However, the high temperature prevented the electronic equipment from operating for a sufficiently long period to give all the information that is desired. Hence this would still justify future studies by orbiting satellites about Venus and Earth-based instrumentation whether on the ground or above the Earth's atmosphere.

REFERENCES

1. Weaver, H., "Some Problems of Planetary Radio Astronomy," Solar System Radio Astronomy, Ch. 17, pp. 371-399, ed. by J. Aarons, Plenum Press (1965).
2. Sinton, W. M. and Strong, J., "Radiometric Observations of Venus," Astrophys. J. 131, pp. 470-490 (1960);
Bottema, M., Plummer, W. J., and Strong, J., "A Quantitative Measurement of Water-Vapor in the Atmosphere of Venus," Ann d'Astrophysique 28, pp. 225-228 (1965);
Plummer, W. J., and Strong, J., "Conditions on the Planet Venus," Astronautics Acta 11, pp. 375-382 (1965).
3. Pollack, J. B., and Sagan, C., "The Infrared Limb Darkening of Venus," J. G. R. 70, pp. 4403-4426 (1965).
4. Evans, J. V., Ingalls, R. P., Rainville, L. P., and Silva, R. R., "Radar Observations of Venus at 3.8 cm Wavelength," Astron. J. 71, pp. 902-915 (1966).
5. Staelin, D. H., and Barrett, A. H., "Spectral Observations of Venus Near 1-Centimeter Wavelength," Astrophys. J. 144, pp. 352-363 (1966).
6. Pettengill, G. H., and Evans, J. V. (to be published).
7. Dollfus, A., "Observation de la vapeur d'eau sur la planète Vénus," Comp. Rend. 256, pp. 3250-3253, Acad. Sci. Paris (1963).
8. Connes, P., Connes, J., Benedict, W. S. and Kaplan, L. P., "Traces of HCl and HF in the Atmosphere of Venus," Astrophys. J. 147, pp. 1230-1237 (1967).

TG# 40

APPENDIX I
(Report of 1967 Summer "TYCHO" Meeting, TG # 31)

SOME COMMENTS ON THE SCATTERING
OF THERMAL MICROWAVE RADIATION BENEATH
A PLANETARY SURFACE

B. G. Smith
July, 1967

Contract No. NSR-24-005-047

Prepared by

UNIVERSITY OF MINNESOTA
Minneapolis, Minnesota

For

HEADQUARTERS, NATIONAL AERONAUTICS & SPACE ADMINISTRATION
Washington, D. C. 20546



SOME COMMENTS ON THE SCATTERING OF THERMAL MICROWAVE
RADIATION BENEATH A PLANETARY SURFACE

ABSTRACT

The microwave radiation thermally emitted by a planet originates in the planetary medium and reaches the surface by a process of radiative transfer. A simple model is used to determine the effect on the transfer process of single scattering from centers randomly distributed in the medium. Particular reference is made to the ability of the scattering mechanism to impose a weak linear polarization upon the radiation. It is found that the polarization from scattering is much weaker than that induced by transmission through the surface. As it stands the model is incapable of providing an explanation of the low value of the surface dielectric constant of the Moon and Venus deduced from measurements of the microwave polarization. The suggestion is made that the development of a multiple scattering model is necessary to provide a complete understanding of the interaction of microwave radiation with a planetary surface.

TABLE OF CONTENTS

<u>Title</u>	<u>Page</u>
Introduction	I-1
Description of the Model	I-4
Conclusions.	I-15
References	I-16

LIST OF ILLUSTRATIONS

<u>Figure</u>	<u>Title</u>	<u>Page</u>
1	A Section of a Planetary Surface	I-5
2	Constituents of the Radiation Reaching the Surface for the Single Scattering Model.	I-9
3	A Comparison of η_s and η_T as a Function of $\bar{\theta}$ Evaluated for $\lambda_A/\lambda_s = 1$, $\epsilon_1 = 2$ and 4 (Remembering $\bar{\mu} = \cos \bar{\theta}$, $\mu = \cos \theta$ and $\sqrt{\epsilon_1}$ $\sin \theta = \sin \bar{\theta}$)	I-14

LIST OF TABLES

<u>Table</u>	<u>Title</u>	<u>Page</u>
1	Values of ϵ_1 (Dielectric Constant of the Surface Layer) Deduced for the Moon and Venus from: a) The Polarization of Thermally Emitted Microwave Radiation b) Radar Backscatter.	I-3

SOME COMMENTS ON THE SCATTERING OF THERMAL MICROWAVE
RADIATION BENEATH A PLANETARY SURFACE

B. G. Smith

July, 1967

INTRODUCTION

The Moon and planets emit microwave radiation and an analysis of the characteristics of the radiation can give information about the physical parameters of the source. The microwave emission from the Moon, Mars and Venus is of low intensity, with weak linear polarization and, apart from solar phase effects, time invariant. The simplest explanation is that the radiation is from an incandescent black body.

The model to describe thermal microwave emission from a planetary surface was first elaborated by Troitskii (ref. 1). (For convenience in this paper the Moon will be included under the general heading of Planets, whenever no confusion will arise). Radiation leaving the surface originates in the planetary medium up to an absorption length deep. The intensity of the radiation is a measure of the brightness temperature of the medium averaged in some way over this depth. Microwave radiometers in present use on Earth have insufficient angular resolution to allow examination of local features on the planets and in fact sample the radiation integrated over the whole planetary disc. Average disc brightness temperatures have been derived for the Moon, Mars and Venus. Those for the Moon and Mars are compatible with the measured infrared temperatures, but a well known discrepancy exists between the two temperatures of Venus, providing fruitful ground for atmospheric model makers.

A second characteristic of thermal radiation is its polarization. If the planetary medium is isotropic and if scattering plays no part in the transfer process by which radiation reaches

the surface, the upward stream of radiation beneath the surface will be unpolarized. Passage through the surface will then impose a linear polarization upon the wave. If the surface may be considered locally as a plane interface between two dielectric media, the magnitude of the induced polarization will depend upon the angles of incidence and refraction, according to Fresnel's transmission equations. The total radiation integrated over a uniformly emitting spherical surface would, however, from arguments of symmetry, be unpolarized. Since the sun is the ultimate source of at least part of the radiated energy, the variation in solar phase angle produces a surface temperature variation with planetary longitude and this in turn causes different parts of the surface to contribute different amounts to the total radiation. The integrated emission will in this case be weakly polarized. In addition, the weighting accorded different contributions depends upon the characteristics of the radiometer used to make the experimental measurement. The orientation of an interferometer axis defines a preferred direction of the planetary disc preferentially weighting the contributions from the surface lying on a diameter perpendicular to the axis. In this case, too, the integrated emission is weakly polarized. A twin-antenna microwave interferometer has been used in this way to study radiation from Venus (ref. 4).

Fresnel's transmission equations contain the dielectric constant of the subsurface medium as a parameter. Measurements of polarization have given values for the dielectric constant, ϵ_1 , of the surface layer of the Moon and Venus quoted in Table 1. There they are compared with values of ϵ_1 deduced from the radar backscatter cross section of those bodies. The discrepancy is striking, and indicates that in each case the polarization of thermally emitted radiation is less than that expected from a surface layer with the radar dielectric constant. Various explanations have been offered. Roughness of the planetary surface would impose less polarization upon the emergent

TABLE I

VALUES OF ϵ_1 (DIELECTRIC CONSTANT OF THE SURFACE LAYER) DEDUCED FOR THE MOON AND VENUS FROM:

a) THE POLARIZATION OF THERMALLY EMITTED MICROWAVE RADIATION.

b) RADAR BACKSCATTER.

Body	a) Thermal microwave radiation	b) Radar backscatter
Moon	1.6 ± 0.2 ($\lambda = 3.2$ cm, ref. 2)	2.72 ($\lambda = 3.6$ cm, ref. 5)
	2.1 ± 0.3 ($\lambda = 21$ cm, ref. 3)	2.79 ($\lambda = 68$ cm, ref. 5)
Venus	2.2 ± 0.2 ($\lambda = 10.6$ cm, ref. 4)	3.75 ± 0.3 ($\lambda = 12.5$ cm, ref. 6)
		4 - 5 ($\lambda = 23$ cm, ref. 7)

radiation than the equivalent smooth surface. Hagfors and Moriello (ref. 8) have examined a rough surface model and are able to explain some, but not all, of the discrepancy. Another explanation is that the planetary medium is inhomogeneous with depth, with compacted material of higher dielectric constant underlying a more diffuse surface layer (ref. 5). It is suggested that radar will sample the dielectric constant of the lower strata while the polarization of the thermally emitted radiation will be induced by passage across the outer boundary of the diffuse top layer.

This paper describes a new model which incorporates scattering of the radiation by subsurface inhomogeneities in the process of radiative transfer through the planetary medium. Scattering mechanisms themselves can impose polarization upon initially unpolarized radiation. Depending upon whether the polarization from scattering reinforces or subtracts from the polarization induced by transmission through the surface, the dielectric constant, according to the simple model, will be over or under-estimated. The possibility of explaining the dielectric discrepancy in terms of a scattering model provided the stimulation for the present study. In anticipation of the conclusion it must be stated that in fact the effect of scattering is to produce a polarization of incorrect sign and of insufficient magnitude to account for the discrepancy.

DESCRIPTION OF THE MODEL

Scattering will play an important role in radiative transfer if the scattering length ℓ_s of radiation in the medium is comparable with or less than the absorption length ℓ_A . A crude model will be used to estimate the effect of scattering centers embedded in the medium. The planetary surface, illustrated in Fig. 1, is locally plane, separating the planetary medium of dielectric constant ϵ_1 from the atmosphere (if any) of dielectric

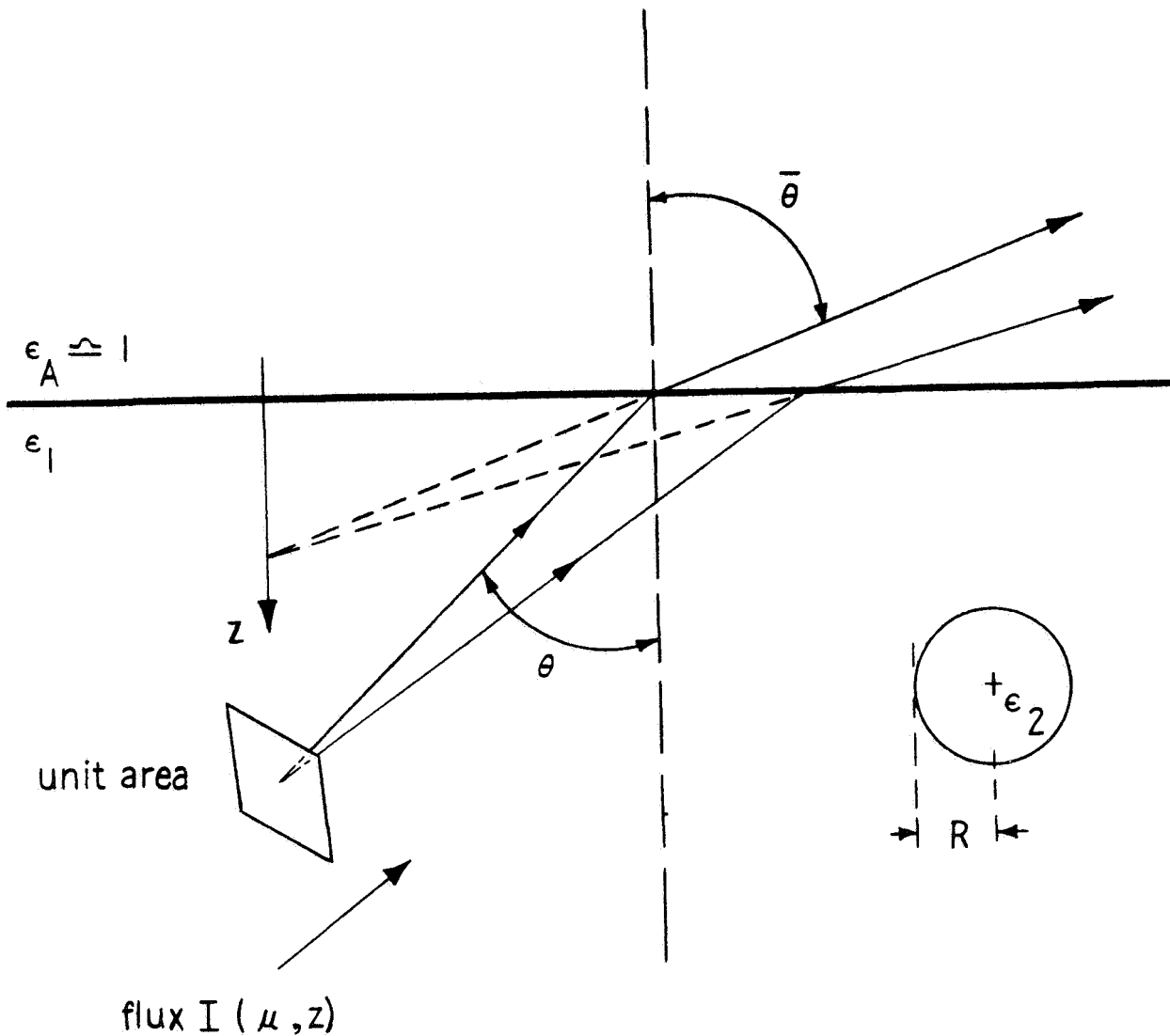


Figure 1. - A Section of a Planetary Surface

constant ϵ_A (≈ 1). The medium is homogeneous except for the presence of a random distribution of inclusions of dielectric constant ϵ_2 ($\neq \epsilon_1$), of characteristic dimension less than a free space wavelength λ . The interaction of radiation with an inclusion

will be approximated by Rayleigh scattering, for which the total scattering cross section σ_s is (ref. 9)

$$\sigma_s = \frac{8\pi}{3} \left(\frac{4\pi^2 \alpha}{\lambda^2} \right)^2 \quad (1)$$

where α is the polarizability of the inclusion. For spherical scattering centers of radius R , α is given by (ref. 10)

$$\alpha = \left(\frac{\epsilon_2 - \epsilon_1}{2\epsilon_1 + \epsilon_2} \right) R^3 \epsilon_1 \quad (2)$$

The scattering length l_s expressed in terms of the scattering cross section and the number density of scattering centers n_s , is

$$l_s = \frac{1}{n_s \sigma_s} \quad (3)$$

If $\beta (= \frac{4\pi}{3} R^3 n_s)$ is the fractional volume of the medium occupied by spherical inclusions

$$l_s = \frac{\lambda}{2\beta} \cdot \frac{1}{(2\pi)^4} \cdot \left(\frac{\lambda}{R} \right)^3 \cdot \left(\frac{2\epsilon_1 + \epsilon_2}{\epsilon_2 - \epsilon_1} \right)^2 \cdot \left(\frac{1}{\epsilon_1} \right)^2 \quad (4)$$

It is not difficult to imagine an inhomogeneous medium for which typical values of the parameters would be $\beta \sim 0.05$, $R \sim 0.1\lambda$, $\epsilon_1 \sim 4$, $\epsilon_2 \sim 2$ and in this case $l_s \sim 10\lambda$. Estimates of the absorption length of microwave radiation beneath the lunar surface have been made (ref. 11); a typical value is $l_A \sim 10\lambda$. Although criticism can be raised about the validity of this estimate, the deduction may be drawn that there is no strong a priori reason why scattering of radiation should not be an important process within the lunar medium. It will be assumed that a similar argument could be advanced for the planets.

The equation of radiative transfer within a plane parallel planetary medium (ref. 9) is, referring to Fig. 1,

$$\begin{aligned}
 -\mu \frac{dI(\mu, z)}{dz} = & - \left(\frac{1}{\ell_A} + \frac{1}{\ell_s} \right) I(\mu, z) + \frac{\epsilon_1}{\ell_A} B(z) \\
 & + \frac{1}{\ell_s} \int_{-1}^{+1} d\mu' \int_0^{2\pi} d\phi' P(\mu\phi, \mu'\phi') I(\mu', z) \quad (5)
 \end{aligned}$$

$I(\mu, z)$ is the radiative energy flux per unit solid angle at a depth z in the medium in a direction (θ, ϕ) making an angle θ with the surface normal. $\mu = \cos \theta$, and because the system has cylindrical symmetry about the z axis I is independent of azimuthal angle ϕ . The term on the left of the equation represents the change of the energy flux in traversing a path length $(-dz/\mu)$ in the medium (z being measured downwards). On the right, the first term represents attenuation of the flux by scattering and absorption. The second term describes the isotropic emission process according to Kirchoff's Law. $B(z)$ is the Planck function at the appropriate wavelength and depends upon temperature which may be a function of depth. The third term represents the enhancement of the flux caused by scattering into unit solid angle in the direction (θ, ϕ) , and $P(\mu\phi, \mu'\phi')$ is the angle dependent part of the angular scattering cross section. Since the radiation can be polarized, it is necessary to differentiate between a flux I_1 polarized with its E vector in the plane containing the direction of the flux and the normal to the surface, and its orthogonal counterpart I_2 . I is thus a two component quantity $\begin{pmatrix} I_1 \\ I_2 \end{pmatrix}$, and P

a two by two matrix, which for Rayleigh scattering has the form (ref. 9)

$$P = \frac{3}{16\pi} \begin{bmatrix} 2(1-\mu^2)(1-\mu'^2) + \mu^2\mu'^2 & \mu^2 \\ \mu'^2 & 1 \end{bmatrix} + Q(\theta\phi, \theta'\phi') \quad (6)$$

where Q is a matrix with the property that

$$\int_0^{2\pi} d\phi' \quad Q(\theta\phi, \theta'\phi') \equiv 0 \quad (7)$$

Q plays no part in the following analysis. B is also a two-component quantity, but for an isotropic medium the components B_1 and B_2 are identical.

If scattering is a less important attenuative process than absorption, equation 5 can be solved by a series expansion in powers of λ_A/λ_s . The first two terms in such an expansion describe the transfer of radiation suffering zero and one scattering process. In order to demonstrate the physical properties of the model more clearly higher order scattering processes will be neglected. Developing the series from an intuitive point of view, there will be two constituents of the radiation reaching the surface, illustrated in Fig. 2. Radiation $I^{(A)}$ emitted by each volume element reaches the surface undeflected after suffering attenuation by absorption and single scattering en route. $I^{(A)}$ satisfies the reduced equation of transfer

$$-\mu \frac{dI^{(A)}}{dz} = - \left(\frac{1}{\lambda_A} + \frac{1}{\lambda_s} \right) I^{(A)} + \frac{\epsilon_1}{\lambda_A} B \quad (8)$$

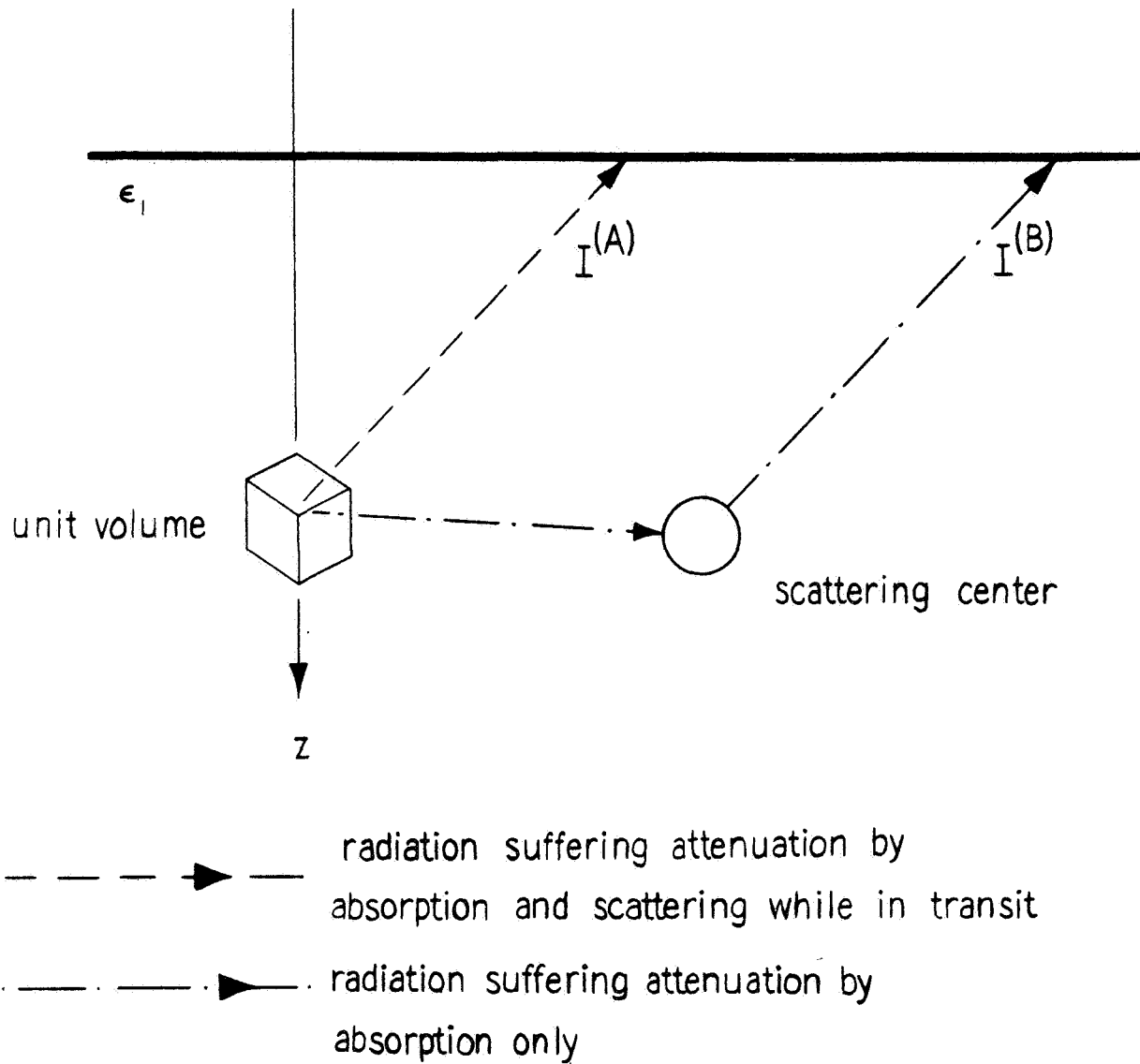


Figure 2. - Constituents of the Radiation Reaching the Surface for the Single Scattering Model

Equation 8 may be integrated to give

$$\begin{aligned}
 \mu > 0; \quad I^{(A)}(\mu, z) &= \frac{\epsilon_1}{\ell_A \mu} \int_z^\infty dz' B(z') e^{-(1/\ell_A + 1/\ell_S) \frac{1}{\mu} (z' - z)} \\
 \mu < 0; \quad I^{(A)}(\mu, z) &= \frac{\epsilon_1}{\ell_A (-\mu)} \int_0^z dz' B(z') e^{-(1/\ell_A + 1/\ell_S) \frac{1}{\mu} (z' - z)}
 \end{aligned}
 \tag{9}$$

where the boundary condition has been imposed that there be no downward radiation stream at the surface ($z = 0$).

The second constituent of the radiation, $I^{(B)}$, reaches the surface after suffering a single scattering, and attenuation by absorption before and after the scattering process. $I^{(B)}$ satisfies an equation of transfer

$$-\mu \frac{dI^{(B)}}{dz} = -\frac{1}{\ell_A} I^{(B)} + \Phi \tag{10}$$

where $\Phi(\mu, z)$, the two component source function for $I^{(B)}$, is

$$\Phi(\mu, z) = \frac{1}{\ell_S} \int_{-1}^{+1} d\mu' \int_0^{2\pi} d\phi' P(\theta_\phi, \theta'_{\phi'}) \bar{I}^{(A)}(\mu', z) \tag{11}$$

and $\bar{I}^{(A)}$ is $I^{(A)}$ evaluated in the limit $\ell_S \rightarrow \infty$, since the source of $I^{(B)}$ is radiation which has suffered no earlier scattering. Implicit in the definition of Φ is a neglect of radiation which suffers single scattering after a reflection from the surface. Its

contribution is small and for ease of calculation will be excluded.

Equation 10 can be integrated to give $I^{(B)}$

$$\mu \geq 0; \quad I^{(B)}(\mu, 0) = \frac{1}{\mu} \int_0^{\infty} dz' \phi(\mu, z') e^{-z/\mu \ell_A} \quad (12)$$

If the brightness distribution with depth, $B(z)$, is specified the integrals in Equations 9, 11 and 12 may be evaluated to give $I^{(A)}$ $(\mu, 0)$ and $I^{(B)}$ $(\mu, 0)$. Their sum, $I(\mu, 0)$, for $\mu \geq 0$, is the upward flux of radiation at the surface within the medium, which subsequently suffers refraction and a transmission loss on crossing the surface. If $J_k(\bar{\mu})$ is the two component radiative energy flux per unit solid angle outside the surface in a direction $(\bar{\theta}, \bar{\phi})$, making an angle $\bar{\theta}$ with the surface normal, and $\bar{\mu} = \cos \bar{\theta}$

$$\mu \geq 0; \quad J_k(\bar{\mu}) = \frac{1}{\epsilon_1} (1 - R_k) I_k(\mu, 0) \quad k = 1, 2 \quad (13)$$

where k is an index denoting one of two polarization components and $\sin \bar{\theta} = \sqrt{\epsilon_1} \sin \theta$ according to Snell's law of refraction. R_k is the appropriate Fresnel surface reflection coefficient given by (ref. 12)

$$R_1 = \frac{\tan^2(\theta - \bar{\theta})}{\tan^2(\theta + \bar{\theta})}; \quad R_2 = \frac{\sin^2(\theta - \bar{\theta})}{\sin^2(\theta + \bar{\theta})} \quad (14)$$

The factor $1/\epsilon_1$ appears in order to allow for the change in solid angle occurring at refraction through the surface (ref. 1).

The purpose of this paper is to compare the polarization induced by scattering with that induced by transmission through the surface. It is convenient to define the polarization η_s caused by scattering alone.

$$\eta_s = \frac{I_1(\mu, 0) - I_2(\mu, 0)}{I_1(\mu, 0) + I_2(\mu, 0)} \quad \mu \geq 0 \quad (15)$$

and to compare it directly with the polarization η_T caused by transmission through the surface in the absence of scattering

$$\eta_T = \left[\frac{J_1(\bar{\mu}) - J_2(\bar{\mu})}{J_1(\bar{\mu}) + J_2(\bar{\mu})} \right]_{\lambda_s \rightarrow \infty} \quad (16)$$

In this limit, $I_1(\mu, 0) = I_2(\mu, 0)$, $\mu \geq 0$, and from equation 13,

$$\eta_T = \frac{(1 - R_1) - (1 - R_2)}{(1 - R_1) + (1 - R_2)} \quad (17)$$

Explicit evaluation of η_s will be made for two brightness distribution functions $B(z)$: that of an isothermal medium, and a linear brightness gradient.

(1) Isothermal medium. $B(z) = \text{constant}$, $B_1 \equiv B_2 = B_0$

Equation 9 can be integrated directly to give $I^{(A)}$. At the surface

$$\mu \geq 0; \quad I_k^{(A)}(\mu, 0) = \left(\frac{\lambda_s \epsilon_1}{\lambda_s + \lambda_A} \right) B_0 \quad k = 1, 2 \quad (18)$$

a result which, in the limit of no scattering, reproduces that of Troitskii (ref. 1). Using equations 9, 11 and 12 the expression for $I_1 - I_2$ in the isothermal medium is

$$\mu \geq 0; \quad I_1(\mu, 0) - I_2(\mu, 0) = 2\epsilon_1 B_0 \left(\frac{\lambda_A}{\lambda_s} \right) f(\mu) \quad (19)$$

where

$$f(\mu) = \frac{3}{16} \mu (1-\mu^2) \left\{ (1-3\mu^2) \log (1+1/\mu) - \left(\frac{3}{2} - 3\mu\right) \right\} \quad (20)$$

The total intensity in the two polarizations is little affected by scattering, and is given approximately by

$$\mu \geq 0; \quad I_1(\mu, 0) + I_2(\mu, 0) \approx 2\epsilon_1 B_0 \quad (21)$$

with the result, from equation 15,

$$\eta_s \approx \frac{\ell_A}{\ell_s} f(\mu) \quad (22)$$

η_s (for $\ell_A/\ell_s = 1$) and η_T , calculated for two values of ϵ_1 , are displayed as functions of $\bar{\theta}$ in Fig. 3. Two features stand out. One, η_s has the same sign as η_T and so for a real surface the two polarization mechanisms will reinforce one another. Two, η_s is at best an order of magnitude smaller than η_T .

(2) Linear brightness gradient. $B_1(z) = B_2(z) = B_0 + B'z$

With this expression for $B(z)$ the integrals in equations 9, 11 and 12 lead to

$$\mu \geq 0; \quad I_1(\mu, 0) - I_2(\mu, 0) = 2\epsilon_1 \left(\frac{\ell_A}{\ell_s}\right) [B_0 + B'\mu\ell_A] f(\mu) - \frac{3}{32} \left(\frac{\ell_A}{\ell_s}\right) (1-\mu^2) B'\ell_A\epsilon_1 \quad (23)$$

A simple interpretation exists for equation 23. The first term to the right of the equality sign is equivalent to the contribution from an isothermal medium of brightness equal to that at a slant depth of one absorption length. The second term, which is of opposite sign, is equal to the difference in the intensities of

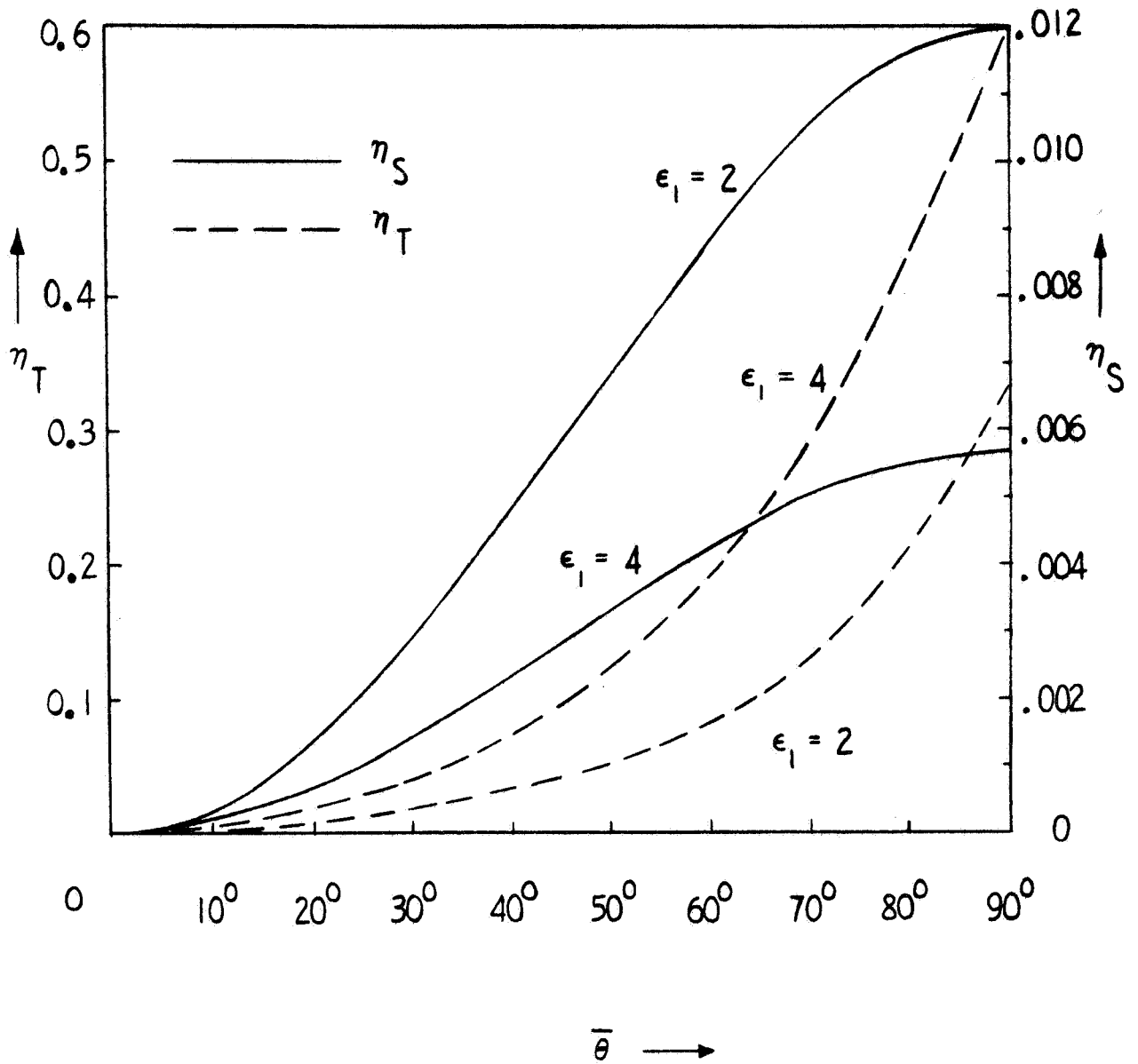


Figure 3. - A Comparison of η_S and η_T as a Function of $\bar{\theta}$ Evaluated for $l_A/l_S = 1$, $\epsilon_1 = 2$ and 4 (Remembering $\bar{\mu} = \cos \bar{\theta}$, $\mu = \cos \theta$ and $\sqrt{\epsilon_1} \sin \theta = \sin \bar{\theta}$).

the two polarized components of scattered radiation produced when a steady vertical flux of total intensity $\frac{\pi}{2} B' \ell_A \mu \epsilon_1$ interacts with the scattering centers contained in one absorption length depth of the planetary medium. The second term is important only if the brightness gradient is steep, in particular only if the brightness more than doubles in the distance of one absorption length below the surface. This is unlikely to be the case for a planet, and so the second model is essentially indistinguishable from the first.

CONCLUSIONS

Disappointingly, it is impossible to understand the dielectric discrepancy in terms of a simple scattering model. Indeed, if such a model were applicable as it stands, current estimates of ϵ_1 from polarization measurements should be slightly reduced rather than increased.

The calculation does, however, provoke thought about the relative importance of absorption and scattering as attenuative mechanisms beneath a planetary surface. The current estimated value of the absorption length for microwave radiation in the lunar medium (ref. 11) is based upon an interpretation of the emission process in terms of radiative transfer without scattering, an interpretation which this paper is calling in doubt. If the absorption length is in reality considerably greater than this estimate, it will be necessary to perform a completely new analysis of a multiple scattering model for the process of transfer by which microwave radiation diffuses through a planetary medium. An analysis of this sort might have interesting conclusions for the interpretation of both microwave emission and radar backscatter experiments from planetary surfaces.

REFERENCES

1. Troitskii, V. S., "A Contribution to the Theory of Radio Emission of the Moon," *Astron. Zh.* 31 (6), 1954, pp. 511-528.
2. Soboleva, N. S., "Measurement of the Polarization of Lunar Radio Emission On a Wavelength of 3.2 cm," *Astron. Zh.* 39 (6), 1962, pp. 1124-1126.
3. Heiles, C. E. and Drake, F. D., "The Polarization and Intensity of Thermal Radiation From a Planetary Surface," *Icarus* 2, 1963, pp. 281-292.
4. Clark, B. G. and Kuz'min, A. D., "The Measurement of the Polarization and Brightness Distribution of Venus at 10.6-cm Wavelength," *Ap.J.* 142, 1965, pp. 23-44.
5. Evans, J. V. and Hagfors, T., "On the Interpretation of Radar Reflections From the Moon," *Icarus* 3, 1964, pp. 151-160.
6. Carpenter, R. L., "Study of Venus by CW Radar - 1964 Results," *Astron. J.* 71, 1966, pp. 142-152.
7. Evans, J. V. et al, "Radio Echo Observations of Venus and Mercury at 23 cm Wavelength," *Astron. J.* 70, 1965, pp. 486-501.
8. Hagfors, T. and Moriello, J., "The Effect of Roughness On the Polarization of Thermal Emission From a Surface," *J. Res. Natl. Bur. Stand.*, 69 (D), 1965, pp. 1614-1615.
9. Chandrasekhar, S., "Radiative Transfer," Chapter 1, Oxford University Press, Oxford, 1950.
10. Stratton, J. A., "Electromagnetic Theory," Chapter III, McGraw Hill Book Company, Inc., New York, 1941.
11. Weaver, H., "The Interpretation of Thermal Emission From the Moon," Chapter 15 of "Solar System Radio Astronomy", edited by J. Aarons, Plenum Press, New York, 1965.
12. Stratton, J. A., "Electromagnetic Theory," Chapter IX, McGraw Hill Book Company Inc., New York, 1941.

TG # 41

APPENDIX J
(Report of 1967 Summer "TYCHO" Meeting, TG # 31)

WATER ON MARS

R. Smoluchowski

July, 1967

Contract No. NSR-24-005-047

Prepared by

UNIVERSITY OF MINNESOTA
Minneapolis, Minnesota

For

HEADQUARTERS, NATIONAL AERONAUTICS & SPACE ADMINISTRATION
Washington, D. C. 20546



WATER ON MARS

ABSTRACT

Water in the form of ice can exist on Mars as permafrost which is either in equilibrium with the water content of the atmosphere or is gradually evaporating through a protective layer of soil. The latter situation is evaluated quantitatively for grains from 0.5 to 1000 microns and for porosities from 0.01 to 0.8. The effective diffusion coefficients are calculated and the required thicknesses of the protective layers estimated. It is concluded that such subsurface ice can exist at Martian latitudes lower than those for which the permafrost is in equilibrium with the atmosphere. This may lead to seasonal variations of radar reflectivity and may explain the higher reflectivity of the dark areas as compared to the bright areas.

TABLE OF CONTENTS

<u>Title</u>	<u>Page</u>
Introduction.	J-1
Effect of Porosity on Diffusion	J-2
Thickness of the Protective Layer	J-6
Seasonal and Diurnal Variations of Surface Temperature. . .	J-8
Effect of Ice or Water Content on Radar Reflectivity. . . .	J-8
References.	J-11

LIST OF TABLES

	<u>Page</u>
1 Effective Pore Size or Hydraulic Radius m	J-3
2 Mean Effective Diffusion Coefficients in Cm ² Sec ⁻¹	J-5
3 Calculated Thickness L.	J-7

WATER ON MARS

R. Smoluchowski

July, 1967

INTRODUCTION

No doubt there is water on Mars⁽¹⁾. The biological, climatological and morphological implications of this fact depend radically upon its actual amount, form and location. The only direct quantitative measurement available is that of precipitable water vapor in the atmosphere in the amount of 14 ± 7 microns. The generally subfreezing surface temperatures⁽²⁾ imply also that there may be considerable amounts of ice as subsurface permafrost⁽³⁾. This has been discussed in detail by Leighton and Murray⁽³⁾. The polar caps now appear to be solid CO_2 rather than ice as previously assumed. One can be sure also that there are no open bodies of water but the occurrence of surface temperatures⁽⁴⁾ as high as 340°K suggests that there may be localized temporary and periodic melting. In fact the best values⁽⁵⁾ of the triple point of water 6.11 mb and 273°K fall right in the middle of the range of pressures deduced from the Mariner IV occultation experiments⁽⁶⁾ and also are bracketed by the calculated and observed surface temperatures. The occurrence of pressures and temperatures appropriate for liquid water, however, is rarer than those for ice and vapor.

The purpose of this note is to look in a quantitative manner into the stability of permafrost, its possible melting and the preservation of moisture in the Martian soil. A possible connection between these phenomena and the behavior of dark areas and their radar reflectivity is also discussed and suitable observations suggested.

EFFECT OF POROSITY ON DIFFUSION

If the mean annual temperature is low enough, permafrost can exist in equilibrium with the water content of the atmosphere. Under this condition permafrost on Mars can exist within a few meters from the surface at latitudes higher than about 45 degrees⁽³⁾. In this paper we are concerned rather with a non-equilibrium situation when the mean temperatures are higher and the ice has a life time determined by the thickness of a protective layer. To a certain extent this resembles the problem of the retention of ice on the moon. It is thus important to estimate the rate of permeation of water vapor through layers of particulate matter which one would expect to encounter on Mars. It is rather certain^(4,7) that the well-known yellow clouds require particles not less than a couple of hundred microns in size but these particles constitute probably only a small fraction of the actual surface coverage. A careful analysis⁽⁸⁾ of the thermal properties of Martian surface suggests that the predominant size is from a few tenths of a micron up to about 20 microns. The larger particles are undoubtedly mixed in but the effective pore size will be determined by the smaller grains.

The effective pore size or the hydraulic radius m depends not only on the grain size but also on porosity. We shall consider here grains with diameter ϕ equal 0.5, 10, 200 and 1000 microns and porosities .01, 0.1, 0.2, 0.5 and 0.8. In Table 1, standard permeability formulae give the corresponding values of m expressed in μ :

Table 1

EFFECTIVE PORE SIZE OR HYDRAULIC RADIUS m

Grain Diameter	Porosity				
	$\epsilon=0.01$	$\epsilon=0.1$	$\epsilon=0.2$	$\epsilon=0.5$	$\epsilon=0.8$
$\phi=0.5\mu$	8×10^{-4}	.01	0.021	0.083	0.332
$\phi=10\mu$	1.7×10^{-2}	.02	0.42	1.7	6.8
$\phi=200\mu$	0.33	3.9	8.3	33	130
$\phi=1000\mu$	1.7	20	42	169	667

Assuming⁽⁶⁾ that the Martian pressure near the surface is 5mb one obtains in the highly diluted CO₂-H₂O mixture for the mean free path λ of CO₂ molecule 4-8 μ for an H₂O molecule for temperatures varying from 160 to 300^oK. These values fall in the middle of the range of pore diameters listed in Table 1 which indicates that the mechanism of transport of water vapor will vary from normal diffusion in large pores to Knudsen flow in small pores. Under these conditions the very complete theory of diffusion in porous media at uniform pressure as given rather recently by Evans, Watson and Mason⁽⁹⁾ has to be used. In the normal diffusion region in a binary gas mixture the flux of molecules A along z axis is given by

$$J_A = D_{AB} (\partial n_A / \partial z) + X_A J \quad (1)$$

where D_{AB} is the usual interdiffusion coefficient, n_A is the number of molecules A per cc., X_A is their mole fraction and $J = J_A + J_B$.

In the Knudsen region

$$J_A = - D_{AK} (\partial n_A / \partial z) \quad (2)$$

applies where D_{AK} is the Knudsen diffusion coefficient or Knudsen permeability for molecules A. In the intermediate region the effective diffusion coefficient is given by the Bosanquet relationship:

$$(D_A)_{\text{eff}}^{-1} = (D_{AB})_{\text{eff}}^{-1} + (D_{AK})^{-1} \quad (3)$$

where

$$(D_{AB})_{\text{eff}} = \frac{3}{16} \frac{\epsilon}{nq} \left(\frac{M_A + M_B}{M_A M_B} 2 \pi RT \right)^{1/2} \frac{1}{S\Omega} \quad (4)$$

and

$$D_{AK} = 3 \frac{m}{q} \left(\frac{2\pi RT}{M_A} \right)^{1/2} \frac{2}{8+\pi b} \quad (5)$$

In these formulae ϵ is porosity, n is the total molecular concentration, q is the tortuosity factor, M_A and M_B are molecular weights, S is the scattering cross section, Ω is the collision integral usually close to unity and b is related to the ratio of diffuse to specular scattering and is also close to unity. For the H_2O-CO_2 system $S = 52 \text{ \AA}^2$ and also (10)

$$D = D_0 (T/T_0)^2 (p_0/p)$$

where we chose $T_0 = 273^\circ\text{K}$ and $p_0 = 1 \text{ atm}$. From Eqs. (4) and (5) one obtains:

$$(D_{AB})_{\text{eff}} = 20.3 \frac{\epsilon}{q} \left(\frac{T}{T_0} \right)^2$$

and

$$D_{AK} = 4.8 \times 10^4 \frac{m}{q} \left(\frac{T}{T_0} \right)^{1/2}$$

The flux of water molecules is then given by

$$J_A = - (D_A)_{\text{eff}} (\partial n_A / \partial z)$$

where $(D_A)_{\text{eff}}$ is given by Eq. (3). The second term in Eq. (1) has been omitted because of the very small values of X_A . The only quantity in these formulae for which there are no reliable theoretical values is q , the tortuosity factor. This factor is supposed to take care of the fact that at low porosities many of the pore paths lead to side-wise or even backward diffusion and it is usually determined from experimental data. For porosities in the range 0.2-0.5 parameter q turns out to be around 5, for lower porosities it is higher.

It appears that between 160 to 300°K the influence of temperature on the effective diffusion coefficient is negligible as compared to the influence of the mean pore diameter. Table 2 shows the resulting mean effective diffusion coefficients in $\text{cm}^2 \text{sec}^{-1}$ for the various structures of the porous material. It is assumed that the tortuosity factor $q = 1$ for $\epsilon = 0.8$, $q = 5$ for $\epsilon = 0.5$ and $q = 10$ for the lower porosities.

Table 2

MEAN EFFECTIVE DIFFUSION COEFFICIENTS IN $\text{CM}^2 \text{SEC}^{-1}$

Grain Diameter	Porosity				
	$\epsilon=0.01$	$\epsilon=0.1$	$\epsilon=0.2$	$\epsilon=0.5$	$\epsilon=0.8$
$\phi=0.5\mu$.0004	.004	.008	.07	1.3
$\phi=10\mu$.004	.06	0.1	.7	9
$\phi=200\mu$.009	.08	0.2	1.1	11
$\phi=1000\mu$.01	.1	0.25	1.2	12

THICKNESS OF THE PROTECTIVE LAYER

Our model consists of ice under a layer of thickness L of porous soil and it is assumed that in order to have appreciable permafrost or subsoil ice on Mars a layer of ice 10m thick should have existed over a period of a billion years. This leads to a maximum loss rate of 3×10^{-13} gr/cm²/sec. The partial vapor pressure of water above ice⁽¹⁰⁾ is given by its temperature T and we assume that at the surface, temperature T_s , the partial pressure of water is zero. Thus one has a system in which the water vapor diffuses down a concentration gradient and along a temperature gradient. In view of the fact, mentioned above, that temperature has only a secondary effect on the diffusion coefficient this influence will be neglected.

With these numerical data one can calculate the thickness L of a layer of a given porosity and grain size which would be sufficient to keep the loss of water vapor from ice at temperature T below the value 3×10^{-13} gr cm⁻² sec⁻¹. The results are given in Table 3. They have primarily relative significance because the absolute values are uncertain at least within a factor of 2 or 3. For $\epsilon = 0.8$ the calculated thicknesses L were greater than 10 meters. It should be stressed that the dependence of L on T reflects the variation of the pressure of water vapor over ice and not the variation of the diffusion rate which as mentioned above is only a slow function of temperature. The range of temperatures in Table 3 covers the range of mean annual temperatures⁽³⁾ on Mars.

It appears that there is a considerable range of particle sizes and porosities for which a layer of ice could be preserved during a time of the order of a billion years under a layer of reasonable thickness. This implies that ice or permafrost may exist at latitudes lower than 45 degrees.

Table 3

CALCULATED THICKNESS L

Grain Diameter (ϕ in μ)	Temperature (T in $^{\circ}$ K)	Porosity			
		$\epsilon=.01$	$\epsilon=.1$	$\epsilon=.2$	$\epsilon=.5$
0.5	240	10m			
	230	3.3m			
	220	1m	10m		
	210	30cm	3m	5.8m	
	200	6cm	60cm	1.2m	9m
	190	1.5cm	15cm	30cm	2.2m
	170		2.5cm	5cm	36cm
160				6cm	
10	220	10m			
	210	3m			
	200	62cm	9m		
	190	15cm	2.2m	3.7m	
	180	2.5cm	36cm	60cm	2.5m
	170		6cm	9cm	36cm
	160			1cm	4cm
200	210	5.8m			
	200	1.2m	9m		
	190	30cm	2.2m	3.7m	
	180	4.8cm	36cm	60cm	
	170		5.4cm	9cm	
	160			2cm	
1000	210	7.3m			
	200	1.5m			
	190	37cm	3.7m	9.3m	
	180	6cm	60cm	1.5m	
	170		9cm	22cm	
	160		1cm	3cm	

SEASONAL AND DIURNAL VARIATIONS OF SURFACE TEMPERATURE

In discussing the existence of ice and water on Mars one has to take into account the seasonal and diurnal variations of the surface temperature at various latitudes. At a sufficient depth below the surface these variations are negligible but they may reach 100° and more at the surface⁽⁴⁾. It follows that the temperature gradient between the layer of ice and the surface is sometimes positive and sometimes negative. In the first case the water vapor will escape as discussed above. In the second case, however, it may condense in the colder outside layers and form ice which will exist until the temperature gradient is gradually reversed. In such pores ice may be very stable since only a small fraction of its surface will be exposed to the atmosphere. In this connection it should be kept in mind that the results shown in the tables above were obtained for a mean pore diameter m given by ϕ and ϵ . There are, however, always some larger and some smaller pores. For instance⁽¹¹⁾ for a fixed porosity 0.5 and grain size decreasing from about 4mm to less than 0.5mm the ratio of capillary volume to non-capillary volume increases from 0.25 to 15. Thus even for a large non-capillary value of m there is a considerable fraction of capillary pores. Since in the warmer regions of Mars, temperatures well above the freezing point were observed, it follows that under favorable circumstances some water may be retained at least for a while in capillary pores. This may have biological consequences.

The existence of ice in intergranular pores implies that ice may also form in cracks of the grains themselves. Such condition leads to a gradual break up of the grains and to a comminution of the surface material in analogy to well known geological phenomena on Earth.

EFFECT OF ICE OR WATER CONTENT ON RADAR REFLECTIVITY

It is interesting to speculate whether ice or water content could affect the radar reflectivity of the soil. An analysis of this reflectivity indicates⁽¹²⁾ that the effective dielectric constant of the bright areas is about 2.2 while for the dark areas one obtains 3.5. Typical values for sand are near 2.8 as compared to the dielectric constant of water about 80 and of ice 3.3 to 130 (depending on frequency and temperature). It appears thus quite possible that the differences in radar reflectivity⁽¹³⁾ could be interpreted as due, at least in part, to ice or water retained in the subsurface layers. The thicknesses of the protective layers listed in Table III and those calculated from equilibrium considerations⁽³⁾ are quite comparable to the penetration depth of the 3.8 to 70cm radar wavelengths used in various Martian studies. Without further knowledge of the gradients of porosity and of particle size below the surface it is not possible to calculate the actual distribution of ice in the soil. Nevertheless, even if the radar does not reach the permafrost itself it will easily reach the seasonal condensation layer discussed above. According to various studies of the thermal properties of the Martian surface^(3,8), the amplitude of seasonal temperature variations decreases by a factor of ten within a layer of the order of several centimeters. If this is the case then the shorter wavelength reflectivity would be more likely to show seasonal variation than the longer wavelengths. Recent radar results⁽¹³⁾ suggest that Martian dark areas are probably lowlands rather than highlands and thus one is tempted to ascribe to them higher humidity content and a higher reflectivity than to the dry bright uplands. One way to check this conclusion would be to measure seasonal and diurnal radar reflectivity changes of bright and dark areas. This may be difficult to accomplish from the Earth because of the small variation of the phase angle and the large variation of distance

between Earth and Mars. On the other hand, an orbiter would be ideally suited for this purpose.

Planetary radar reflectivity is a function of many parameters and thus its seasonal variation, if it exists, could be accounted for on several models. Nevertheless, the ice-water mechanism seems more realistic and more attractive than an analogous mechanism based on variable photoconductivity⁽¹⁴⁾ of the soil.

REFERENCES

1. Dollfus, A., "Mesure de la Quantite' de Vapeur d'Eau Contenue dans l'Atmosphere de la Planete Mars," Compt. Rend. Acad. Sci. (Paris) 256, pp. 3009-3011 (1963).
2. de Vaucouleurs, G., "Physics of the Planet Mars," Faber and Faber, London (1954).
3. Leighton, R. B. and Murray, B. C., "The Behavior of Carbon Dioxide and Other Volatiles on Mars," Science 153, pp. 136-144 (July 8, 1966).
4. Opik, E. J., Science 153, p. 255 (1966).
5. Landolt-Bornstein Tables, Springer, Berlin (1965).
6. Kliore, A., Cain, D. L., Levy, G. S., Eshelman, V. R., and Fjeldbo, G., "Results of the First Direct Measurement of Occultation Experiment: Mars' Atmosphere and Ionosphere," Science 149, pp. 1243-1248 (1965).
7. Ryan, J. A., J. Geophys. Res. 69, p. 3759 (1964).
8. Leovy, C., Icarus 5, p. 1 (1966).
9. Evans, R. B., Watson, G. M., and Mason, E. A., J. Chem. Phys. 15, p. 2076 (1961).
10. Kennard, E. H., "Kinetic Theory of Gases," McGraw Hill, New York (1938).
11. Baver, L. D., "Soil Physics," J. Wiley & Sons, New York (1940).
12. Evans, J. V., private communication.
13. Pettengill, G. H., and Rinvile, L., to be published in Astron. J.
14. Smoluchowski, R., Science 148, p. 964, (1965).